VALIDITY AND LIMITATIONS OF HORIZONTAL FLOW MODELS IN PHREATIC AQUIFERS

by

Mohamed A. Elbakhbekhi

Submitted in Partial Fulfillment
of the Requirements for the Degree of
Doctor of Philosophy

NEW MEXICO INSTITUTE OF MINING AND TECHNOLOGY

Socorro, New Mexico

July, 1976

ABSTRACT

Horizontal flow models are widely used as a means for determining hydraulic head distribution and aquifer parameters in phreatic aquifers. They do not account for several physical factors including 1) the flow zone thinning, 2) vertical flow and anisotropy of permeability, and 3) flow in the unsaturated zone.

This study is an attempt to determine the significance of these physical factors and consequently to establish the validity and limitations of the horizontal flow models using existing solutions.

The physical problems under consideration are axisymmetric flow to a well, flow to parallel drainage ditches bounded by an impervious horizontal bottom, and artificial groundwater recharge.

Correlation of the horizontal flow model and the vertical flow model for the problems named above, indicates that the vertical flow effects and anisotropy of permeability are insignificant provided that the transformed aspect ratio (horizontal dimension relative to aquifer thickness times the square root of the anisotropy ratio) is equal to or greater than 4.0. Correlation of the vertical flow model and the variably saturated flow model indicates that the flow in the unsaturated zone is practically insignificant if the ratio of the critical height or thickness of the unsaturated zone to the aquifer thickness is equal to or less than 0.07. The flow zone thinning can be neglected provided that the ratio of the drawdown to the initial saturated thickness is equal to or less than 0.2 in axisymmetric flow

to a well, the ratio of the drainable depth to the aquifer thickness is equal to or less than 0.2 in linear flow to parallel ditches, and the recharge ratio (recharge relative to horizontal hydraulic conductivity times the ratio of the square of half the recharge basin length to the initial saturated thickness) is equal to 0.01 in artificial groundwater recharge. Practically speaking it is also concluded that the nonlinear horizontal flow model is valid provided that the transformed aspect ratio is equal to or greater than 4.0 and the ratio of the critical height of the unsaturated zone to the initial saturated thickness is equal to or less than 0.07. A correction which accounts for the combined effects of flow zone thinning and vertical flow was developed for the horizontal flow model in the case of the well flow problem. A new field equation suitable for numerical simulations, combining the above effects, has been obtained.

ACKNOWLEDGMENTS

The author is grateful to his major professor, Dr. Lynn W. Gelhar, for his guidance, encouragement and many helpful suggestions throughout the course of this research. Appreciation is also extended to graduate committee members, Dr. Gerardo W. Gross and Dr. Alan Sharples, for their assistance. Discussions with Dr. Shlomo P. Neuman of University of Arizona, Dr. G. Dagan of the Technion and suggestions and advice of Dr. U.I. Kroszynski of the Technion are very much appreciated.

Finally, the author wishes to thank his family for their patience and understanding during the course of this study.

TABLE OF CONTENTS

TABLE OF CONTENTS (continued)

TABLE OF CONTENTS (continued)

TABLE OF CONTENTS (continued)

LIST OF FIGURES

LIST OF FIGURES (continued)

LIST OF FIGURES (continued)

LIST OF FIGURES (continued)

LIST OF FIGURES (continued)

LIST OF FIGURES (continued)

LIST OF TABLES

LIST OF SYMBOLS

A	cross sectional area of flow	$[L^2]$
B	length of the aquifer	[L]
B'	dimensionless length of the aquifer (B/L)	
c	nonlinearity parameter ($c = Q/2\pi K_H D^2$)	
D	initial saturated thickness	[L]
d	saturated thickness below the drain	[L]
H	drainable depth	[L]
h	height of the phreatic surface below a datum	[L]
h_{cr}	critical height or thickness of the unsaturated zone	[L]
K	hydraulic conductivity of isotropic aquifer	$[LT^{-1}]$
K_H, K_x, K_r	horizontal hydraulic conductivity	$[LT^{-1}]$
K_v, K_z	vertical hydraulic conductivity	$[LT^{-1}]$
L	half length of the recharge basin or drain spacing	[L]
n	effective porosity of the aquifer	
$\vec{n}$	unit normal vector	
P	nonlinearity parameter ($RL^2/K_H D^2$)	
p	pressure	$[ML^{-1}T^{-2}]$
Q	discharge	$[L^3T^{-1}]$
q	specific discharge	$[LT^{-1}]$
R	recharge rate	$[LT^{-1}]$
r	radial distance from the pumping well	[L]
S	storage coefficient	
S_y	specific yield	

LIST OF SYMBOLS (continued)

s	average drawdown	[L]
s°	free surface drawdown	[L]
s_r	rise of the phreatic surface	[L]
s_e	effective saturation	
T	transmissivity of the aquifer	$[L^2T^{-1}]$
t	time	[T]
t'	dimensionless time (tK_HD/S_yL^2)	
t^*	dimensionless time (K_vt/S_yD)	
U, U_y	dimensionless time ($4Tt/r^2S_y$)	
$\vec{v}$	velocity vector of the flow	$[LT^{-1}]$
W	well function ($4\pi Ts/Q$)	
W°	free surface well function ($4\pi Ts^\circ/Q$)	
x	horizontal longitudinal coordinate	[L]
x'	dimensionless horizontal longitudinal coordinate (x/L)	
y	horizontal transverse coordinate	[L]
z	vertical coordinate	[L]
∇	del operator	
α	a parameter describing the vertical flow ($K_vh/3S_y$)	$[L^2T^{-1}]$
α	dimensionless parameter ($K_H(d + H/2)/S_y$)	
β_1	compressibility of the water	
γ	specific weight of the fluid	$[ML^{-2}T^{-2}]$
σ	storage coefficient to specific yield ratio (S/S_y)	

LIST OF SYMBOLS (continued)

η	transformed aspect ratio ($\sqrt{K_v/K_H}\,\frac{r}{D}$)	
θ	volumetric moisture content	
λ	a parameter of the soil depending on its pore size distribution	
ρ	density of the water	$[ML^{-3}]$
μ	dynamic viscosity of the water	$[ML^{-1}T^{-1}]$
ξ	transformed aspect ratio ($\sqrt{3K_v/K_H}\,\frac{r}{D}$)	
τ_a	dimensionless time ($4Tt/r^2S$)	
τ_y	dimensionless time ($4Tt/r^2S_y$)	
ϕ	piezometric head	[L]
ψ	capillary head	[L]

CHAPTER 1

INTRODUCTION

Horizontal flow models are approximate theoretical models applicable mainly to "hydraulic flows," the theory in which the flow is averaged over the depth (Muskat, 1946). This theory was originally proposed by Dupuit in 1863 and was later generalized by Forchheimer in 1886. It is based on a number of assumptions resulting from the observation that in most groundwater flows the slope of the free surface is very small, and hence the streamlines can be taken as parallel to the impervious bed. Consequently the piezometric head along any vertical line is a constant equal to the elevation of the free surface at that line. The hydraulic gradient is equal to the slope of the free surface and is independent of the depth z. This leads to the conclusion that flow is essentially horizontal and that vertical flow velocities can be neglected. The important advantages gained by employing these assumptions (Dupuit assumptions) are that the vertical coordinate z is eliminated, and the nonlinear boundary condition at the free surface can be dispensed with.

The horizontal flow model (Dupuit approximation) is among the most powerful tools for treating unconfined flows. It is the only simple tool available to most engineers and hydrologists for solving such problems (Bear, 1972).

The primary objective of this study is to determine the relative importance of some of the physical factors and effects of certain assumptions in the physical analysis of a phreatic aquifer, using the

horizontal flow model. These factors can be categorized as 1) thinning of the flow zone, 2) vertical flow and anisotropy of permeability, 3) compressibility of the aquifer, 4) seepage face, and 5) the unsaturated zone. The ultimate objective is to determine quantitatively the validity and limitations of these models from a practical standpoint. To achieve these objectives, specific quantitative criteria describing the limitations of the horizontal flow models will be developed. To improve these models relaxation of the severe limitations will also be developed whenever possible.

A systematic analysis will be made of the existing literature dealing with well flow analysis, agricultural drainage, and artificial groundwater recharge problems. In well flow analysis a reliable estimate of the aquifer parameters is necessary for the overall planning and management of water resources. Accurate prediction of the rise and fall of the water table due to added water from deep percolation is a prerequisite for optimum design of a drainage system or groundwater recharge facility. Consequently it is very important to establish quantitatively the limitations of the horizontal flow model as a tool with which to analyze these problems.

The main factors considered in the choice of these study problems were 1) the availability of literature necessary for an adequate analysis of the physical factors omitted in the horizontal flow models, and 2) the significance of the problem from a practical point of view.

All of the problems considered here have to deal with anisotropic homogeneous unconfined aquifers bounded by impervious horizontal bottoms. Though the well flow problem is restricted to fully penetrating

pumping and observation wells, it is a very basic and practical problem in hydrology. The artificial recharge problem involves a typical water recharge system for unconfined aquifer receiving uniform vertical percolation. The rate of percolation is maintained by a spreading area in the form of a long strip located above the unconfined aquifer. After the percolation rate has been applied for some time, a groundwater ridge will develop. A problem was required for which adequate literature existed. This lead to the choice of a very idealized drainage problem as a subject of study. It is limited to shallow horizontal aquifers; the drainage systems considered are restricted to fully penetrating parallel open ditches.

CHAPTER 2

Basic Equations, Literature Survey and Objectives of the Present Investigation

2.1 Introductory Remarks

This chapter is a compilation of the significant developments pertaining to groundwater flow in an unconfined aquifer. The basic mathematical equations are presented along with derivations of some of the governing partial differential equations and boundary conditions, and the assumptions underlying these equations. The objectives of the related mathematical models are considered, (based on a literature survey) and specific approaches to the solution are explained for the various models.

2.2 Basic Equations

A. Equation of Continuity

A mathematical expression for the conservation of mass principle can be developed (Bear, 1972) for any arbitrarily shaped fixed volume (see Figure 1). The mass outflow per unit time through the surface of the volume is

$$\int_A \rho(\vec{q}\cdot\vec{n})\, dA$$

where dA = differential element of the surface A enclosing the volume

$\vec{q}$ = specific discharge

$\vec{n}$ = outward pointing unit-normal vector

and ρ = density of the fluid.

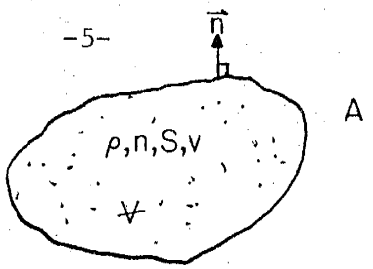

FIGURE 1. Control Volume

This must equal the rate of decrease of mass within the fixed volume,

$$-\int_v \frac{\partial}{\partial t}(\rho n S_w)\ dv$$

where n = porosity of porous medium

S_w = degree of saturation = $\frac{\text{liquid volume (water)}}{\text{void volume}}$

Thus the principle of conservation of mass becomes

$$\int_v \frac{\partial}{\partial t}(\rho n S_w)\ dv + \int_A \rho(\vec{q}\cdot\vec{n})\ dA = 0$$

Using the divergence theorem for the second term and rearranging gives

$$\int_v \{\frac{\partial}{\partial t}(\rho n S_w) + \nabla\cdot(\rho\vec{q})\}\ dv = 0$$

or

$$\frac{\partial}{\partial t}(\rho n S_w) + \nabla\cdot(\rho\vec{q}) = 0 \qquad (2.1)$$

This equation applies to any arbitrary volume. However, to develop an equation useful in describing flow in porous media we must consider a volume element sufficiently large that the irregularities of the

flow in individual pores are effectively averaged, facilitating the use of an average velocity to describe flow across the surface; it must also be small enough that its properties vary little within it.

B. Dynamic Equation

Water in a porous medium moves in response to potential differences and in the direction of decreasing potential. The steady flow of a viscous, incompressible, and chemically inactive fluid through a saturated, homogeneous, porous medium, at low Reynolds number and constant temperature, obeys Darcy's law stated in terms of Cartesian tensor notation as follows:

$$q_i = -K_{ij} \frac{\partial \phi}{\partial x_i} \tag{2.2}$$

where K_{ij} = the hydraulic conductivity tensor, i,j = 1,2,3

x_i = cartesian coordinates, i = 1,2,3.

q_i = components of the specific discharge vector, i = 1,2,3.

$\phi = p/\rho g + z$

where p = pressure

$\rho g = \gamma$, specific weight of the fluid

z = elevation above a datum.

C. Variably Saturated Model (Exact)

From equation (2.1) we obtain

$$-(\rho \nabla \cdot \vec{q} + \vec{q} \cdot \nabla \rho) = \frac{\partial \rho n S_w}{\partial t} \tag{2.3}$$

Assuming that the spatial variation of fluid density with pressure change

is small enough that $\nabla\cdot(\rho\vec{q})\approx\rho\nabla\cdot\vec{q}$, and that the wetting fluid (water of this study) is incompressible, equation (2.3) can be written as

$$\rho\,\frac{\partial\theta}{\partial t} = -\rho\nabla\cdot\vec{q} \tag{2.4}$$

where $\theta = nS_w$ is the volumetric moisture content. Substitution of equation (2.2) into this equation gives the Richards equation (Richards, 1931),

$$\frac{\partial\theta}{\partial t} = \frac{\partial}{\partial x_i}\left(K_{ij}\,\frac{\partial\phi}{\partial x_j}\right) \tag{2.5}$$

This equation with the necessary initial and boundary conditions, specifies flow in saturated and unsaturated porous medium, when the flowing fluid and medium are both incompressible.

D. Potential Theory (Laplace Equation)

If contribution to flow from the unsaturated zone of the porous medium is neglected and only flow below the water table (where all the pores are regarded as filled with water) is considered, equation (2.1) may be written as

$$-\nabla\cdot\rho\vec{q} = \frac{\partial n\rho}{\partial t} \tag{2.6}$$

If the matrix, as well as the water, is compressible, the density of the water will be a variable ($d\rho = \beta_1\rho_0\,dp$); also the porosity of the medium and the vertical dimension of the elemental volume are variables (assuming that the changes of the lateral dimensions are negligible). Using the above assumptions and equations (2.6) and (2.2) Cooper, 1966, has shown that

$$\frac{\partial}{\partial x_i}\left(K_{ij}\frac{\partial \phi}{\partial x_j}\right) = S_s \frac{\partial \phi}{\partial t} \tag{2.7}$$

where $S_s = \rho g(n\beta_1 + \alpha)$ is specific storage; ρ_0 is a reference water density (constant); β_1 and α are the compressibility of water and matrix respectively.

If we consider two-dimensional flow of a constant density fluid in a homogeneous, incompressible medium, the equation can be written as

$$K_x \frac{\partial^2 \phi}{\partial x^2} + K_z \frac{\partial^2 \phi}{\partial z^2} = 0 \tag{2.7a}$$

where K_x and K_z are hydraulic conductivities in x and z directions, which are principal axes of the conductivity tensor.

FREE SURFACE BOUNDARY CONDITION

If we neglect capillary fringe, a free surface may be defined as the uppermost line of saturation. Hydrodynamically it represents a line of atmospheric pressure. The shape of the free surface is generally unknown in the problem as formulated according to the potential theory. It can be determined in conjunction with the governing partial differential equation derived above. An unsteady free surface with accretion is a surface on which the pressure is maintained constant ($p = 0$). A formulation of this free surface for the two-dimensional case is presented below.

The piezometric head has been defined as

$$\phi = p/\rho g + z$$

Rearranging results in

$$p = \rho g(\phi - z) \tag{2.8}$$

Since the pressure is uniform over the free surface, we have

$$Dp/Dt = 0 \tag{2.9}$$

where the total or substantial derivative Dp/Dt is expressed as (Bear, 1972, p. 72)

$$\frac{\partial p}{\partial t} + \vec{v}\cdot\nabla p = 0 \tag{2.10}$$

Physically, the velocity of propagation of the moving free surface $\vec{v}$ may be related to the vectorial sum of seepage velocity $\vec{q}/n$ and recharge velocity $\vec{R}/n$ (Bear, 1972, p. 258)

$$\vec{n}\cdot\vec{v} = \vec{n}\cdot(\vec{q}-\vec{R})/n \tag{2.11}$$

Considering vertical accretion with $\vec{R} = -\hat{k}R$ where $\hat{k}$ is a unit vector in the vertical direction, and substituting equations (2.8) and (2.11), into (2.10), the two-dimensional form of the phreatic surface condition becomes

$$S_y \frac{\partial\phi}{\partial t} - [K_x (\partial\phi/\partial x)^2 + K_z (\partial\phi/\partial z)^2 - \frac{\partial\phi}{\partial z}(K_z + R) + R] = 0 \tag{2.12}$$

where $n \cong S_y$, the specific yield.

If $R = 0$ this leads to

$$S_y \frac{\partial\phi}{\partial t} - [K_x(\partial\phi/\partial x)^2 + K_z (\partial\phi/\partial z)^2 - K_z \frac{\partial\phi}{\partial z}] = 0 \tag{2.13}$$

These are the required two-dimensional, non-linear, dynamic boundary conditions which must be satisfied at the free surface; equations (2.12) and (2.13) apply beneath and outside the recharge basin, respectively.

E. Approximate Theory (Horizontal Flow Model)

Determination of the location of free surface is one of the objectives of the solution of gravity flow problems. The nonlinearity of this boundary condition, together with the fact that the location of the boundary is unknown, makes an exact analytical solution of the flow problem practically impossible. This is the reason for the development of approximate methods in which the flow is averaged over the depth of the aquifer. The theory was originally proposed by Dupuit (1863), and it stems from two assumptions.

i) For small inclinations of the free surface of a gravity flow system, the streamlines can be taken as parallel to the impervious bed. Consequently the piezometric head along any vertical line is a constant equal to the elevation of the free surface at that location.

ii) The hydraulic gradient is equal to the slope of the free surface and is invariant with depth; this establishes that the flow is essentially horizontal, or that we have a hydrostatic pressure distribution. The advantages of these assumptions are (1) the non-linear boundary condition at the free surface can be dispensed with, and (2) the potential $\phi(x,y,z,t)$ at an arbitrary point $P(x,y,z)$ of the flow domain may be replaced by the corresponding elevation $h(x,y,t)$ of the free surface, leaving only one unknown h and eliminating the

vertical coordinate z.

With these assumptions, the nonlinear equation describing unsteady two-dimensional flow in a saturated unconfined aquifer bounded by an impervious horizontal bottom can be derived from the continuity equation and Darcy's law; this has been done by several authors, including Boussinesq(1904), Baumann (1965), and Bear, Zaslavsky and Irmay (1968).

Using equation (2.2) in equation (2.7),

$$-\frac{\partial}{\partial x_i} q_i = S_s \frac{\partial \phi}{\partial t} \tag{2.14}$$

Integrating each term in equation (2.14) over the depth of flow h (Hantush, 1964) gives in the (x,y,z) cartesian coordinates,

$$-\left[\int_0^h \left(\frac{\partial q_x}{\partial x} + \frac{\partial q_y}{\partial y} + \frac{\partial q_z}{\partial z}\right) dz\right] = S_s \int_0^h \frac{\partial \phi}{\partial t}\, dz \tag{2.15}$$

or

$$-\left[\frac{\partial}{\partial x}\int_0^h q_x dz - q_x\Big|_{z=h} \frac{\partial h}{\partial x} + \frac{\partial}{\partial y}\int_0^h q_y dz - q_y\Big|_{z=h} \frac{\partial h}{\partial y} + q_z\Big|_{z=h} - q_z\Big|_{z=0}\right]$$

$$= S_s\left[\frac{\partial}{\partial t}\int_0^h \phi dz - \phi\Big|_{z=h} \frac{\partial h}{\partial t}\right] \tag{2.16}$$

The kinematic boundary conditions at the free surface (z=h(x,y,t)) can be written as (Lamb, 1945)

$$S_y \frac{\partial h}{\partial t} + q_x \frac{\partial h}{\partial x} + q_y \frac{\partial h}{\partial y} - q_z - R = 0 \tag{2.17}$$

and $q_z\big|_{z=0} = 0$ (impervious horizontal boundary condition)

Substituting (2.17) into (2.16) gives

$$-\left[\frac{\partial}{\partial x}\int_0^h q_x dz + \frac{\partial}{\partial y}\int_0^h q_y dz + S_y\frac{\partial h}{\partial t} - R\right] = S_s\left[\frac{\partial}{\partial t}\int_0^h \phi dz - \phi\Big|_{z=h}\frac{\partial h}{\partial t}\right] \tag{2.18}$$

Integration of Darcy's equation results in

$$\int_0^h q_x dz = -K_x\int_0^h \frac{\partial \phi}{\partial x}\,dz = -K_x\left[\frac{\partial}{\partial x}\int_0^h \phi dz - \phi\Big|_{z=h}\frac{\partial h}{\partial x}\right] \tag{2.19}$$

where $$\bar{\phi} = \frac{1}{h}\int_0^h \phi(x,y,z,t)dz \tag{2.20}$$

and $$\phi = h(x,y,t) \text{ at } z=h. \tag{2.21}$$

Combining equations (2.18), (2.19), (2.20), and (2.21) leads to

$$K_x\frac{\partial^2}{\partial x^2}(h\bar{\phi} - h^2/2) + K_y\frac{\partial^2}{\partial y^2}(h\bar{\phi} - h^2/2) + R = S_s\frac{\partial}{\partial t}(\bar{\phi}h - h^2/2) + S_y\frac{\partial h}{\partial t} \tag{2.22}$$

Now neglecting the variation of piezometric head over the depth of flow h by assuming $\bar{\phi} \approx h$ or $\partial\bar{\phi}/\partial x = \partial h/\partial x$ results in

$$K_x\frac{\partial}{\partial x}\left(h\frac{\partial h}{\partial x}\right) + K_y\frac{\partial}{\partial y}\left(h\frac{\partial h}{\partial y}\right) + R = S_s h\frac{\partial h}{\partial t} + S_y\frac{\partial h}{\partial t} \tag{2.23}$$

The only assumption used in the above derivation is that $\partial\bar{\phi}/\partial x \approx \partial h/\partial x$, i.e., the pressure is hydrostatic in the flow domain.

Equation (2.23) is a nonlinear second order partial differential equation (called the Boussinesq equation); with the proper boundary and

initial condition, it will be referred to as the horizontal flow model.

2.3 Literature Survey

This section covers the past research and major developments in well hydraulics, agricultural drainage, and artificial recharge.

A. Well Flow Hydraulics

HORIZONTAL FLOW MODEL

Thiem (1906) was probably first to present an analytical solution to the Dupuit equation for steady state flow in confined and unconfined aquifers; his solution is known as the equilibrium formula. In 1935 Theis solved the problem of unsteady state flow in a confined aquifer by analogy to heat conduction in solids. Jacob (1940) verified this solution directly from hydraulic concepts; he also used Theis' (1935) mathematical model to analyze unconfined aquifers and developed an approximation (the Jacob correction) (Jacob, 1963) for thinning of the flow zone.

Boulton (1963) introduced the concept of delayed yield for unconfined aquifers; he assumed that the total storage is the sum of an instantaneous storage coefficient $S = S_s D$ (aquifer compressibility) and gravitational drainage coefficient, S_y (responding with an exponential time delay). In his solution, drawdown is governed by the instantaneous storage coefficient at short times and by the gravitational drainage coefficient (specific yield) at long times. This concept has been criticized (Neuman, 1972) on the grounds that the delay index lacks a firm physical basis.

Using numerical methods Kriz et al. (1966) solved the nonlinear horizontal flow equation, for a well fully penetrating an unconfined aquifer. Dagan (1966) obtained an analytical solution for the same boundary and initial value problem using a perturbation expansion in series of a small parameter, effectively linearizing the nonlinear horizontal flow equation.

POTENTIAL FLOW MODEL (VERTICAL FLOW)

Boulton (1951, 1954) assumed that when pumping starts, the flow in the neighborhood of the well is vertical. This gives rise to his linearized vertical flow model (1954) which he solves analytically. Type curves were developed by Boulton and Stallman (1961) for drawdown at the free surface. Dagan (1967a) extended Boulton's model to account for partial penetration.

Neuman (1972, 1974) generalized Dagan's (1967a) solution by incorporating the compressibility of the unconfined aquifer into the flow equation. His results are similar to those of Boulton (1963), i.e. the compressibility of the aquifer initially dominates drawdown and specific yield becomes important at large time, but his solution has no artificial coefficients and depends only on the compressibility and specific yield of the aquifer.

VARIABLY SATURATED FLOW MODEL (EXACT THEORY)

The above models account only for flow in the saturated portion of the aquifer, though an unsaturated region draining to the water table also exists. Taylor and Luthin (1969) solved the variably saturated

model numerically; Brutsaert, et al. (1971) and Cooley (1971) used fully implicit finite difference methods to solve the problem. Neuman (1972) developed numerical solutions using the finite element method.

B. Agricultural Drainage and Artificial Groundwater Recharge

HORIZONTAL FLOW MODEL

Boussinesq (1904) was the first to find an exact solution for the nonlinear horizontal flow model; he used the separation of variables method, and the similarity transformation method for certain boundary conditions. Irmay (1966), using appropriate transformations, extended the above technique and found a solution to the nonhomogeneous equation by introducing additional assumptions. Polubarinova-Kochina (1952) used the Boltzman transformation to solve the problem of seepage by variable water level in reservoirs.

Karadi, et al. (1968), Yeh (1970), Hornberger (1970) and Verma (1969) solved the nonlinear horizontal flow equation by numerical techniques, for one- and two-dimensional flow situations. Glover (1965), Bower (1965), Van Schilfgaarde (1965), and De Wiest (1965) showed the limitations and validity of the Dupuit-Forchheimer equations by comparing their results to experimental and field results. Problems of ground water recharge were analytically solved by Polubarinova-Kochina (1962), Glover (1961), Bittinger and Trelease (1960) and Baumann (1965), using the linearized horizontal flow equation in h. An example of the second linearization (linear in h^2) is given by Hantush (1967) and Marino (1967); their solutions extend the validity

of the corresponding solutions to the linear equation in h for one- and two-dimensional cases of growth and decay of groundwater mounds in aquifers of infinite extent. Terzidis (1968) used both explicit and implicit finite difference techniques to solve the one-dimensional nonlinear equation numerically. Bibby and Sunada (1971) used an implicit finite difference scheme to solve the transient two-dimensional nonlinear equation (as related to a leaky aquifer).

POTENTIAL FLOW MODEL (VERTICAL FLOW)

Davidson (1936) was probably the first to present an analytical solution of Laplace equation with a nonlinear free surface boundary condition. He used the complex potentials to solve the problem of steady two-dimensional flow through a dam of rectangular cross section. Bazanov (1938) (see Bear, et al., 1968) used the hodograph technique to solve the steady state problem of drainage of an infinite aquifer toward a curved drainage ditch. Muskat (1946) employed the hodograph technique for steady state seepage of water through a dam with vertical faces; he computed the quantity of seepage as well as the pressure distribution under the base of the dam. Polubarinova-Kochina (1962) applied the technique used by Davidson to an unsteady free surface, using Zhukovsky's mapping function for the nonlinear free surface boundary condition. The resulting expression was linearized and an estimate of accuracy of the solution was obtained by successive approximations.

Dagan (1964, 1966, and 1967) presented solutions to several free surface ground water flow problems. He used a perturbation

technique which effectively linearizes the free surface boundary condition. Kirkham (1950, 1964, and 1966) has presented solutions, for both flow toward a ditch and axisymmetric flow toward a well, in which separation of variables and Fourier series methods are applied.

De Wiest (1969) solved the problem of damping of the unsteady free surface flow through a dam by the method of power series expansion of unsteady potential (a time dependent perturbation of the final steady state flow). There was good agreement between his results and those from experiments on a Hele-Shaw model.

Hunt (1970) extended Dagan's linearization above to the two-dimensional case for aquifers of finite and infinite depth.

Murray(1970) corrected the flaw in Kirkham's analysis (1964) and extended it to include the seepage face.

Gelhar (1974) used the stochastic approach to solve the Laplacian aquifer for a partially penetrating stream. Kirkham and Gaskel (1951) used the relaxation technique to solve the problem of water table recession in tile drained land, but the method required considerable computation. Later Isherwood (1959) refined the technique and obtained a relatively rapid convergence. Jeppson (1968) solved the problem of seepage from ditches using a finite difference scheme in the complex potential plane, where the position of the free surface is known. Verma and Brutsaert (1971) used the successive over relaxation technique to solve for the fall of unsteady free surface groundwater seepage.

Amar (1973) solved the nonlinear boundary value problem of artificial groundwater recharge using the accelerated Liebman relaxation method. Also, Singh (1972) solved the nonlinear problem for recharge

from a long strip and for a circular pond.

VARIABLY SATURATED MODEL (EXACT THEORY)

In 1931 Richards derived an equation of flow in unsaturated porous media by combining Darcy's law and the continuity equation; a detailed account of the physics of the capillary flow phenomena has been given by Klute (1952), Miller and Miller (1956) and by Swartzendruber (1966). Rubin (1968), Taylor and Luthin (1969), and Verma and Brutseart (1970) solved the Richards equation numerically for the problem of flow in stream connected aquifer.

2.4 Objectives of the Present Investigation--Specific Approach

As indicated by the literature survey, a considerable amount of work has been done on the subject of groundwater flow in phreatic aquifers; a large amount of literature on this subject is continually appearing. However, practicing hydrologists still prefer to use simple models which are easy to use and cheap to operate; due to the numerous assumptions used to reach an analytical solution, these models are not an exact description of the physical systems in consideration.

It is therefore of theoretical and practical interest to attempt an analysis of the problems in question, to substantially increase the accuracy and generality of the conclusions reached and to provide a better understanding of the dynamics of flow in phreatic aquifers. Accordingly, it is an objective of the present research to direct attention toward an evaluation and correlation of the various existing solutions of the different models in order to establish quantitatively the validity and limitations of the horizontal flow model.

Three general categories of models will be considered. One is based on the Dupuit assumption of hydrostatic pressure distribution, and is known as the horizontal flow model; another is based on potential flow and emphasizes vertical flow, and the third is the exact theory or the so-called variably saturated model. A systematic analysis of the existing solutions will be undertaken, to separate and investigate the significance of the physical factors omitted in the horizontal model. More specifically, in the well flow problem, a correlation of the nonlinear and the linearized horizontal flow models will be used to separate the effects of the flow zone thinning. A comparison between the linearized vertical flow model and the linearized horizontal flow model will be used to analyze the vertical flow effects and the anisotropy of permeability. A correlation of the linearized vertical flow model and the variably saturated model for small drawdown will be used to analyze contributions of the unsaturated zone. The same procedure will be followed in examining the other physical factors omitted in the horizontal flow model. It will also be followed in the examination of artificial recharge and drainage problems. An over-all comparison of the variably saturated model and the horizontal flow model will be made to establish the latter's validity. Existing solutions both analytical and numerical, will be utilized in this investigation; new numerical results will be obtained using the computer programs of the numerical solutions.

Specific quantitative criteria will be obtained to establish the limitations of the horizontal flow model. Relaxation of the limitations

to improve the horizontal flow model will be found by deriving simple corrections whenever possible.

CHAPTER 3.

Theoretical Models for Unconfined Flow to a Well

3.1 Introduction

The investigation and analysis of the theoretical models will be based upon an idealized flow situation which approximates actual field situations. A simplified physical model of an unconfined aquifer with a cross-section as shown in figure 2 was selected for the well flow problem. An evaluation of the different theoretical models for radial flow to a fully penetrating pumping well in a phreatic aquifer will be developed to provide a better understanding of the hydrodynamics of flow in these aquifers.

Three general categories of mathematical models are considered (see table 1)

(i) Horizontal flow model based on the Dupuit assumption of nearly horizontal flow.

(ii) Potential flow model which emphasizes vertical flow,

(iii) Exact theoretical model based on a variably saturated medium.

The solutions developed here and by previous investigators, corresponding to the various theoretical formulations, will be compared and analyzed to establish or recommend an over-all model which will satisfy the objectives sought in well flow problems.

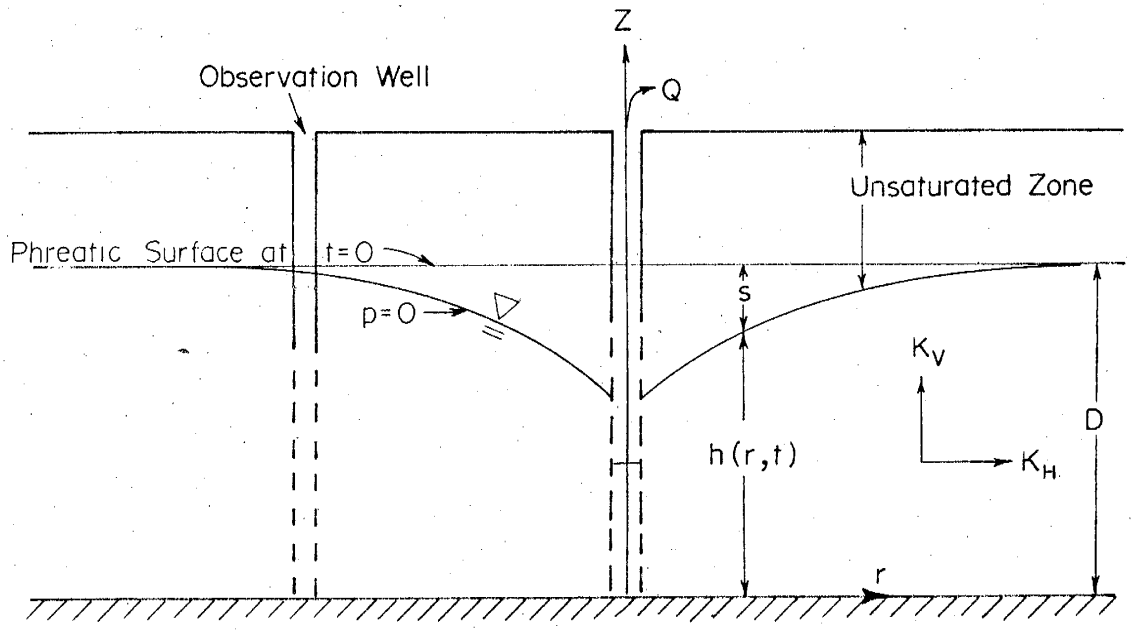

Figure 2. Schematic diagram of an unconfined aquifer

Table 1 Models and their limitations considered in the well flow problem; $h = h(r,t)$ is the height of the phreatic surface above a datum and D is the initial saturated thickness.

Theoretical Model		Assumptions				Author
		Vertical flow	Flow zone thinning ($h \neq$ constant)	Unsaturated Zone	Elastic Storage	
Horizontal Flow Model	linear in h	no	no	no	no	Theis(1935)
					yes	Boulton(1963)
	linear in h^2	no	yes ($h \approx D$ in storage term)	no	no	Jacob(1963)
	nonlinear	no	yes	no	no	Kriz,et al. (1966)
Potential Flow Model	linearized free surface	yes	no	no	no	Boulton(1954) Dagan(1967a)
					yes	Neuman(1972)
	nonlinear free surface	yes	yes	no	yes	no solution available
Variably Saturated Flow Model	linearized model	yes	no	yes	no	Kroszynski & Dagan(1974)
	nonlinear model	yes	yes	yes	no	Kroszynski & Dagan(1974)
					yes	Neuman & Feddes(1974)
Improved Horizontal Flow Model	linear in h	yes	no	no	yes	Streltsova (1972)
	linear in h^2	yes	yes ($h \approx D$ in storage term)	no	yes	Present Research

3.2 Horizontal Flow Models

A. Linearized Model in h

Equation (2.23) (Boussinesq equation) is the basic partial differential equation in the development of the mathematical models for horizontal flow. With no accretion, this equation can be written in axisymmetric cylindrical coordinates as

$$K_r \frac{1}{r} \frac{\partial}{\partial r} \left(rh \frac{\partial h}{\partial r}\right) = S_s h \frac{\partial h}{\partial t} + S_y \frac{\partial h}{\partial t} \tag{3.1}$$

If we assume $S_y >> S_s h$, (3.1) becomes

$$K_r \frac{1}{r} \frac{\partial}{\partial r}\left(rh \frac{\partial h}{\partial r}\right) = S_y \frac{\partial h}{\partial t} \tag{3.2}$$

This is nonlinear in h, and no general analytical solution is available. However, the linearized version of this equation can be obtained by replacing h with D-s where s is the drawdown and assuming $s << D$. This gives

$$\frac{1}{r} \frac{\partial}{\partial r}\left(r \frac{\partial s}{\partial r}\right) = \frac{S_y}{K_r D} \frac{\partial s}{\partial t} \tag{3.3}$$

Theis (1935) solved the above equation subject to the following boundary and initial conditions:

$$s(r, t=0) = 0$$

$$\lim_{r \to \infty} s(r,t) = 0$$

$$\lim_{r \to 0} r \frac{\partial s}{\partial r} = \frac{-Q}{2\pi K_r D}$$

The solution to equations (3.3) and (3.4) is given by

$$s = \frac{Q}{4\pi T} \int_u^\infty e^{-u} \frac{du}{u} = \frac{Q}{4\pi T} W(u) \tag{3.5}$$

where $T = K_r D$ is the transmissivity,

$$u = r^2 S_y / 4Tt$$

and $$W(u) = \int_u^\infty \frac{e^{-u}}{u} \, du$$

($W(u)$ is usually called the well function for confined aquifers, or the Theis well function after C. V. Theis who developed equation (3.5) in 1935.) Equation (3.5) is shown in figure 3.

B. Linearized Model in h^2

If h is replaced by D-s in equation (3.2) we get

$$\frac{1}{r} \frac{\partial}{\partial r}[rD \frac{\partial}{\partial r} (s - s^2/2D)] = \frac{S_y}{K(1 - s/D)} \frac{\partial}{\partial t} (s - s^2/2D) \tag{3.6}$$

Denoting the corrected drawdown s' as

$$s' = s - s^2/2D \tag{3.7}$$

equation (3.6) can be written

$$\frac{1}{r} \frac{\partial}{\partial r} (r \frac{\partial s'}{\partial r}) = \frac{S_y}{KD(1 - s/D)} \frac{\partial s'}{\partial t} \tag{3.8}$$

This can be linearized by taking $(1 - s/D) \approx 1$ or assuming that $s \ll D$ (only in the storage term) to get

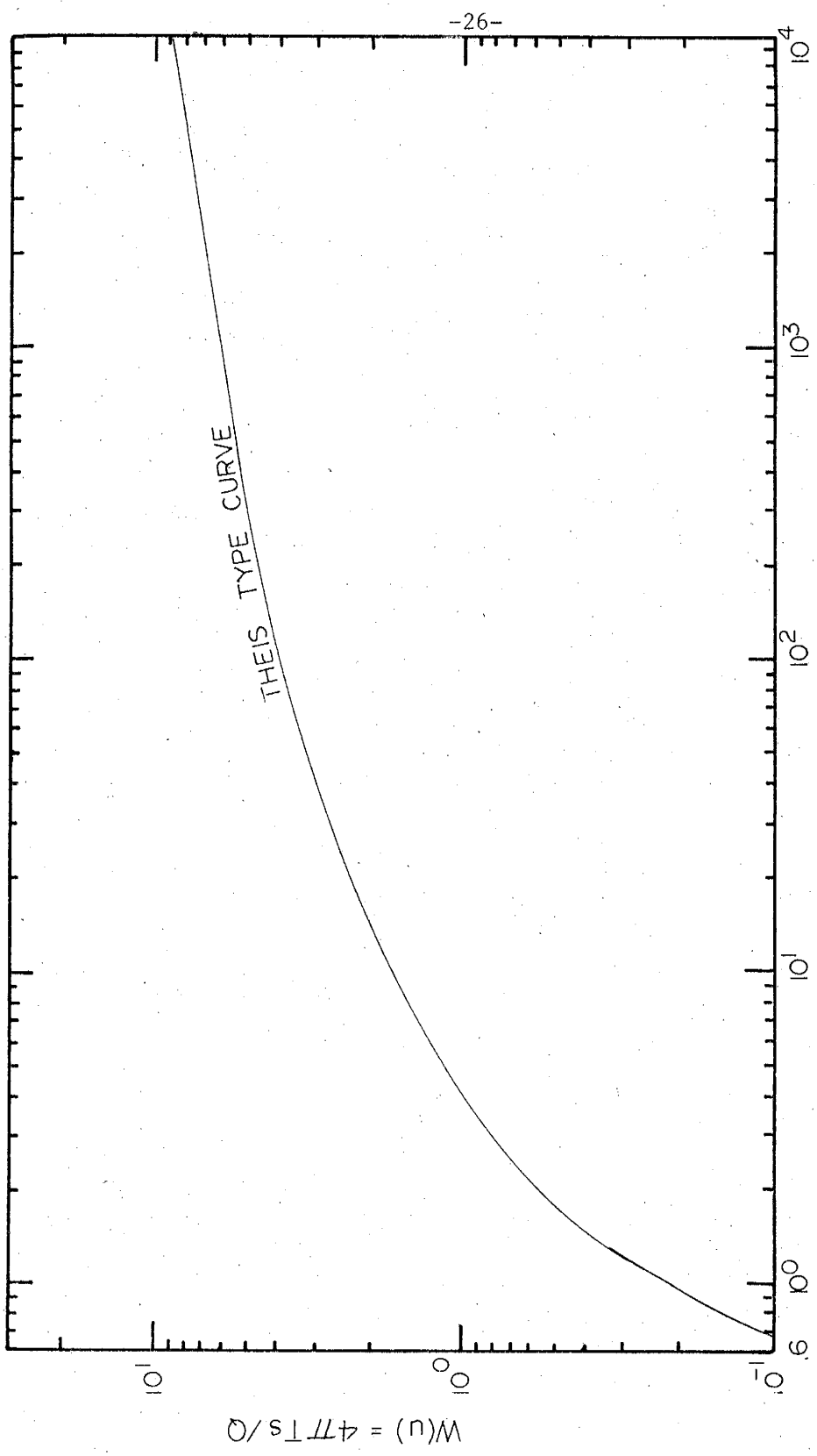

Figure 3. Theoretical curve corresponding to Theis (1935) solution

$$\frac{1}{r}\frac{\partial}{\partial r}\left(r\frac{\partial s'}{\partial r}\right) = \frac{S_y}{T}\frac{\partial s'}{\partial t} \tag{3.9}$$

Equation (3.9) is subject to the following boundary and initial conditions:

$$s'(r,t=0) = 0$$

$$\lim_{r\to\infty} s'(r,t) = 0 \tag{3.10}$$

$$\lim_{r\to 0} r\frac{\partial s'}{\partial r} = -Q/2\pi T$$

This is analogous to the problem mentioned earlier solved by Theis (equation 3.5); thus the solution is

$$s' = s - s^2/2D = (Q/4\pi T)\, W(u) \tag{3.11}$$

or
$$4\pi Ts/Q = \frac{4\pi KD^2}{Q}\left[1 - (1 - W(u)c)^{1/2}\right] \tag{3.12}$$

where $c = Q/2\pi KD^2$

With the aid of equation (3.12) and tabulated values of the Theis solution for W(u), we can easily develop the corresponding type curves for the linear horizontal model in h^2 for different values of the parameter c.

Figure 4 shows a graphical representation and comparison of this model (equation (3.12)) with the linear horizontal model in h (Theis solution).

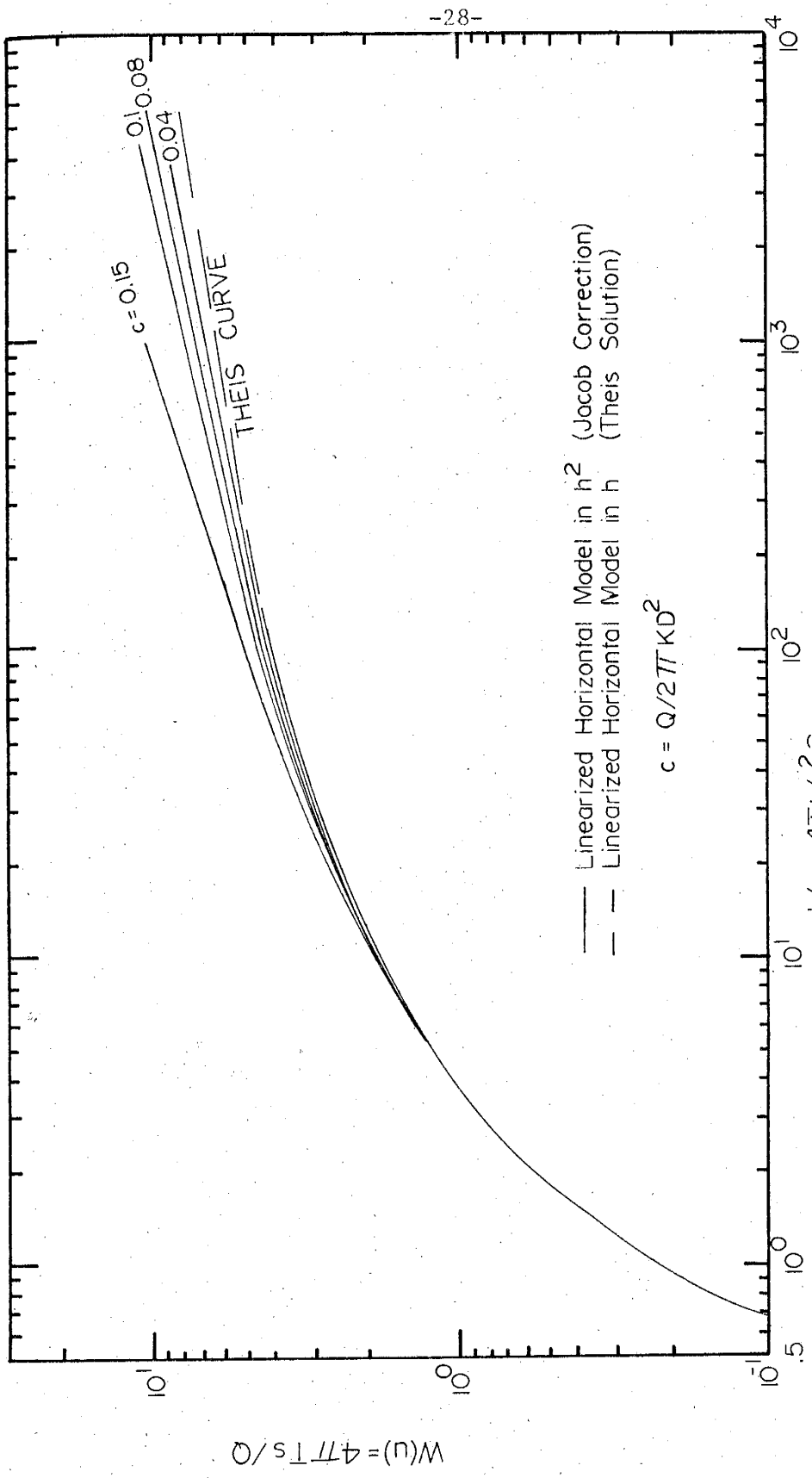

Figure 4. Comparison between linearized horizontal model in h (Theis, 1935) and the linearized horizontal model in h^2 (Jacob, 1963) for different values of c

C. Nonlinear Model

Kriz, et al. (1966) solved the nonlinear Boussinesq equation (equation (3.2)) numerically in the form

$$\frac{d^2\omega}{d\xi^2} + \left(\frac{1}{\xi} + \frac{1}{\sqrt{\omega}}\right) \frac{d\omega}{d\xi} = 0 \qquad (3.13)$$

where $\omega = (h/D)^2$, $\xi = (r^2 S_y)/(4Tt)$.

They used a generalization of Runge Kutta formulas; the results of the solution are shown in figure 5.

3.3 Correlation of Horizontal Flow Models

The horizontal flow models have been derived using the Dupuit assumption of hydrostatic pressure distribution along any vertical in the flow domain. They are used in practice to find aquifer parameters, the coefficients of storage and transmissivity. These factors, along with a long range forecast of drawdown, are the ones to be considered when we evaluate the models.

Figure 6 shows a comparison between the nonlinear model and linear horizontal flow models in h and h^2. Qualitatively, the linear model in h differs significantly from the other two models for large time, whereas at small time they all merge to one type curve. However, for all practical purposes there is hardly any difference between the nonlinear model and the linear model in h^2.

Quantitatively, figure 7 shows that for all practical values of the parameter $c = Q/2\pi KD^2$ in the range of $1/u \leq 2 \times 10^2$, the difference between dimensionless drawdown predicted by the linear horizontal model in h and the nonlinear model is $\leq 10\%$. But for $1/u \geq 2 \times 10^2$

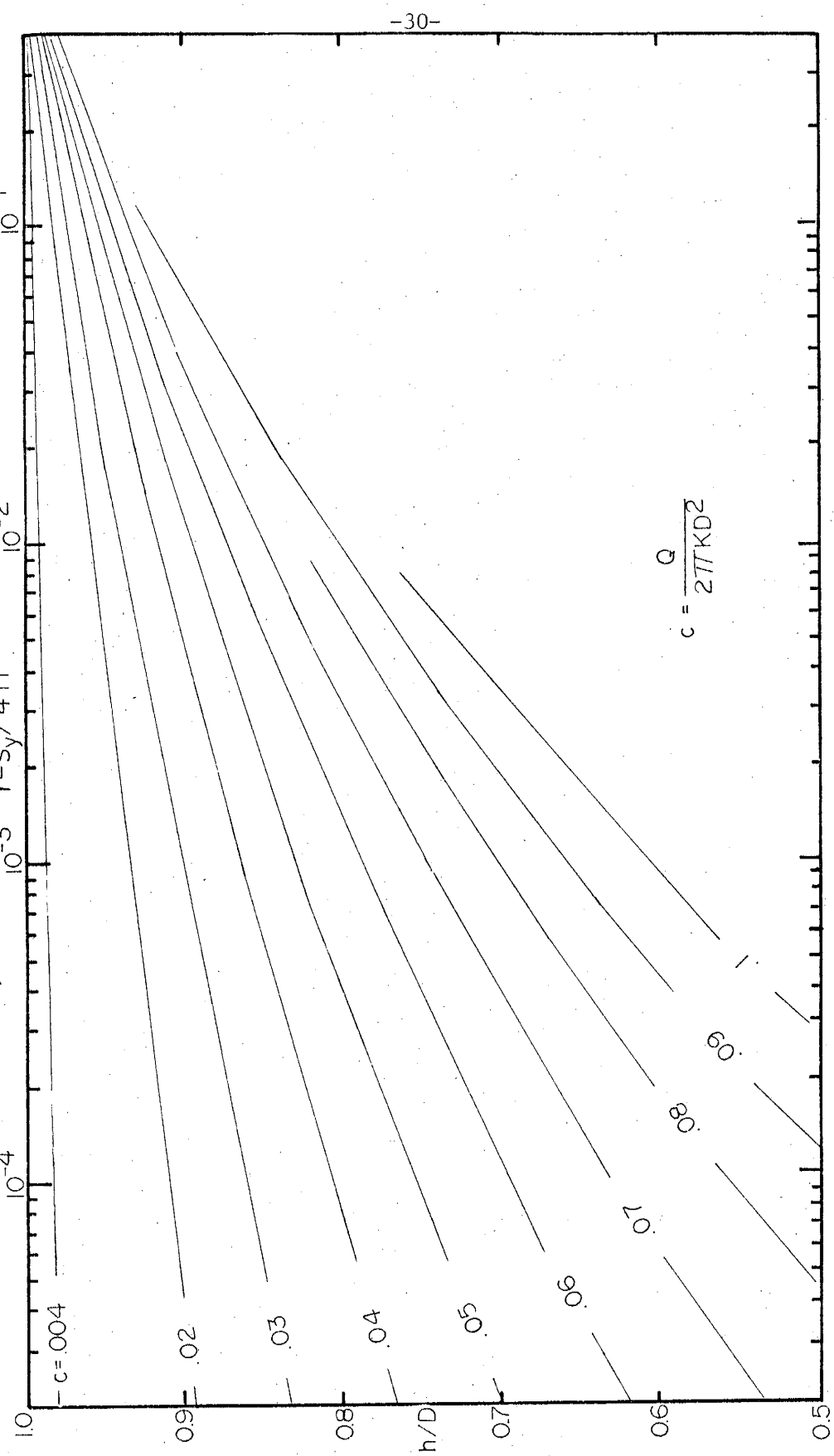

Figure 5. Type curves for nonlinear horizontal model (Kriz, et al., 1966)

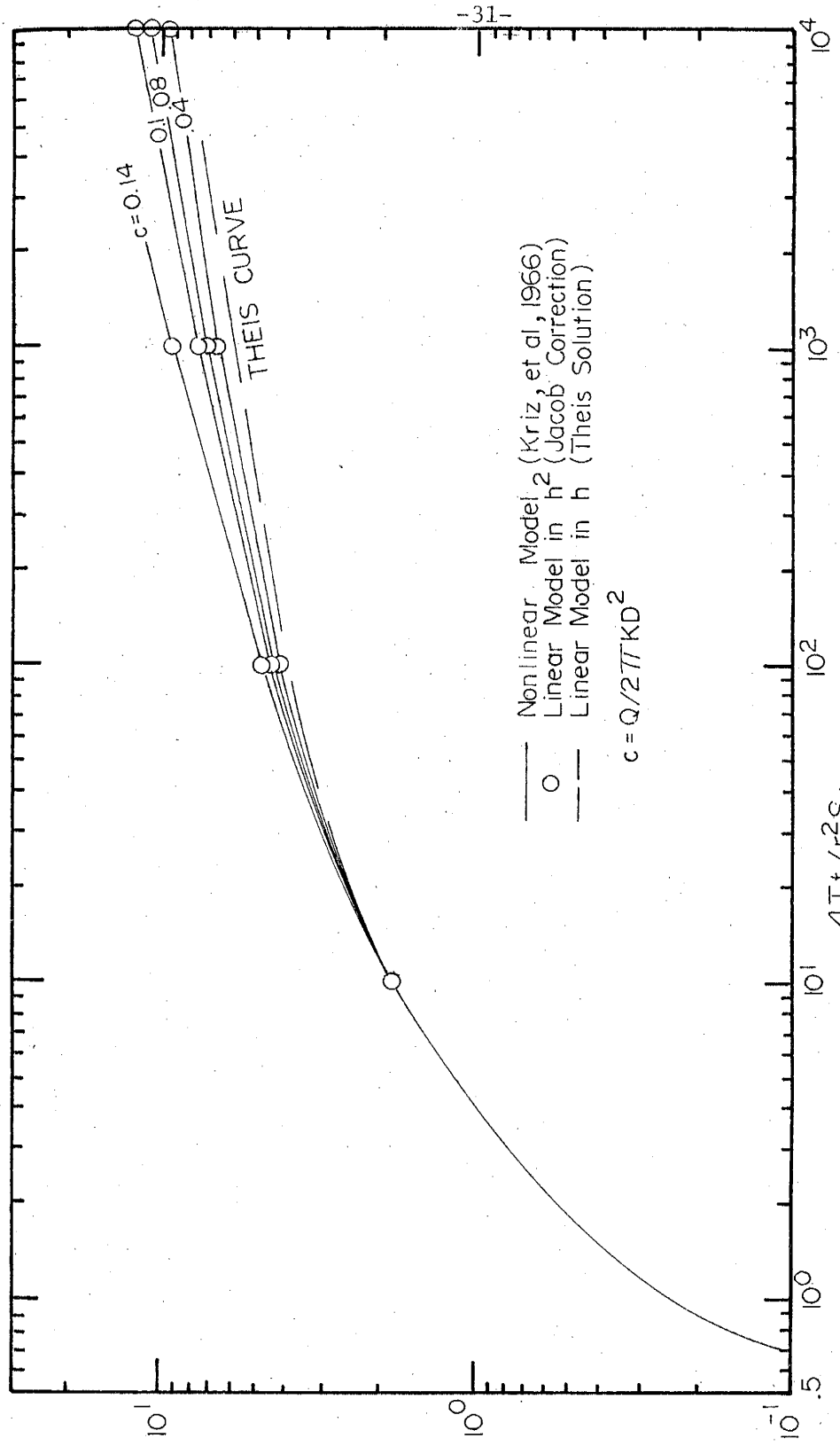

Figure 6. Comparison between the nonlinear horizontal model and the linearized horizontal models in h^2 (Jacob, 1963) and h(Theis, 1935)

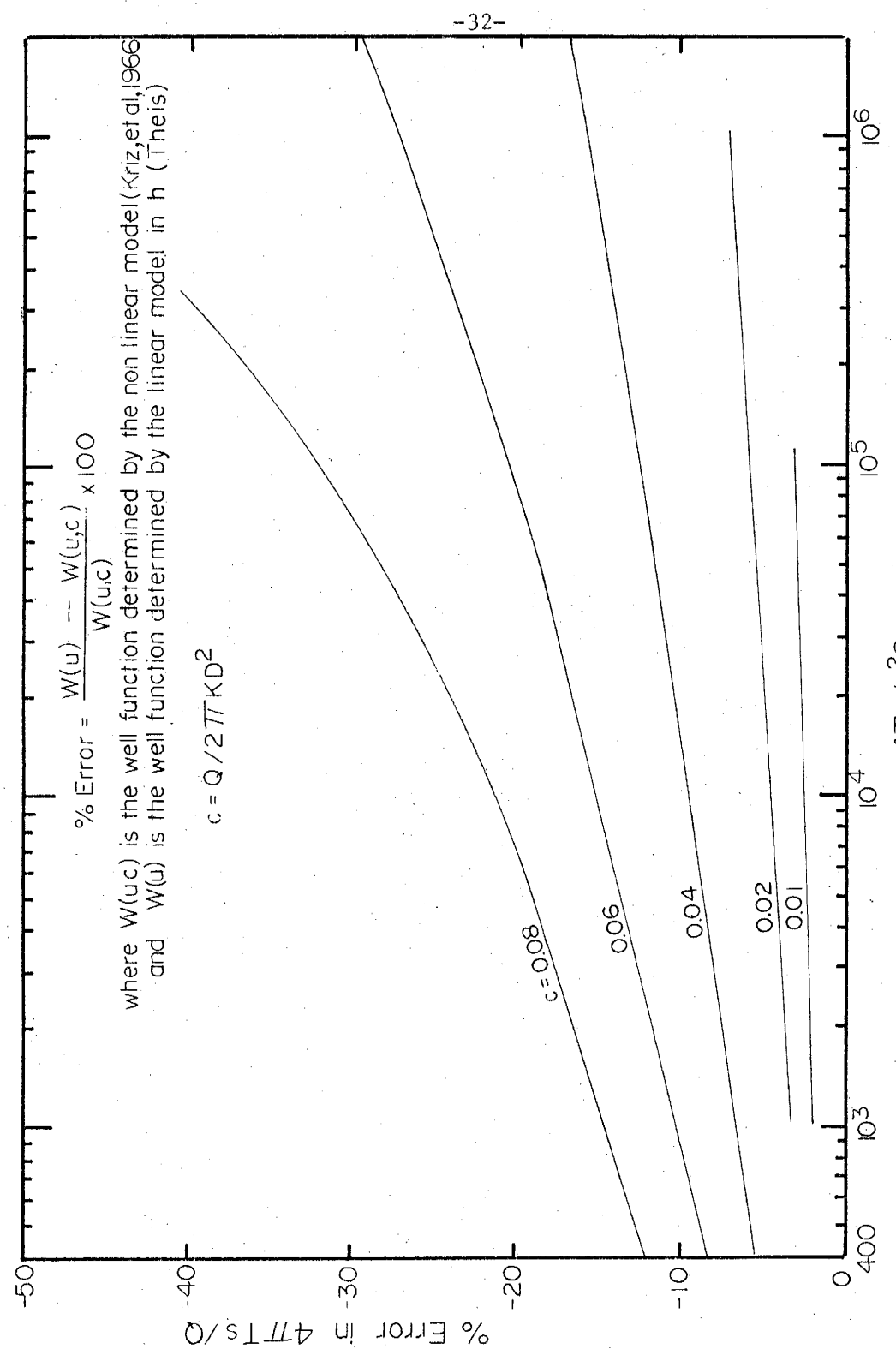

Figure 7. Relative error due to the linearization of the horizontal flow model

the difference depends on the value of the parameter c. For instance, in an aquifer with c = 0.08 (D = 50 feet, K = 1000 gallons per day per foot^2, and Q = 870 gallons per minute) we find that at $1/u = 10^5$ there is about a 32% difference in dimensionless drawdown between the nonlinear model and the linear model in h (Theis solution). The higher the value of c, the larger the difference.

Figure 8 shows another way of analyzing the difference between the type curves, using the ratio of drawdown to total saturated thickness determined by the nonlinear horizontal model. For s/D = 0.2, there is a 10% difference which increases linearly to about 40% for s/D = 0.8; thus the error introduced in the Theis solution by the linearization of the horizontal model is mainly a function of the ratio of drawdown to the initial saturated thickness s/D regardless of what the value of the parameter c is.

Analysis of the well functions in figure 7 shows a good agreement between the linear model in h^2 and the nonlinear model for all values of 1/u. It is expected from theory that this will be the case, since the discharge boundary conditions are essentially the same. The flux terms of both equations (3.2) and (3.9) are also the same. The difference existing between the two models is in the storage term, where the coefficient for the linear model in h^2 is $DS_y/(D-s)$; this was linearized assuming $D \approx D-s$, to permit finding an analytical solution for equation (3.8). This difference between the solutions of the models is very small for all practical purposes. For instance, for c = 0.08 and $1/u = 10^5$, there is only a 1.0% difference (the linear model in h^2 shows higher drawdown than the nonlinear model).

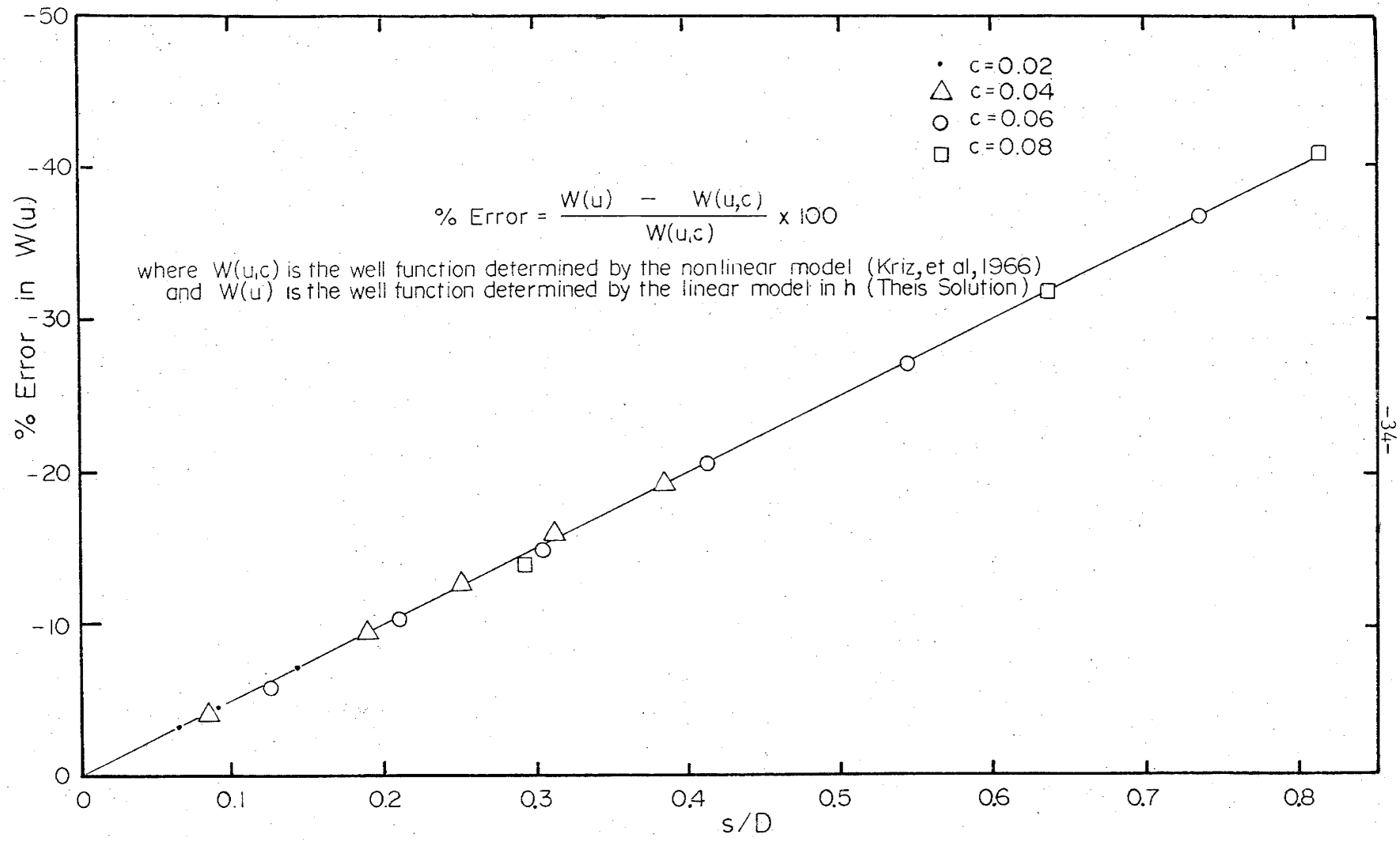

Figure 8. Relative error in W(u) as a function of dimensionless drawdown (s/D)

To conclude the discussion of the horizontal flow models, we note that the dimensionless drawdown predicted by the linear horizontal model in h^2 (Jacob correction) is practically identical to that of the nonlinear model, even for large time and large drawdowns. This proves that it is a good approximation for the nonlinear horizontal model, which is an exact interpretation of the Dupuit assumptions. However, this still does not represent precisely the physical problem under consideration.

3.4 Potential Flow Model (Vertical Flow)

We have shown (see section 2.2B) that according to the horizontal flow model, a hydrostatic pressure distribution is assumed along any vertical of the flow region. This is not justified near the pumping well. Boulton (1951) showed experimentally that in the neighborhood of a pumping well, the vertical component of the specific discharge $\vec{q}$ is of considerable magnitude.

The potential flow model (see section 2.2D) takes into account this vertical component of the specific discharge vector. Rewriting equation (2.7) in cylindrical coordinates, and assuming a homogeneous medium, gives

$$K_r \frac{1}{r} \frac{\partial}{\partial r} \left(r \frac{\partial \phi}{\partial r}\right) + K_z \frac{\partial^2 \phi}{\partial z^2} = S_s \frac{\partial \phi}{\partial t} \tag{3.14}$$

Equation (3.14) and the following boundary and initial conditions,

$$\phi(r,z,t=0) = D \tag{3.15a}$$

$$\frac{\partial \phi}{\partial z}(r,z=0,t) = 0 \tag{3.15b}$$

$$\lim_{r\to 0} \int_0^h r \frac{\partial \phi}{\partial r}\, dz = Q/2\pi K_r \qquad (3.15c)$$

$$\lim_{r\to \infty} \phi(r,z,t) = D \qquad (3.15e)$$

$$K_r \left(\frac{\partial \phi}{\partial r}\right)^2 + K_z \left(\frac{\partial \phi}{\partial z}\right)^2 - K_z \frac{\partial \phi}{\partial z} = S_y \frac{\partial \phi}{\partial t} \quad \text{at } z = h \qquad (3.15f)$$

describe the potential flow model.

Equation (3.15f) makes the solution very difficult to obtain. However, if the quadratic terms are dropped, the condition is taken at z = D instead of z = h, i.e., $[(D-h)/D] \ll 1$, this linearizes the boundary condition to

$$\frac{K_v}{S_y} \frac{\partial \phi}{\partial z} + \frac{\partial \phi}{\partial t} = 0 \qquad \text{at } z = D \qquad (3.15g)$$

where $K_v = K_z$ and $K_H = K_r = K_x$.

The solution to this problem, neglecting the seepage face and the compressibility term in equation (3.14), was given by Boulton (1954) for the drawdown at the free surfaces as

$$s = \frac{Q}{2\pi KD} \int_0^\infty \frac{J_0(\lambda\rho)}{\lambda} \{1 - \exp(-\tau\lambda \tanh \lambda)\}\, d\lambda \qquad (3.16)$$

where s = D-h = drawdown

$\rho = r/D$

$\tau = K_v t/S_y D$

and λ is a variable of integration and J_0 is a Bessel function.

Usually equation (3.16) is expressed as

$$s = \frac{Q}{2\pi T} v(\tau,\rho) \tag{3.17}$$

where $v(\tau,\rho)$ is tabulated as a function of τ for different values of ρ (see Hantush, 1964).

Dagan (1967a) solved the problem in a more general way. He used the perturbation expansion method, considering a partially penetrating well, and found the first order approximation in the following series:

$$s/D = 2\pi c s_1/D + (2\pi c)^2 s_2/D + \ldots \tag{3.18}$$

where $c = Q/2\pi K_H D^2$

For a fully penetrating pumping well, his solution reduces to that of Boulton (1954). A comparison between the drawdown, at the free surface predicted by the two solutions, is shown in figure 9 for 3 type curves. The curves are identical except for a small deviation as dimensionless time becomes very small.

Neuman (1972, 1974) solved the linearized problem by taking into account the compressivility of the aquifer. Hoffman, G.L. (personal communication, 1975) compared the solutions by Neuman (1972) and Dagan (1967a) and showed that as time increases, the two curves merge.

To demonstrate the significance of the unconfined aquifer compressibility, different ratios of S/S_y are shown in figure 10. The period of time occupied by the early segment of the time drawdown curve becomes less as S/S_y decreases; when it approaches zero this segment disappears completely, and hydraulic heads everywhere below

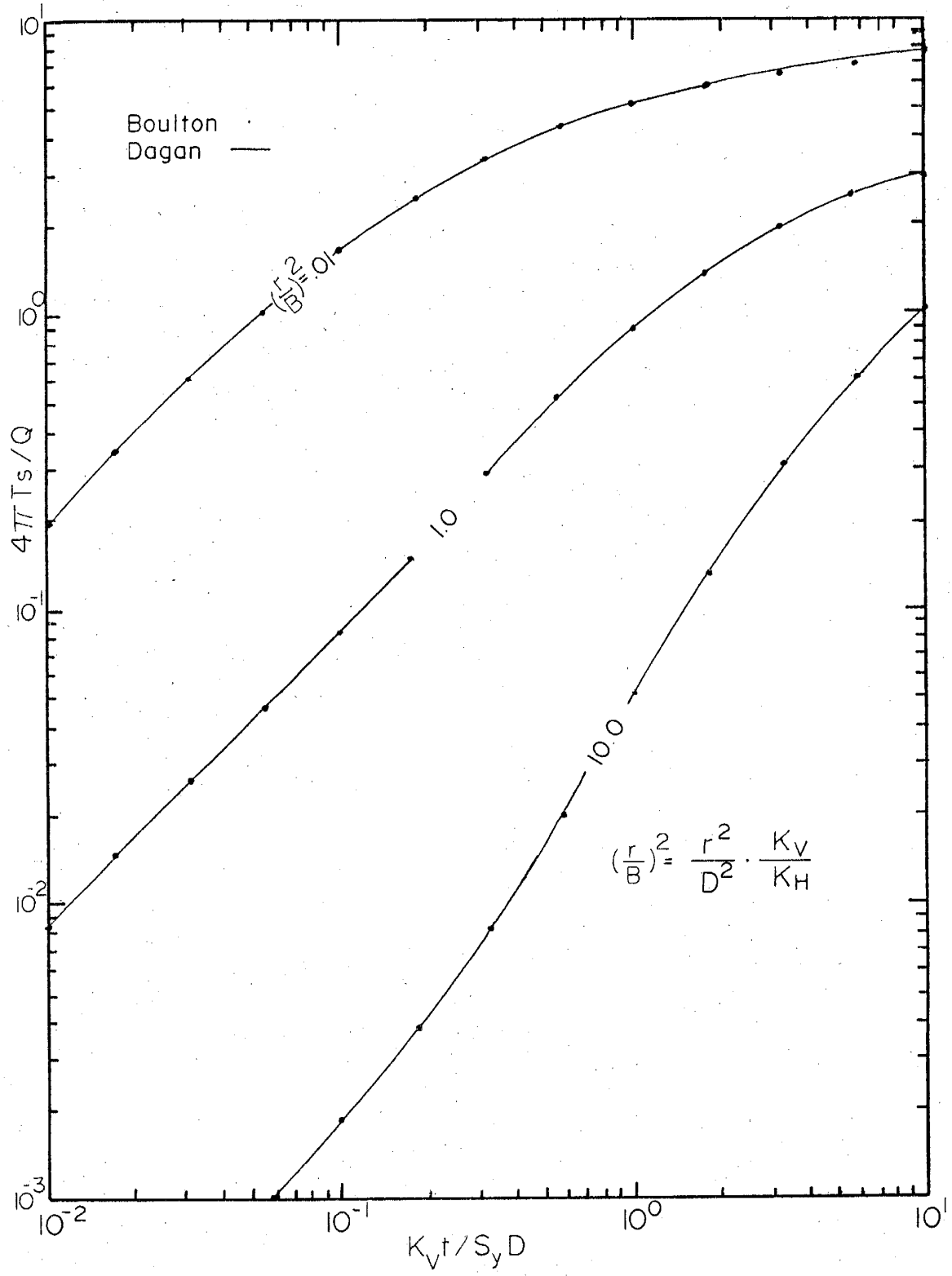

Figure 9. Comparison of Boulton (1954) and Dagan (1967a) type curves for dimensionless drawdown at the free surface

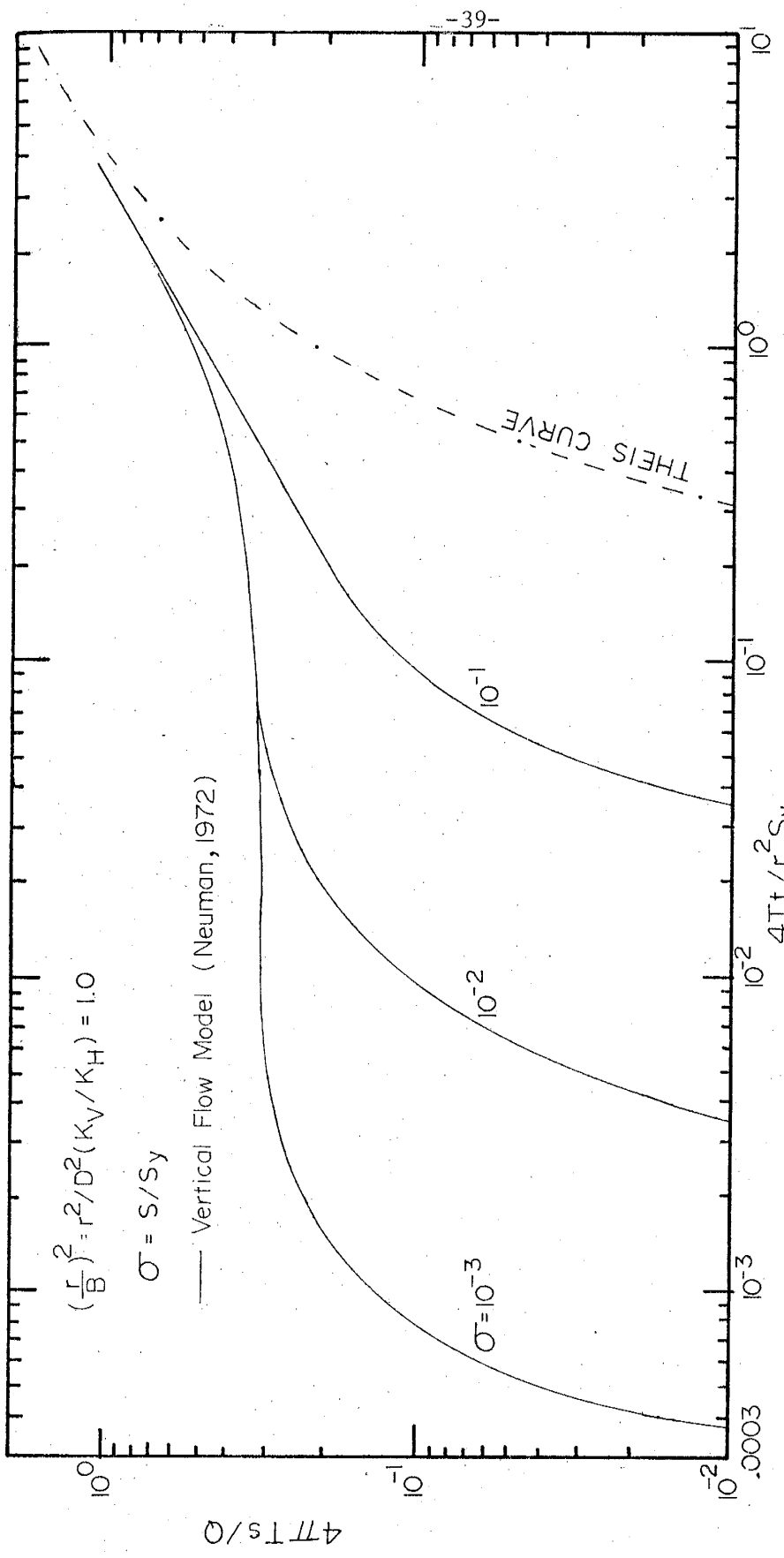

Figure 10. Dimensionless drawdown versus dimensionless time for different values of σ

the water table drop instantaneously when pumping starts. The general lack of data on the compressibility of an unconfined aquifer makes it difficult, however, to answer the question of the significance of elastic storage S of an unconfined aquifer in relation to S_y.

3.5 Correlation of the Vertical and Horizontal Flow Models

Now that we have discussed some of the distinguishing features of the horizontal and vertical flow models, we can correlate the two.

Figure 11 shows a comparison between the linearized horizontal model in h by Theis and the linearized potential flow model. Close examination reveals that the vertical flow effects are very significant at early time, depending on the value of the parameter $(r/B)^2 = \frac{r^2}{D^2}\frac{K_y}{K_H}$. The smaller the value of r/B, the higher the drawdown predicted by the vertical flow model, and vice versa. For $(r/B)^2 \geq 16$ the vertical flow effects are insignificant, and we can say that the two models practically coincide. At intermediate times, depending on the value of $(r/B)^2$, the two models gradually merge into one type curve. For instance, when $(r/B)^2 = 0.01$, the two models merge to one type curve at the dimensionless time $1/u = 6 \times 10^1$, and for $(r/B)^2 = 1.0$ they merge at $1/u = 6 \times 10^0$.

At large times the vertical model and the linearized horizontal model in h together form one type curve which differs significantly from that of the nonlinear horizontal model (figure 12). This difference increases with increase of the parameter c, or s/D, as we have shown in section 3.3. This is expected from theory, since the vertical model and the Theis equation were both linearized by assuming

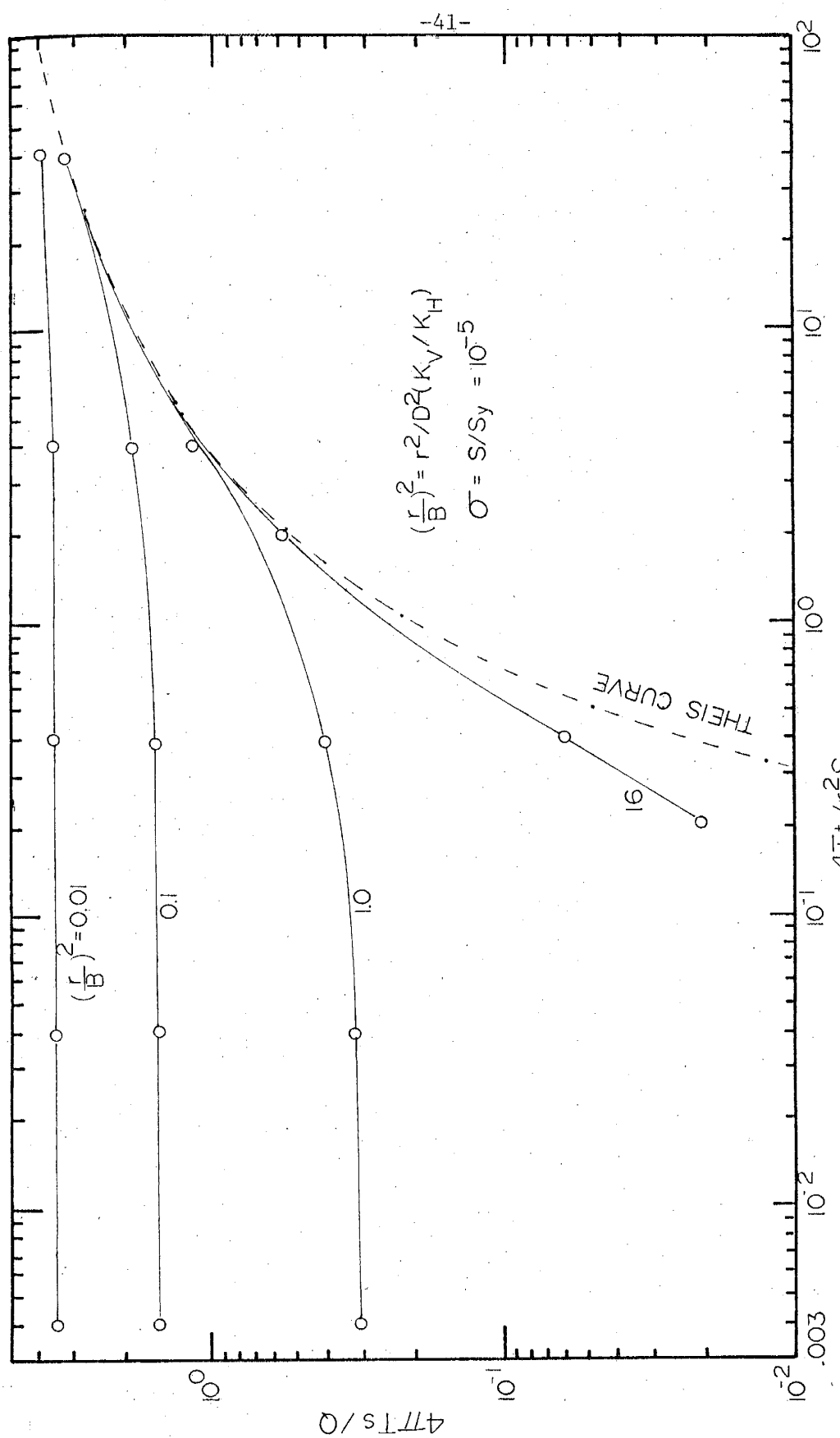

Figure 11. Comparison between linearized potential flow model (Neuman, 1972) and linearized horizontal model (Theis, 1935)

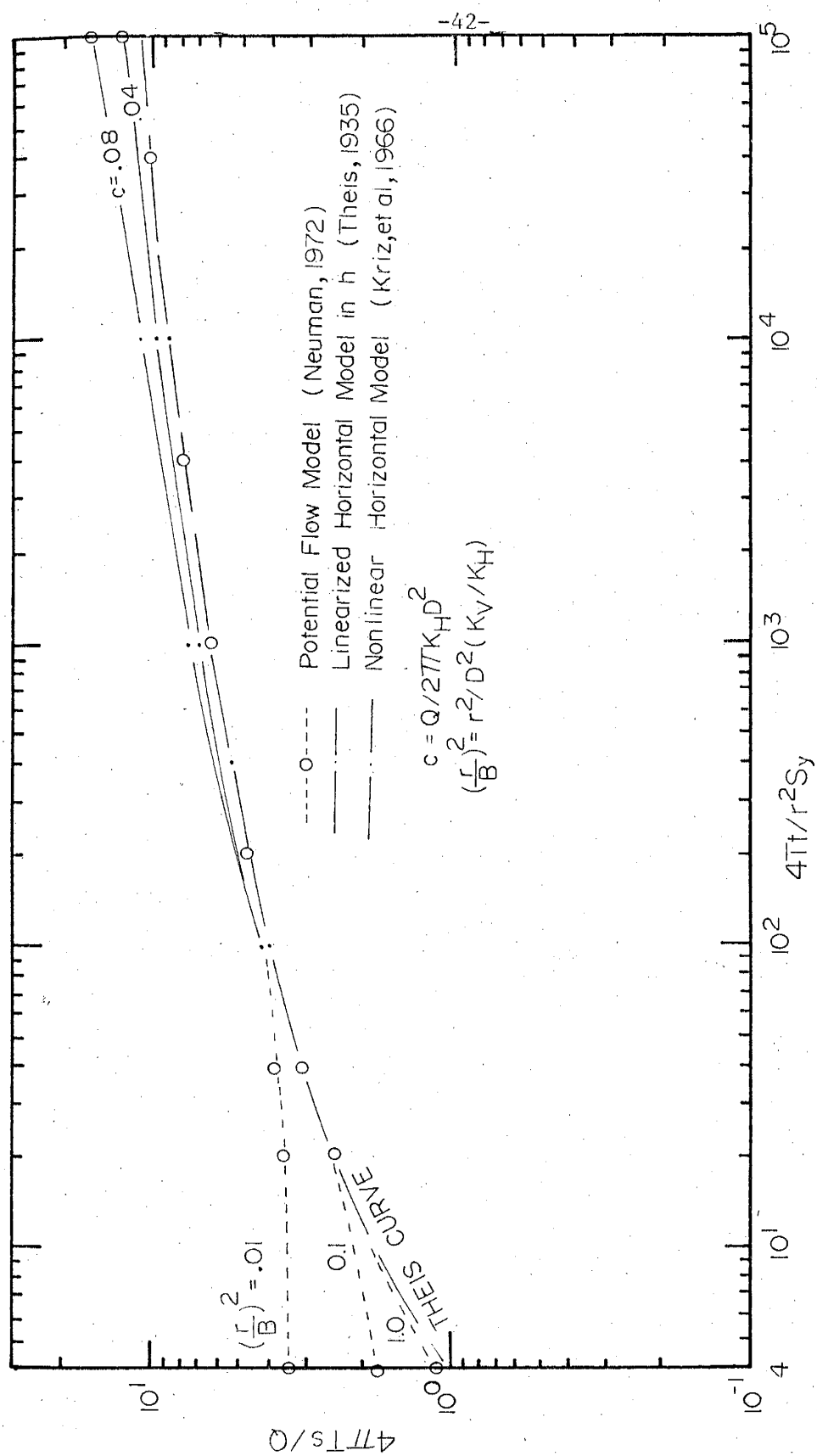

Figure 12. Comparison between the nonlinear horizontal flow model, the linearized potential flow model and Theis solution

that $s<<D$.

So far we have analyzed two significant factors, (1) the linearization effects or the thinning of the saturated thickness, and (2) the vertical flow effects. Fortunately the linearized horizontal model in h^2 handles the first factor with reasonable accuracy and very little difficulty. To neglect the vertical flow effects, either the parameter r/B has to be greater than 4, or the dimensionless time $4Tt/r^2S_y$ must be greater than 5×10^1.

3.6 Variably Saturated Model (exact theory)

A. Introduction

The theoretical models presented in sections 3.2 and 3.4 are based on several approximations, (1) linearization of the free surface boundary condition, which includes neglect of the quadratic terms, (2) the assumption of a constant saturated thickness (assumed in all of the previous models except the nonlinear horizontal model), (3) replacement of the well screen, a boundary of constant head beneath the water level in the well at any time, by a sink line of uniformly distributed strength, (4) the transfer of the upper lateral boundary of the flow domain to infinity and, most important, (5) the neglect of the unsaturated zone.

To check the accuracy of these models, the exact mathematical model, representing precisely the physical problem, had to be solved numerically. The equation describing the variably saturated flow model for the aquifer in figure 2 is equation (2.5). It is nonlinear because of the dependence of hydraulic conductivity $K(\theta)$ on the moisture

content θ. Relationships are needed between θ and ϕ, and between $K(\theta)$ and θ before one can attempt to solve this equation.

Brutsaert (1967) suggested the following relationship, which can be written as

$$K(\theta) = K_0 S_e^N \quad , \quad S_e = \frac{\theta - \theta_r}{\theta_0 - \theta_r} \tag{3.19}$$

or as

$$S_e = A/(A + \psi^\lambda) \quad , \quad \psi = z - \phi$$

where K_0 is a saturation hydraulic conductivity (constant), S_e is a normalized moisture content, generally called effective saturation; the constant N depends mainly on the pore size distribution of the soil; A and λ are parameters of the soil and depend upon its capillary fringe and pore size distribution respectively.

The advantage of equation (3.19) is that it gives a smooth transition from the capillary fringe to the drying curve. Verma (1969) used equation (3.19) for the problem of variably saturated flow in a stream-connected aquifer. He found that the parameter $A^{1/\lambda}/D$ can be used as a criterion to determine the importance of the unsaturated zone.

Assuming hydrostatic pressure, Myers and Van Bavel (1962) came up with a somewhat different and physically more satisfying approximation. They defined an effective thickness h_e of a saturated layer with the same transmissivity as the entire region above the water table as

$$h_e = \int_{z_0}^{z_1} \frac{K(z)}{K_0} \, dz \tag{3.20}$$

where z_0 is the elevation of the water table and z_1 is that of the soil

surface.

Bouwer (1964) was the first to define critical pressure analogous to h_e as

$$p_c = \int_0^{p_w} \frac{K(p)}{K_0} \, dp \tag{3.21}$$

where p_w is the negative soil water pressure at the soil surface. He integrated equation (3.21) using a planimeter and calculated p_c for 28 different soils ranging from sands to clays.

We will use equation (3.21) to define the critical thickness $h_{cr} = p_c/\gamma$ as

$$h_{cr} = \int_0^{\infty} \frac{K(\psi)}{K_0} \, d\psi \tag{3.22}$$

where γ is the specific weight of water.

Substitution of this into equation (3.22) gives

$$h_{cr} = \int_0^{\infty} [A/(A + \psi^{\lambda})]^N \, d\psi$$

which, when integrated simplifies to

$$h_{cr} = \frac{A^{1/\lambda}}{\lambda} \left[\frac{\Gamma(1/\lambda) \cdot \Gamma(N - 1/\lambda)}{\Gamma(N)} \right] \tag{3.23}$$

where $\Gamma(n) = \int_0^{\infty} e^{-x} x^{n-1} \, dx$ for $n<0$ and $n>0$, is the gamma function.

The parameter h_{cr} is physically satisfying and easy to visualize, and gives us common grounds to compare the variably saturated flow models that apply different hydraulic conductivity and moisture content relationships, just by determining their corresponding h_{cr} values.

Experimental data reported by various investigators for different types of soils were analyzed to obtain the parameters A, λ, and N; these were used to determine h_{cr}/D for various depths of D of the aquifer. Details of the soils and their values of A, λ and h_{cr}/D are given in table 2. Typical values of h_{cr} for sand, for instance, range between 0.1m and 0.5m.

B. Linearized Variably Saturated Model

Kroszynski and Dagan (1974) solved equation (2.5), with the appropriate boundary and initial conditions for a well flow problem, by means of perturbation expansion, in series of a small parameter. (This effectively linearizes the equation of unsaturated flow and the free surface boundary condition.) They assumed that the flow departs slightly from equilibrium, which is equivalent to the assumption in sections 3.2 and 3.4 that the drawdown s is small compared to the initial satruated thickness D. They also approximated the variable coefficient of the unsaturated flow equation by applying the following relationships:

$$K(\theta)/K_0 = e^{a'(\psi - \psi_c)}$$

and

$$\frac{\theta - \theta_r}{\theta_s - \theta_r} = e^{a'(\psi - \psi_c)} \qquad (3.24)$$

where ψ_c = the saturated capillary rise, defining the free surface

ψ = capillary head = $z - \phi$

θ_r and θ_s are the residual and saturation moisture contents respectively

Table 2. Values of λ, $A^{1/\lambda}$, and h_{cr} for Different Soils

Soil	Textural Percentage			λ	$A^{1/\lambda}$(m)	h_{cr}(m)	D(m)	h_{cr}/D	Calculated from the experimental results of
	Clay	Silt	Sand						
Oso Flaco			fine sand	5.43	0.37	0.24	20 10 2.67	0.012 0.024 0.090	Day and Luthin (1956)
gravely sand				1.4	0.83	0.44	20 10 2.67	0.022 0.044 0.164	Reisenauer (1963)
Columbia silt loam				6	0.95	0.76	17.5 10 2.67	0.044 0.076 0.284	Nielsen and Biggar (1961)
Webster 24"	38	31	31	3	0.36	0.24	20 10 3.55	0.012 0.024 0.07	Nielsen, Kirkham and Perrier (1960)
Yolo loam	18	31	51	1.5	0.95	0.51	20 10 2.67	0.026 0.05 0.19	Davidson, et al. (1969)

and a' = a parameter characterizing the unsaturated zone.

Substituting equation (3.24) into equation (3.22) and integrating gives

$$h_{cr} = 1/a' + \psi_c$$

Figure 13 represents the results of the linearized variably saturated model (as a function of r/B) for $h_{cr}/D = 0.044$.

C. Nonlinear Variably Saturated Flow Model

The numerical scheme used here is based on the finite element method by Neuman (1972) as modified by Kroszynski and Dagan (1974). He solved equation (2.5) and the appropriate initial and boundary conditions. For a detailed description of the scheme and related computer program, see Kroszynski and Dagan (1974). We used this program to investigate the effects of the well storage and the seepage face, and the nonlinear effect of the unsaturated zone. The computer program for the nonlinear variably saturated model was run twice, once with well storage and seepage face considered, and once without. (For grid system and the time and space increments, see appendix A.)

The time-drawdown curves obtained for various observation wells are plotted in figure 14. As seen from the figure, the well storage and seepage face have some influence for a short time after the beginning of pumping. For a well diameter of 0.3m., Q = 800 m^3/day, T = 400 m^2/day, S_y = 0.2, and r/B = 0.27, 0.59 and 1.24, if we consider the well storage and seepage face, the drawdown after 1.44 minutes of pumping is 6 cm., 2 cm. and 0.4 cm. respectively; neglecting these,

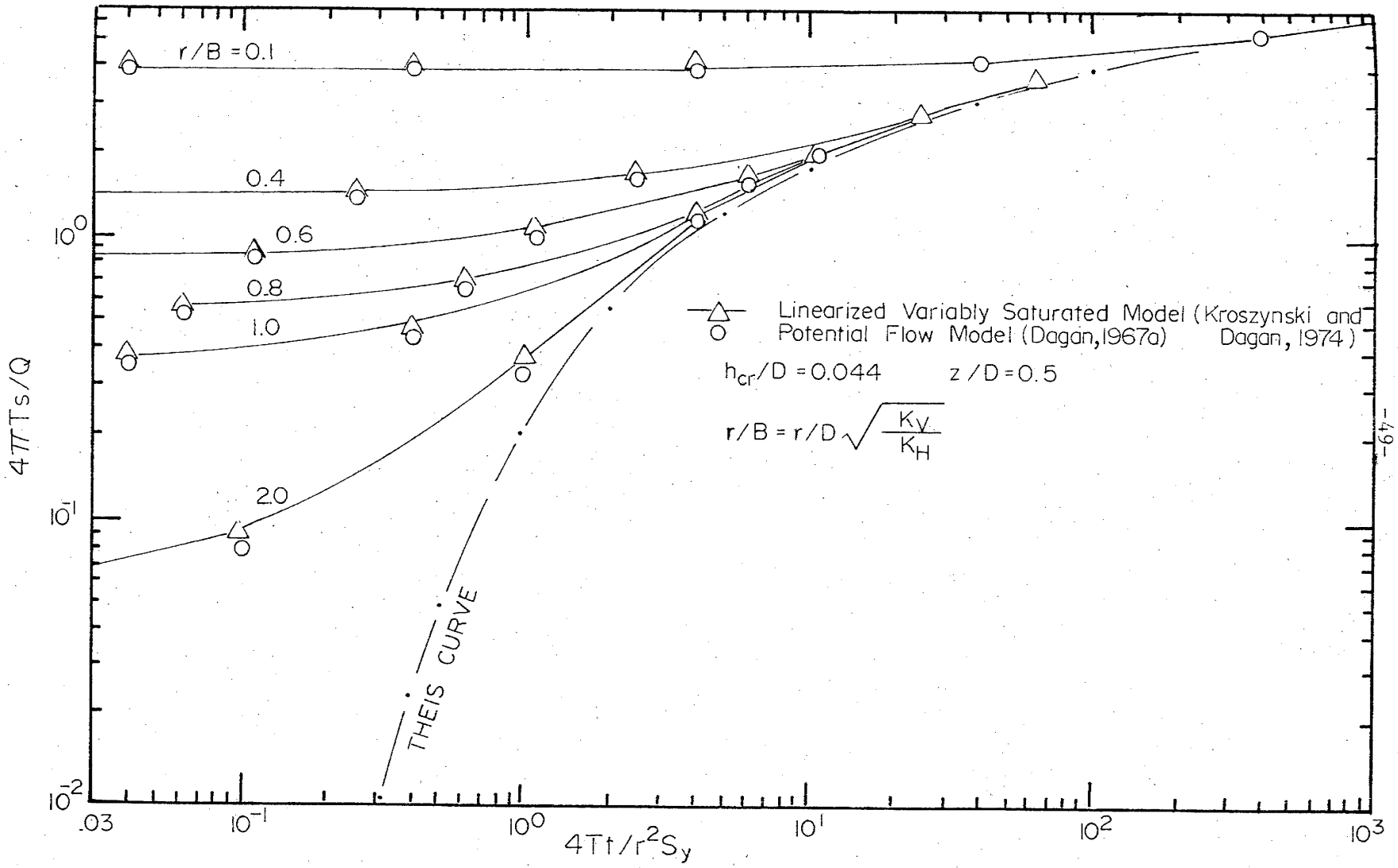

Figure 13. Dimensionless drawdown versus dimensionless time obtained from the linearized variably saturated model

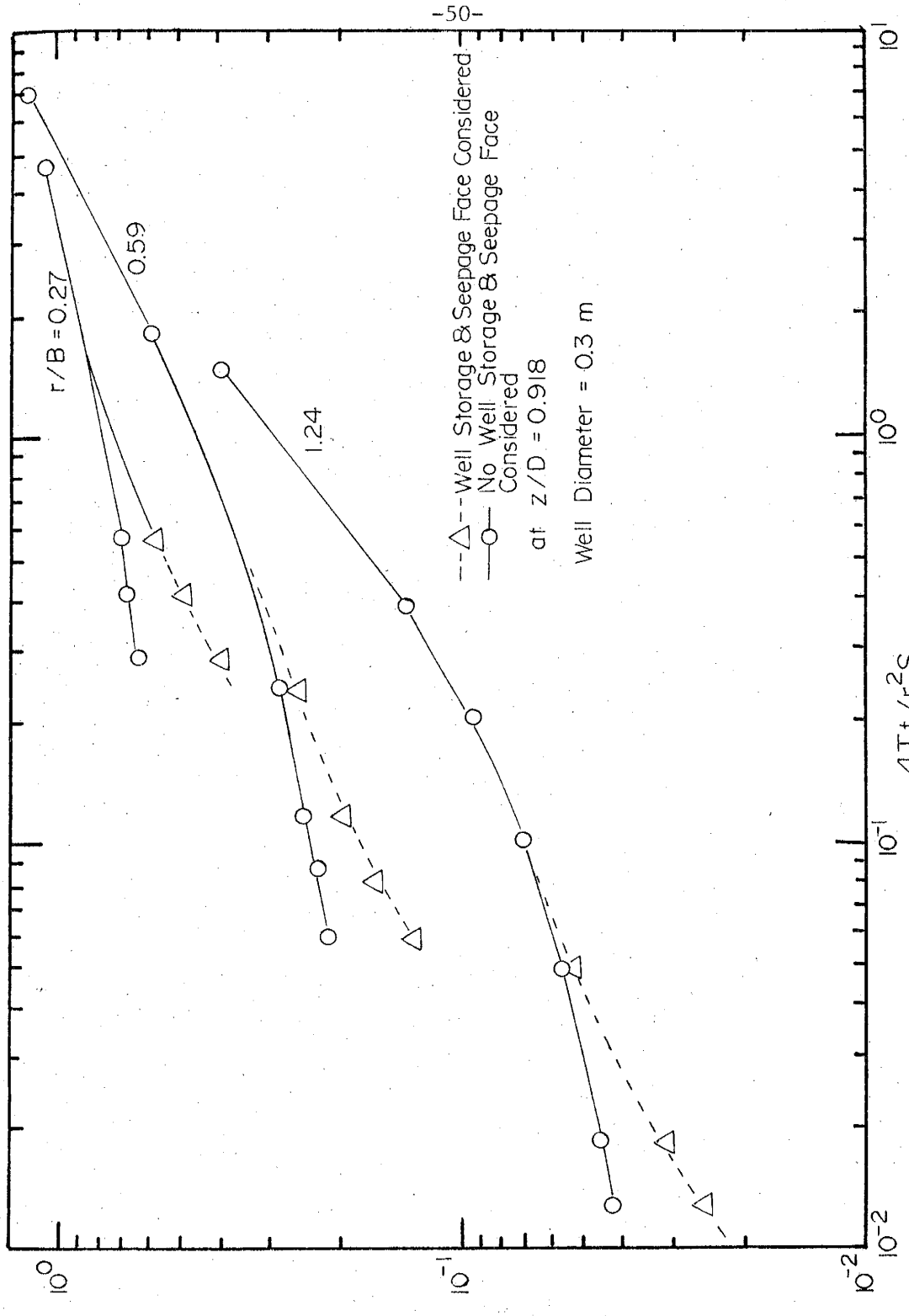

Figure 14. Dimensionless drawdown curves obtained from the numerical solution of the variably saturated model (Kroszynski and Dagan, 1974)

we find that the drawdown is 10 cm, 3.4 cm, and 0.7 cm respectively. The difference in drawdown seems significant, but does not last long. If we analyze the same drawdown curves for time t = 14.4 minutes we find that they practically coincide. This is similar to the conclusions reached by Kipp (1973), and justifies the analytical approximation to the boundary condition of the well.

D. Comparison of the Variably Saturated Models

Figure 15 compares the linearized variably saturated model and the nonlinear model for $c = Q/(2\pi K_H D^2) = 0.032$ and $z/D = 0.5$. The results (obtained using a computer program from Kroszynski and Dagan, 1974) of the two models coincide, demonstrating that the linearized model can be used with high confidence as long as the drawdown is small compared to the initial saturated thickness. They also show that the approximation of the soil characteristic curves by equation (3.24) has little if any influence on the drawdown in the saturated zone, as compared to that of the more accurate representation given by equation (3.19) which was used in the numerical solution.

3.7 Comparison of the Variably Saturated Model and the Potential Model (Vertical Flow)

The objective here is to analyze the significance of the unsaturated zone for different soils and different depths of the aquifer. In doing so we will attempt to obtain a critical value of the parameter h_{cr}/D, below which the effects of the unsaturated zone can be neglected. Dimensionless drawdown curves predicted by the linearized variably saturated model ($h_{cr}/D = 0.044$) and potential flow model for

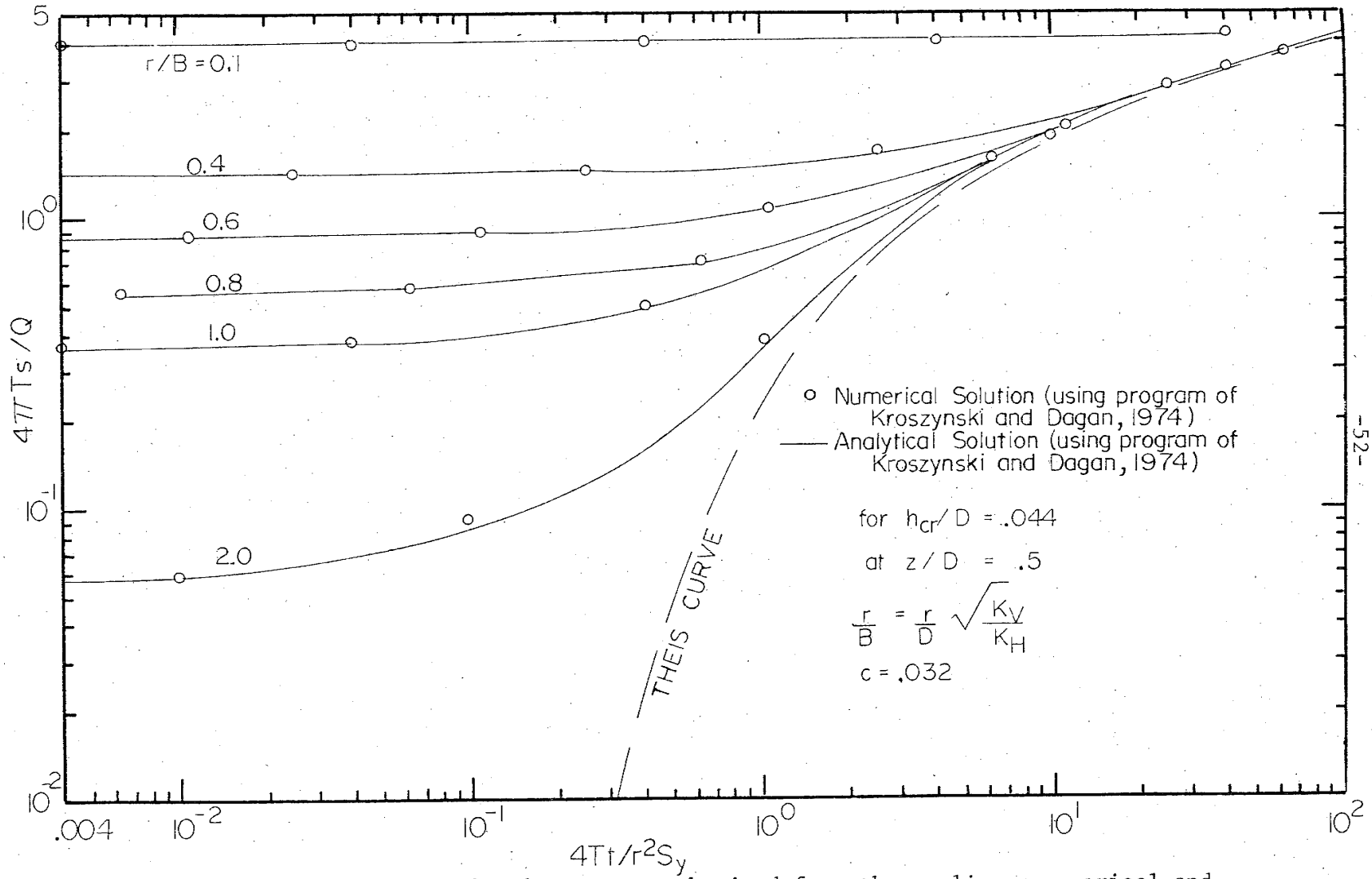

Figure 15. Comparison between drawdown curves obtained from the nonlinear numerical and linearized analytical variably saturated models

a fully penetrating pumping well and for the same values of r/B and z/D are shown in figures 13, 16a and 16b. The figures indicate that flow in the unsaturated zone causes faster drawdown than that predicted by the potential flow model. The discrepancy between their predicted dimensionless drawdown is very small and practically insignificant for deep observation wells ($z/D \leq 0.5$), but for shallow observation wells ($z/D = 0.95$), the difference becomes apparent, especially at intermediate times.

To emphasize the role of the unsaturated zone, a relatively high value, $h_{cr}/D = 0.1$, was selected for our analysis. Drawdown curves predicted by the two models for the same values of z/D and r/B are shown in figures 17 and 18. These figures show that the difference in dimensionless drawdown for shallow observation wells ($z/D = 0.95$) is very significant, especially at early time. For deep observation wells ($z/D \leq 0.5$) the difference is less apparent. Table 3 shows quantitatively the difference between dimensionless drawdown predicted by the linearized variably saturated model ($h_{cr}/D = 0.044$, 0.067 and 0.1) and the potential flow model. For $h_{cr}/D = 0.1$ a maximum error of 15% is encountered in deep observation wells at dimensionless time $K_v t/S_y D = 1 \times 10^{-1}$, as compared with 40% error in shallow observation wells at $K_v t/S_y D = 5 \times 10^{-2}$. If D = 10 m, K_v = 10 m/day and S_y = 0.2, the actual times t are 28.8 and 14.4 minutes. For an intermediate value ($h_{cr}/D = 0.067$), table 3 shows a difference of less than 6% for $r/B \leq 0.4$ and $z/D = 0.5$. At $r/B = 1$, there is about 10% difference, but this still is not very significant because at early time and far from the pumped well, the drawdown is very small for all practical

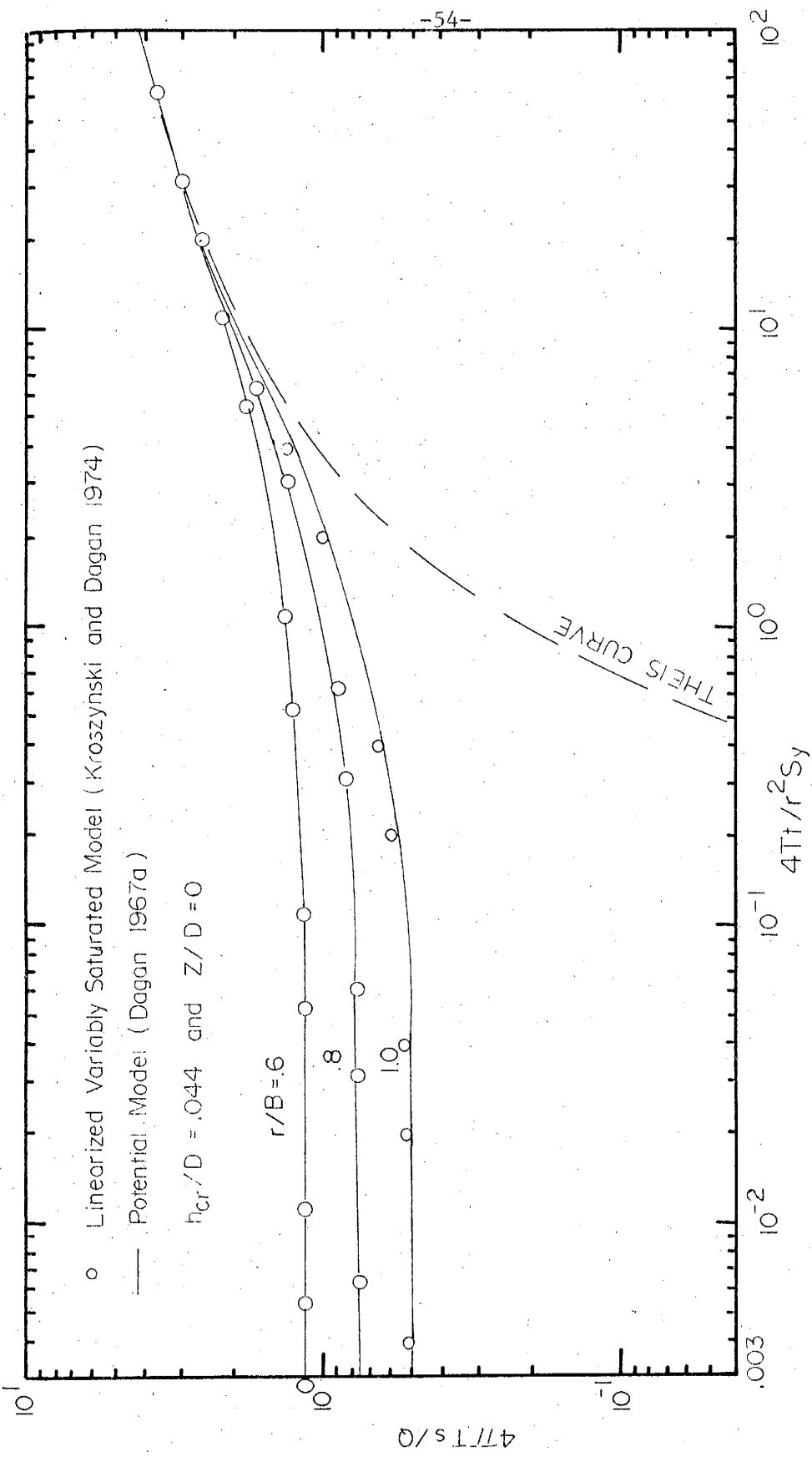

Figure 16a. Comparison between the variably saturated model and the vertical flow model for z/D = 0.0 and h_{cr}/D = 0.044

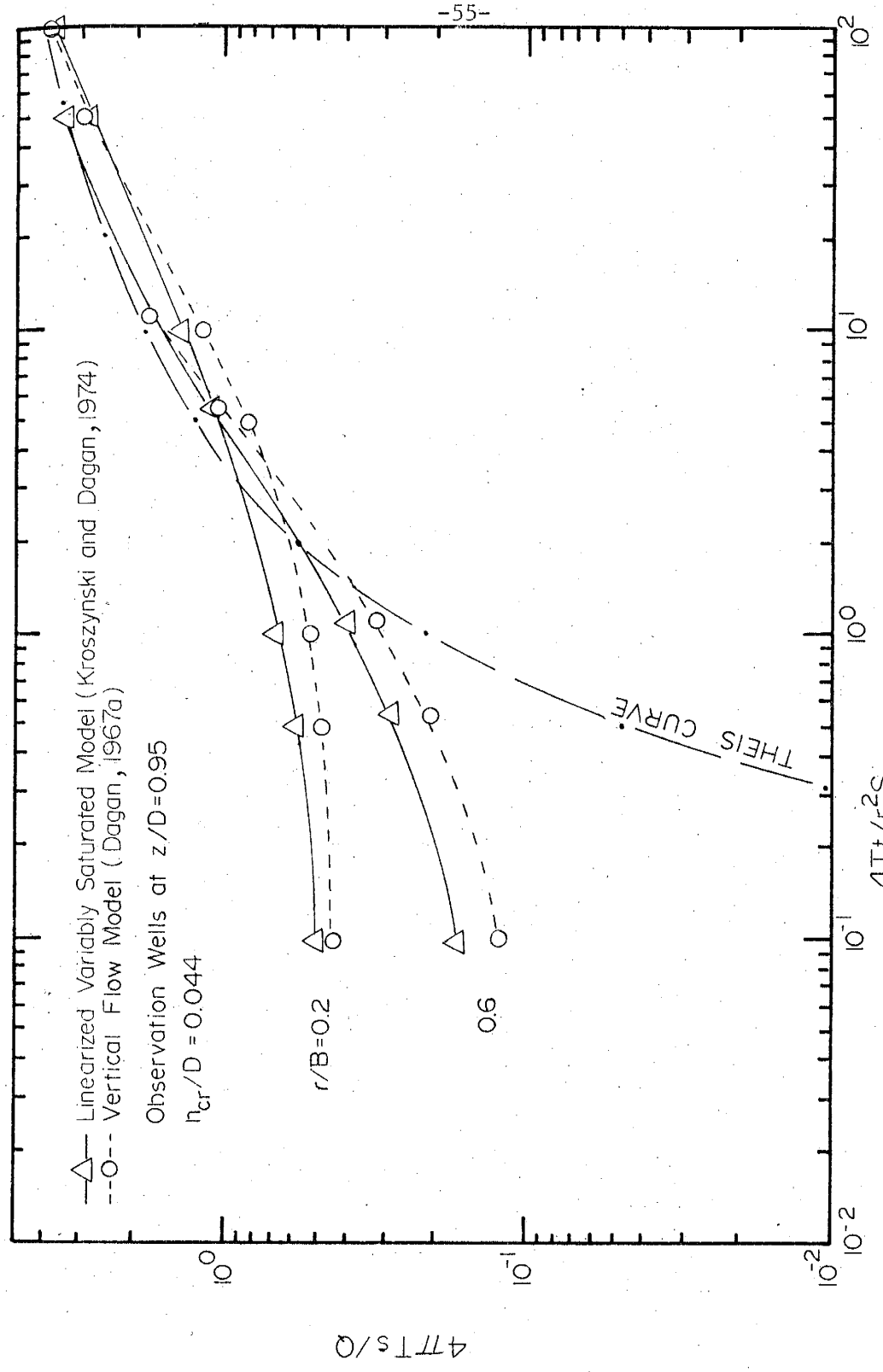

Figure 16b. Comparison between the variably saturated model and the vertical flow model for $z/D = 0.95$ and $h_{cr}/D = 0.044$

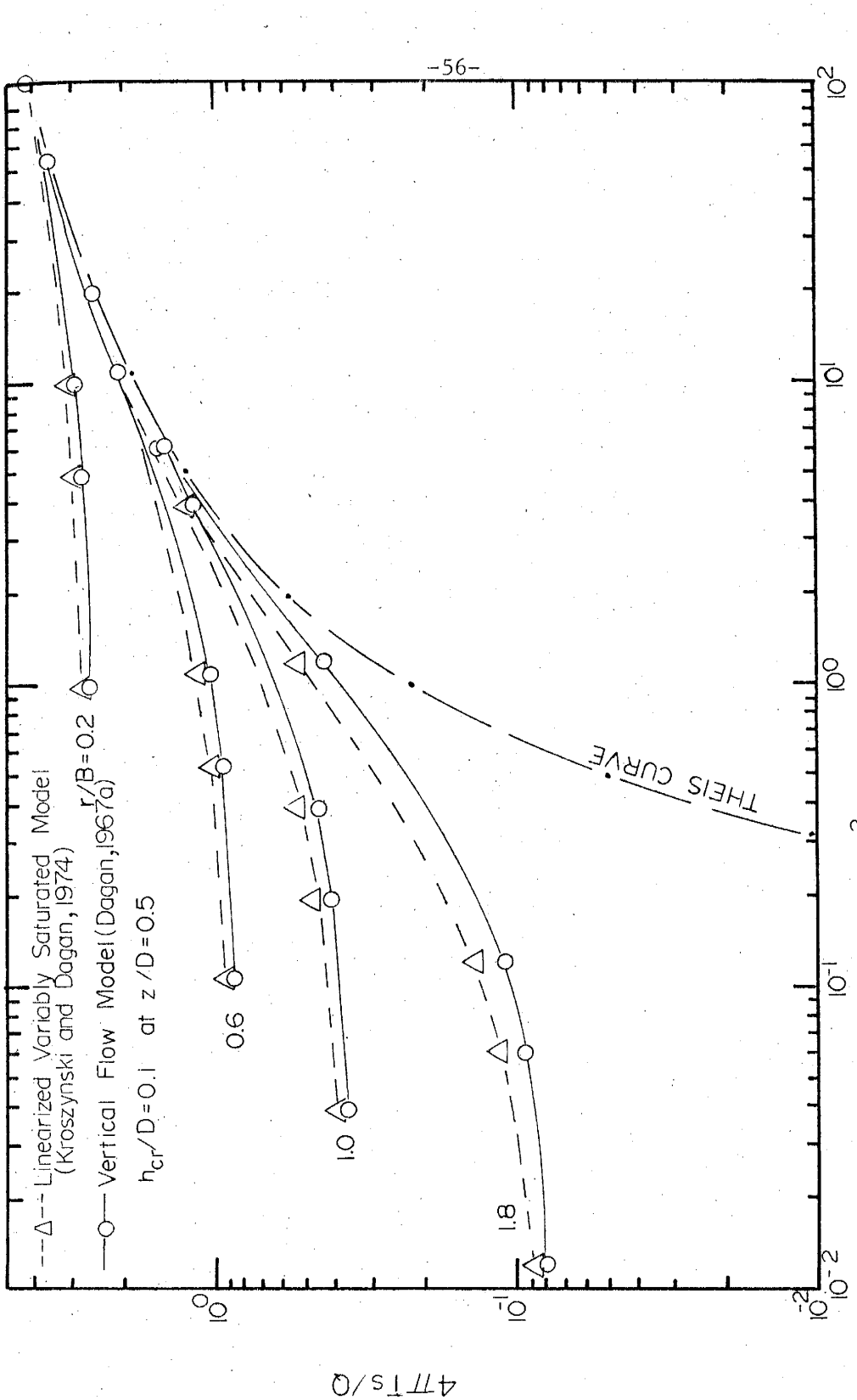

Figure 17. Comparison between the variably saturated model and the vertical model for $z/D = 0.5$ and $h_{cr}/D = 0.1$

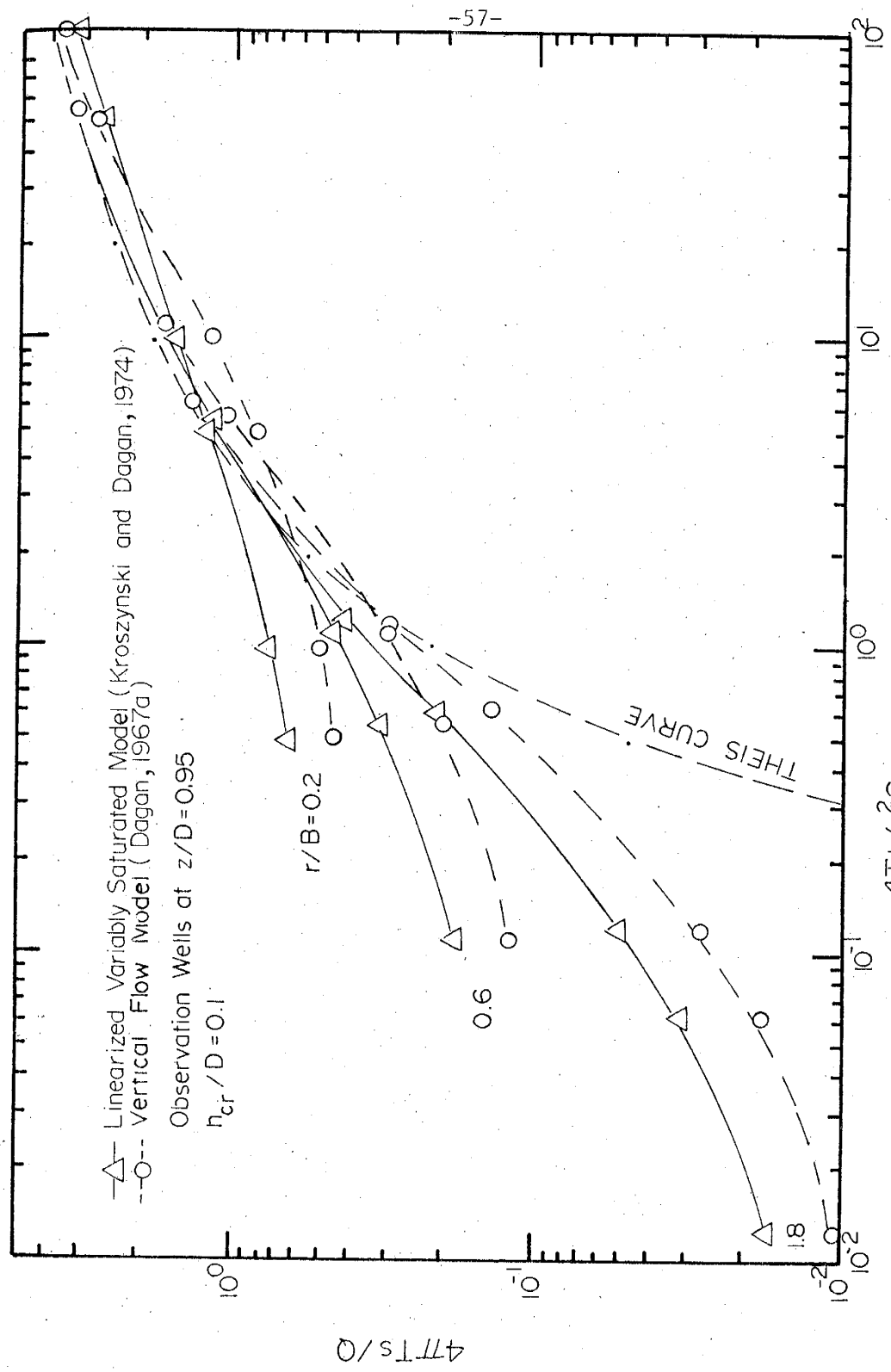

Figure 18. Comparison between the variably saturated model and the vertical flow model for z/D = 0.95 and $h_{cr}/D = 0.1$

Table 3. Comparison between Dimensionless Drawdown Obtained from Variably Saturated Model and Potential Flow Model

$$\% \text{ error} = \frac{\frac{4\pi Ts}{Q} \text{ (potential flow model)} - \frac{4\pi Ts}{Q} \text{ (variably saturated model)}}{\frac{4\pi Ts}{Q} \text{ (variably saturated model)}} \times 100$$

$z/D = 0.95$

$\frac{K_v t}{S_y D}$	$h_{cr}/D = 0.044$			$h_{cr}/D = 0.1$			$h_{cr}/D = 0.0667$		
r/B =	0.2	0.4	1.0	0.2	0.4	1.0	0.2	0.4	1.0
1×10^{-2}	-23.1	-24.2	-24.5	-32.4	-34.1	-35.9	-27.7	-29.1	-30.6
5×10^{-2}	-21.1	-24.3	-27.4	-31.1	-35.9	-40.3	-26.2	-30.1	-33.8
1×10^{-1}	-14.3	-19.2	-23.8	-22.4	-30.3	-37.1	-18.3	-24.6	-30.3
5×10^{-1}	3.7	-2.2	-10.6	5.6	-4.6	-19.7	4.7	-3.3	-14.8
1×10^{0}	5.8	1.4	-5.7	10.5	2.8	-11.3	8.1	2.0	-8.2
5×10^{0}	4.8	1.76	-2.3	9.3	3.9	-4.4	6.8	2.7	-3.3
1×10^{1}	3.8	0.9	-2.7	7.3	2.3		5.4	1.5	-3.8
1×10^{2}	-0.5			-0.2	2.0		-0.5		

+ sign indicates overestimate - sign indicates underestimate

Table 3. Comparison between Dimensionless Drawdown Obtained from Variably Saturated Model and Potential Flow Model (continued)

z/D = 0.5

$\frac{K_v t}{S_y D}$	$h_{cr}/D = 0.044$			$h_{cr}/D = 0.1$			$h_{cr}/D = 0.0667$		
r/B =	0.2	0.4	1.0	0.2	0.4	1.0	0.2	0.4	1.0
5×10^{-2}	-2.9	-4.6	-8.2	-4.8	-7.2	-12.7	-3.8	-5.6	-10.0
1×10^{-1}	-2.7	-4.2	-7.9	-4.9	-7.4	-13.9	-3.7	-5.7	-10.7
1×10^{0}	0.4	-0.1	-3.3	0.0	-0.6	-7.0	0.4	-0.3	-5.0
5×10^{0}	0.5			0.1	0.1	-4.3	0.7	-0.1	-3.2
1×10^{1}	0.0	-0.6	-2.8	0.0			0.0	0.0	

z/D = 0.0 $h_{cr}/D = 0.1$

1×10^{-2}	-1.8	-2.8	-5.7
1×10^{-1}	-3.2	-5.0	-10.5
1×10^{0}	-0.4	-1.3	-5.8
1×10^{1}	±3.4	-0.2	-4.2

purposes.

Figure 19a shows the difference in dimensionless average drawdowns predicted by the nonlinear variably saturated and potential flow models ($h_{cr}/D = 0.044$). The discrepancy between average drawdowns is small, as was found earlier for deep observation wells. This indicates that the effects of the unsaturated zone are insignificant and the vertical flow model is valid.

Also interesting is the comparison of dimensionless drawdown curves with the same values of z/D and h_{cr}/D but different values of r/B. Table 3 shows that the influence of the unsaturated zone is more significant for high values of r/B, but the fact that at early time the drawdown is very small at distant observation wells makes this observation less important from a practical point of view.

Thus we may say that for actual applications, where aquifers are not excessively shallow, the unsaturated zone can be safely neglected provided that $h_{cr}/D \leq 0.067$. This is especially true for deep observation wells ($z/D \leq 0.5$) or for wells penetrating the entire aquifer.

The fact that at early time the variably saturated model predicts higher drawdown than the saturated model can be explained physically as a result of the unsaturated moisture content profile that trails by vertical translation after the moving free surface. The time required for the unsaturated zone to adjust itself to the free surface drop depends mainly on the parameter h_{cr}/D. If it is small, the influence of the unsaturated zone upon the flow in the saturated zone is negligible. The time required for the unsaturated zone to adjust itself to the free surface drop, along with the

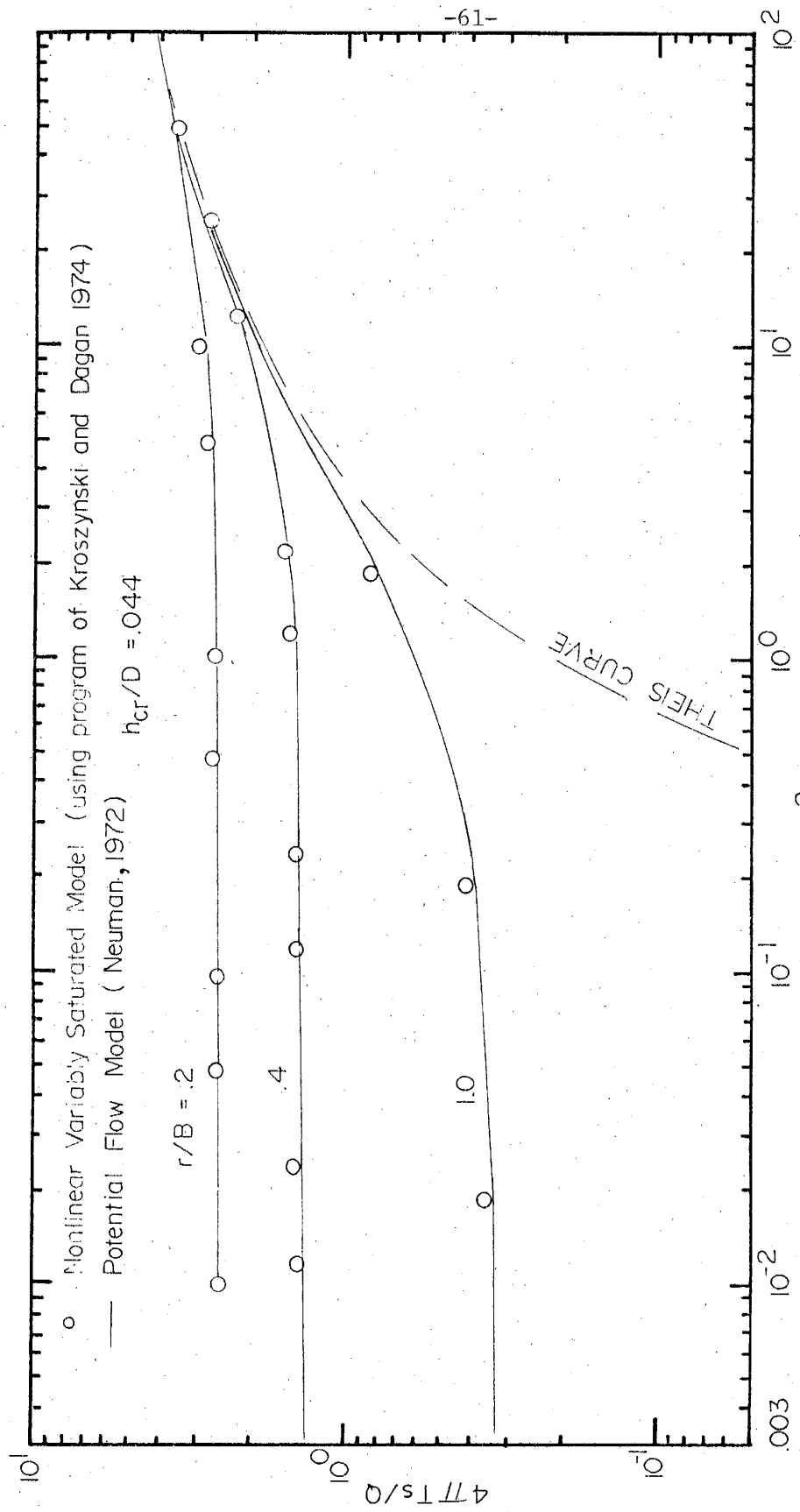

Figure 19a. Dimensionless average drawdown versus dimensionless time

dimensionless time $K_v t/S_y D$, may explain the observation that the maximum specific yield is reached only after a drainage period of considerable length, (Meinzer, 1923, Wenzel, 1942, and Prill, et al., 1965) ranging from a few hours for coarse-textured materials to months for the fine-textured materials. Table 3 shows that for $h_{cr}/D = 0.1$, $r/B = 1$, $K_v = 10$ m/day, $D = 10$ m, and $S_y = 0.2$, it takes about 2 days for the unsaturated zone to completely adjust itself to the free surface drop, whereas if $K_v = 1$ m/day it takes about 20 days.

3.8 Comparative Evaluation of Different Models

We have presented three types of mathematical models to describe the flow of water to wells in unconfined aquifers. The first is called the horizontal flow model, the second is the potential model (vertical flow) and the third is the variably saturated flow model. In section 3.2 we mentioned that the horizontal flow models were derived under the Dupuit assumption of hydrostatic pressure distribution. In section 3.4 we relaxed this assumption by introducing the vertical flow model, but we still assumed small drawdown compared to the total saturated thickness and neglected the quadratic terms in the free surface boundary condition. Since none of these is an exact description of the physical system under consideration, we considered another mathematical model to describe the physical system. This is the variably saturated flow model presented in section 3.6.

In section 3.7 we concluded that the linearized vertical flow model at early and intermediate time is valid provided that $h_{cr}/D \leq 0.067$ and deep observation wells are being used. But in section 3.5 we

showed that the existing vertical flow model's solutions at large time merge with Theis curve, forming one type curve and predicting less drawdown than the nonlinear horizontal flow model solution. To investigate this we computed average dimensionless drawdown at large time using the numerical solution of the variably saturated model (Kroszynski and Dagan, 1974) for $h_{cr}/D = 0.044$ and $c = Q/2\pi K_H D^2 = 0.032$, and compared it to the results of the nonlinear horizontal flow model (figure 19b). Close inspection of the figure shows that the two solutions practically coincide, predicting higher drawdown than either the linearized horizontal model in h (Theis) or the vertical flow model (Neuman, 1972).

In section 3.5 we concluded that the vertical flow effects are insignificant and can be neglected if $r/B \geq 4.0$. We can now also conclude that for actual applications both the nonlinear horizontal model and the linearized horizontal model in h^2 (Jacob correction) are valid provided that $r/B = (r/D)(K_V/K_H)^{1/2} \geq 4.0$ and $h_{cr}/D \leq 0.067$.

It should be emphasized that the ratio of anisotropy of permeability K_V/K_H is a very important factor in determining the location of the observation well. If the thickness of the aquifer is 50 feet and the aquifer is isotropic ($K_H = K_V$), the observation well should be at least 200 feet away from the pumping well for the horizontal flow model to be valid, whereas if $K_V/K_H = 0.1$ the observation well must be at least 632 feet away. However, the ratio of anisotropy of permeability is usually unknown, and locating the observation well far away from the pumping well requires a very long expensive pumping test from which the drawdown curve may be obtained. One alternative is to use a

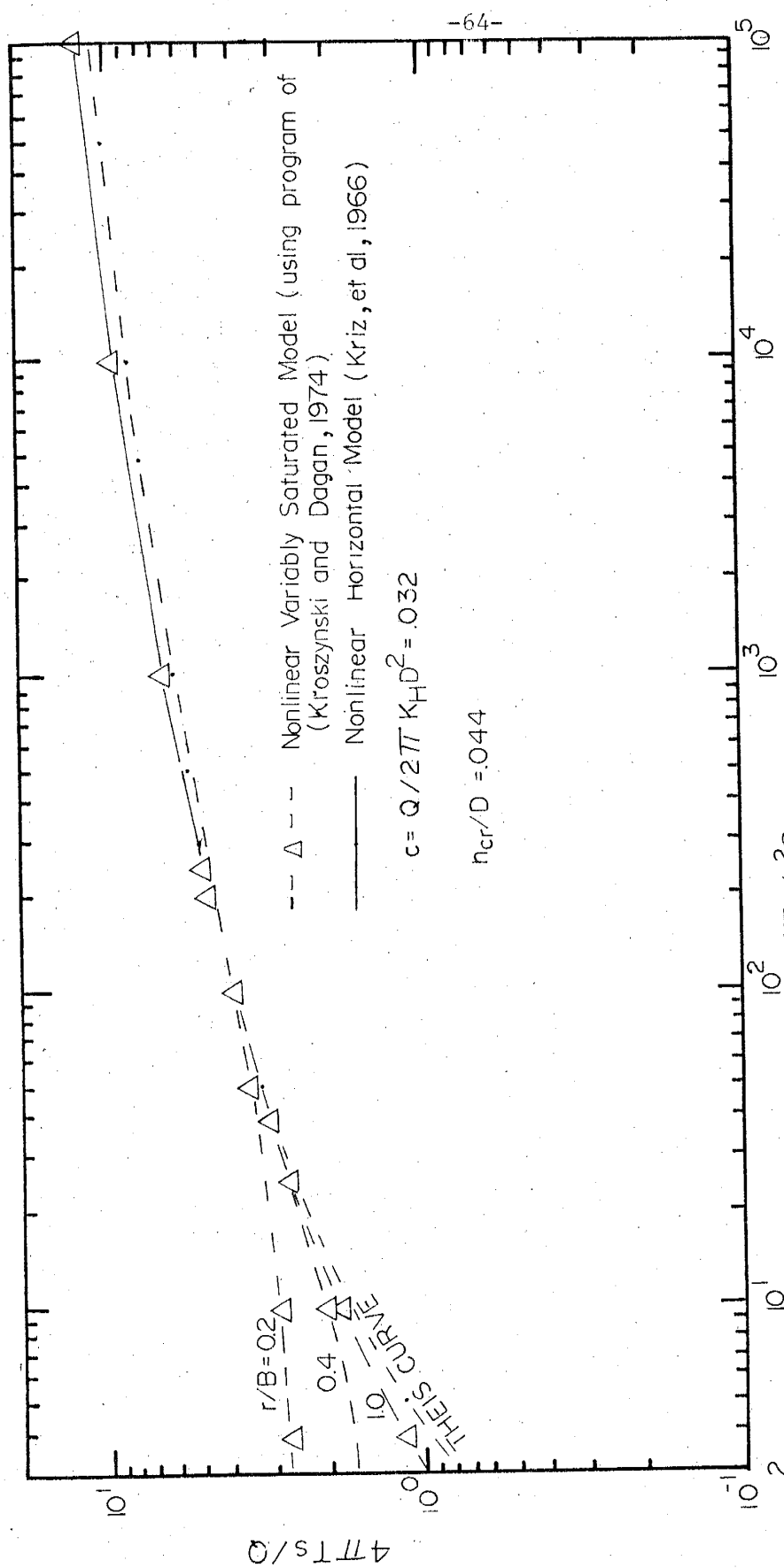

Figure 19b. Comparison between the average dimensionless drawdown predicted by the horizontal flow models and the variably saturated model

vertical flow model by Neuman (1972, 1974) or Dagan (1967a) with available computer programs, for early time, and to use the linearized horizontal model in h^2 (Jacob correction) for large time.

These recommendations are based on the limiting cases (correlation of the different models at early time and large time), with no theoretical support, and do not take into consideration the interaction between the vertical flow effects and the flow zone thinning. Consequently we will attempt next to provide a simple mathematical model that will approximate both the vertical flow effects and the thinning of the flow zone, as well as the interaction between the two.

3.9 Improved Horizontal Flow Model

A. Introduction

In section 3.8 we concluded that the horizontal flow model is valid provided that $r/B \geq 4.0$ and $h_{cr}/D \leq 0.067$, and that the linearized vertical flow models are valid only for small drawdown. However we also showed that the condition $r/B \geq 4.0$ severely limits the use of the horizontal flow model. Thus we need to formulate a mathematical model that will relax the severe assumptions in the above models, and will provide new information concerning the interaction between the vertical flow effects and flow zone thinning.

B. Mathematical Development

Consider the general case of groundwater flow in an unconfined aquifer bounded by an impervious horizontal bottom. The aquifer is anisotropic with principal axes horizontal and vertical. The water is

released from storage by compaction of the aquifer material, expansion of the water, and gravity drainage at the free surface.

Recalling the derivation of the horizontal flow model shown in section 2.3, equation (2.22) without accretion can be written as

$$K_x \frac{\partial}{\partial x}\left(\frac{\partial}{\partial x}(h\bar{\phi}) - h\frac{\partial h}{\partial x}\right) + K_y \frac{\partial}{\partial y}\left(\frac{\partial}{\partial y}(h\bar{\phi}) - h\frac{\partial h}{\partial y}\right) =$$

$$S_s\left(\frac{\partial}{\partial t}(h\bar{\phi}) - h\frac{\partial h}{\partial t}\right) + S_y\frac{\partial h}{\partial t}$$

or

$$K_x \frac{\partial}{\partial x}\left(\frac{\partial}{\partial x}(h\bar{\phi} - h^2/2)\right) + K_y \frac{\partial}{\partial y}\left(\frac{\partial}{\partial y}(h\bar{\phi} - h^2/2)\right) =$$

$$S_s\left(\frac{\partial}{\partial t}(h\bar{\phi} - h^2/2)\right) + S_y \frac{\partial h}{\partial t} \qquad (3.25)$$

At this point in the derivation of the Boussinesq equation it is usually assumed that the average head $\bar{\phi}$ approximately equals the height h of the free surface above a datum. If, instead of this assumption,

$$\phi^{*2} = h\bar{\phi} - h^2/2 \qquad (3.26)$$

is substituted into equation (3.25), the result is

$$K_x \frac{\partial^2\phi^{*2}}{\partial x^2} + K_y \frac{\partial^2\phi^{*2}}{\partial y^2} = S_s \frac{\partial\phi^{*2}}{\partial t} + S_y \frac{\partial h}{\partial t} \qquad (3.27)$$

APPROXIMATION OF THE VERTICAL FLOW COMPONENT

A linearized form of the free surface boundary condition can be obtained by neglecting the quadratic terms in equation (2.17) with no accretion. This gives

$$\frac{\partial h}{\partial t} = - \frac{K_z}{S_y} \frac{\partial h}{\partial z} \tag{3.28}$$

which relates the change of the water table elevation and the intensity of the vertical flow. Streltsova (1972) assumed that the specific rate of the vertical flow varies linearly with the difference between average head $\bar{\phi}$ and the free surface head h. Following this assumption, equation (3.28) can be approximated by

$$\frac{\partial h}{\partial t} = \alpha(\bar{\phi} - h) \tag{3.29}$$

where $\alpha = K_v/S_y b$ and b is the thickness of the vertical flow zone. For homogeneous aquifers, Streltsova (1972) found that $b = h/3$.

Equation (3.29) will be used here to approximate the vertical flow. Assuming α is approximately a constant (the most severe assumption made so far in this model), equation (3.26) may be rearranged and the result substituted in equation (3.29) to give

$$\frac{\partial h}{\partial t} = \alpha(2\phi^{*2} - h^2)/2h \tag{3.30}$$

or

$$\frac{\partial h^2}{\partial t} = \alpha(2\phi^{*2} - h^2) \tag{3.31}$$

The general solution of this equation (see Jeffreys and Swirles, 1951) is

$$h^2 = 2\alpha \int_{\tau=0}^{t} \phi^{*2} \, e^{-\alpha(t-\tau)} \, d\tau \tag{3.32}$$

Integrating by parts and using the static initial condition

$$h = \bar{\phi} = D$$

or $$\phi^{*2} = D^2/2 \qquad \text{at } t = 0$$

leads to

$$(2\phi^{*2} - h^2) = 2\int_{\tau=0}^{t} e^{-\alpha(t-\tau)} \frac{\partial \phi^{*2}}{\partial \tau} \, d\tau \tag{3.33}$$

Substitution of equations (3.33) and (3.31) into equation (3.27) results in

$$K_x \frac{\partial^2 \phi^{*2}}{\partial x^2} + K_y \frac{\partial^2 \phi^{*2}}{\partial y^2} = S_s \frac{\partial \phi^{*2}}{\partial t} + \frac{S_y \alpha}{h} \int_{\tau=0}^{t} e^{-\alpha(t-\tau)} \frac{\partial \phi^{*2}}{\partial \tau} \, d\tau \tag{3.34}$$

Rewritten in cylindrical coordinates, with angular symmetry assumed, this takes the form

$$\frac{\partial^2 \phi^{*2}}{\partial r^2} + \frac{1}{r} \frac{\partial \phi^{*2}}{\partial r} = \frac{S}{T} \frac{\partial \phi^{*2}}{\partial t} + \frac{S_y \alpha}{T} \frac{D}{h} \int_{0}^{t} e^{-\alpha(t-\tau)} \frac{\partial \phi^{*2}}{\partial \tau} \, d\tau \tag{3.35}$$

where $T = K_H D$ is transmissivity

and $S = S_s D$ is the storage coefficient.

This equation is nonlinear; to solve analytically, we still have to linearize it by assuming $h \approx D$ in the storage term (similar to the assumption used by Jacob (1963); see section 3.2). This leads to the following equation:

$$\frac{\partial^2 \phi^{*2}}{\partial r^2} + \frac{1}{r} \frac{\partial \phi^{*2}}{\partial r} = \frac{S}{T} \frac{\partial \phi^{*2}}{\partial t} + \frac{S_y \alpha}{T} \int_{\tau=0}^{\tau=t} e^{-\alpha(t-\tau)} \frac{\partial \phi^{*2}}{\partial \tau} \, d\tau \tag{3.36}$$

EQUATION FOR FREE SURFACE

Writing the combined head ϕ^{*2} in terms of the free surface head h (equation (3.31)) gives

$$\phi^{*2} = (\frac{\partial h^2}{\partial t} + \alpha h^2)/2\alpha \tag{3.37}$$

Then, by substituting (3.37) into (3.27), simplifying, and writing the results in cylindrical coordinates,

$$\frac{1}{r}\frac{\partial}{\partial r}(r\frac{\partial h^2}{\partial r}) + \frac{1}{r\alpha}\frac{\partial^2}{\partial t \partial r}(r\frac{\partial h^2}{\partial r}) =$$

$$\frac{S}{T\alpha}\frac{\partial^2 h^2}{\partial t^2} + \frac{S}{T}\frac{\partial h^2}{\partial t} + \frac{S_y}{T}\frac{D}{h}\frac{\partial h^2}{\partial t} \tag{3.38}$$

This is a nonlinear partial differential equation for the free surface head in unsteady radial flow in a phreatic aquifer; it accounts for the compressibility of the aquifer. For an analytical solution, it must be linearized by assuming that $h \approx D$ in the last term of the storage. This leads to the following equation:

$$\frac{1}{r}\frac{\partial}{\partial r}(r\frac{\partial h^2}{\partial r}) + \frac{1}{r\alpha}\frac{\partial^2}{\partial t \partial r}(r\frac{\partial h^2}{\partial r}) = \frac{S}{T\alpha}\frac{\partial^2 h^2}{\partial t^2} + \frac{S}{T}\frac{\partial h^2}{\partial t} + \frac{S_y}{T}\frac{\partial h^2}{\partial t} \tag{3.39}$$

To express equations (3.36) and (3.39) in terms of drawdown, equation (3.26) is first rewritten as

$$\phi^{*2} = (D - s^\circ)(D - s) - (D - s^\circ)^2/2$$

or

$$\phi^{*2} = D^2/2 - D(s - ss^\circ/D - s^{\circ 2}/2D) = D^2/2 - Df \tag{3.40}$$

where $f = (s - ss^\circ/D + s^{\circ 2}/2D)$

Then,

$$h^2 = (D - s^\circ)^2 = D^2 - 2D(s^\circ - s^{\circ 2}/2D) = D^2 - 2Ds^{\circ\prime} \tag{3.41}$$

where $s^{\circ\prime} = s^\circ - s^{\circ 2}/2D$, $s = D - \bar{\phi}$ is the average drawdown, and

s° is drawdown at the free surface.

A substitution of equations (3.40) and (3.41) into equations (3.36) and (3.39) respectively produces

$$\frac{\partial^2 f}{\partial r^2} + \frac{1}{r}\frac{\partial f}{\partial r} = \frac{S}{T}\frac{\partial f}{\partial t} + \frac{S_y}{T}\alpha \int_{\tau=0}^{\tau=t} e^{-\alpha(t-\tau)} \frac{\partial f}{\partial \tau}\, d\tau \tag{3.42}$$

and

$$\frac{1}{r}\frac{\partial}{\partial r}\left(r\frac{\partial s^{\circ\prime}}{\partial r}\right) + \frac{1}{r\alpha}\frac{\partial^2}{\partial t \partial r}\left(r\frac{\partial s^{\circ\prime}}{\partial r}\right) = \frac{S}{T\alpha}\frac{\partial^2 s^{\circ\prime}}{\partial t^2} + \left(\frac{S+S_y}{T}\right)\frac{\partial s^{\circ\prime}}{\partial t} \tag{3.43}$$

To solve for the average drawdown and the free surface drawdown as a combined problem, equation (3.33) written in terms of drawdown as

$$s^{\circ\prime} = f - \int_{\tau=0}^{\tau=t} e^{-\alpha(t-\tau)} \frac{\partial f}{\partial \tau}\, d\tau \tag{3.44}$$

and equation (3.42) have to be solved with the following initial and boundary conditions:

$$f(r, t=0) = 0 \qquad 0 \leq r \leq \infty$$

$$f(r,t) = 0 \qquad r \to \infty \text{ and } t \geq 0 \tag{3.45a}$$

and

$$Q = 2\pi r K_H \frac{\partial \phi^{*2}}{\partial r} = -2\pi r K_H D \frac{\partial f}{\partial r} \quad \text{as } r \to 0 \tag{3.45b}$$

The free surface drawdown may be solved as a separate problem using equation (3.43) and another set of initial and boundary conditions at the free surface, written as

$$s^{\circ\prime}(r,t=0) = 0 \qquad 0 \leq r \leq \infty$$

$$s^{\circ\prime}(r\ \ ,t) = 0 \qquad t \geq 0 \tag{3.46}$$

and $$Q^{\circ} = -2\pi r K_H D \frac{\partial s^{\circ\prime}}{\partial r} \qquad \text{as } r \to \infty$$

The last boundary condition can be written in terms of Q (equation 3.45b). To do this, equations (3.40) and (3.41) may be substituted into equation (3.31), resulting in the following expression in terms of drawdown:

$$f = s^{\circ\prime} + \frac{1}{\alpha}\frac{\partial s^{\circ\prime}}{\partial t} \tag{3.47}$$

Then substituting equation (3.47) into (3.45b) gives

$$Q = -2\pi r K_H D \left(\frac{\partial s^{\circ\prime}}{\partial r} + \frac{1}{\alpha}\frac{\partial}{t}\frac{\partial s^{\circ\prime}}{\partial r}\right)$$

or, from equation (3.46),

$$\frac{\partial Q^{\circ}}{\partial t} = \alpha(Q - Q^{\circ}) \tag{3.48}$$

This equation is linear; its solution, when Q is constant, is

$$Q^{\circ} = Q\ (1 - e^{-\alpha t}) \tag{3.49}$$

SOLUTION FOR FREE SURFACE DRAWDOWN AND AVERAGE DRAWDOWN

1. Double integral solution

Boulton (1963) obtained an equation of the same form as equation (3.42), assuming delayed yield from storage approximated it by an exponential function of time. By analogy, the solution of equation (3.42) and the initial and boundary conditions (3.45a,b) can be written as

$$f = \frac{Q}{4\pi T} W(\xi,u) \tag{3.50}$$

where: $W(\xi,u) = \int_0^\infty 2J_0(\xi,x)[1 - (\frac{1}{x^2+1})\exp(-\alpha t x^2/x^2+1) - G]\, dx/x$

$$G = \frac{x^2}{x^2+1} \exp[-\alpha N t(x^2+1)]$$

$$\xi = \sqrt{3K_v/K_H} * r/D = \sqrt{3} * r/B$$

$$N = (S + S_y)/S = 1 + S_y/S = 1 + 1/\sigma$$

and J_0 denotes the Bessel function of the first kind of zero order. The function G vanishes for $t > 0$, but is finite as t approaches zero and σt approaches a finite value.

To obtain a solution for the average drawdown s, it is necessary to first solve equation (3.44) to get

$$s^{\circ\prime} = s^\circ - s^{\circ 2}/2D = \frac{Q}{4\pi T} W^\circ(\xi,u) \tag{3.51}$$

where $W^\circ(\xi,u) = W(\xi,u) - \int_0^t e^{-\alpha(t-\tau)} \frac{\partial W(\xi,u)}{\partial \tau}\, d\tau$

Now, this quadratic equation may be solved for the free surface drawdown, giving

$$s^\circ/D = [1 - (1 - W^\circ(\xi,u)c)^{1/2}] \tag{3.52}$$

where $c = Q/2\pi K_H D^2$

The solution written in practical form is

$$(4\pi T/Q)\ s^\circ = \frac{4\pi K_H D^2}{Q}\ [1 - (1 - W^\circ(\xi,u)c)^{1/2}] \tag{3.53}$$

Now knowing s° and f, we can solve for average drawdown s using equation (3.40) written in dimensionless form as

$$\frac{4\pi Tf}{Q} = \frac{4\pi Ts}{Q} + \frac{2\pi K_H D^2}{Q}\frac{s^{\circ 2}}{D^2} - \frac{4\pi Ts}{Q}\frac{s^\circ}{D} \tag{3.54a}$$

or

$$\frac{4\pi Ts}{Q} = \left(\frac{4\pi Tf}{Q} - \frac{1}{c}\frac{s^{\circ 2}}{D^2}\right)/(1-s^\circ/D) \tag{3.54b}$$

Equations (3.50) and (3.51) were integrated numerically using Simpson's rule; equations (3.53) and (3.54b) were then evaluated numerically to obtain the dimensionless free surface drawdown and average drawdown. The results as a function of c, ξ, and τ_y are tabulated in appendix b, and shown graphically in figures 20 and 21a.

2. Single Integral Solution

If we assume S = 0 in equation (3.43) and consider the initial and boundary conditions given by equations (3.46) and (3.49), we

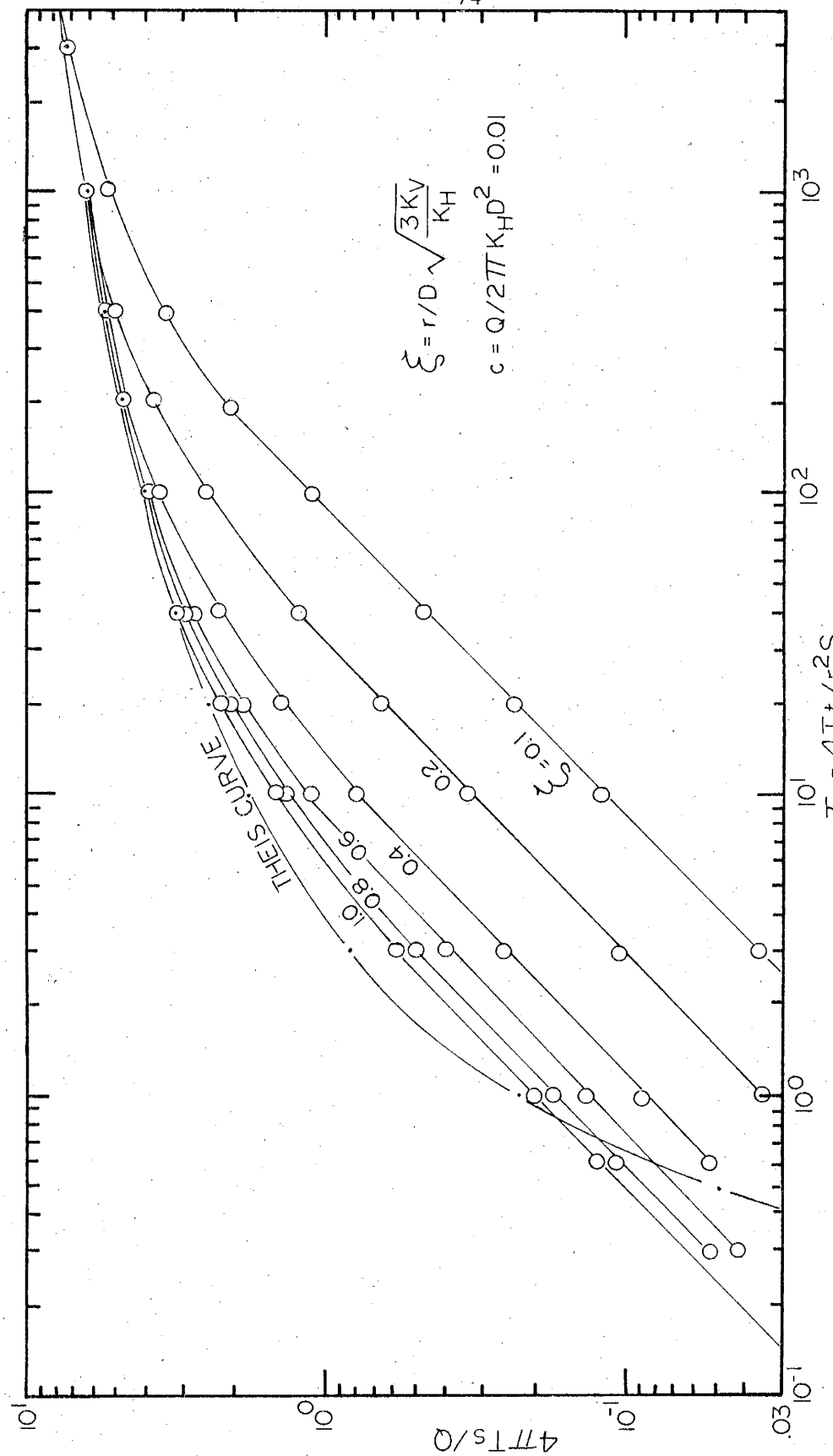

Figure 20. Dimensionless drawdown versus dimensionless time at the free surface predicted by the improved horizontal flow model (equation 3.53)

10^0 10^1 10^2 10^3 $\tau_a = \frac{4Tt}{r^2S}$ 10^4 10^5 10^6 10^7 10^8

ξ = 0.1
0.2
0.4
0.6
0.8
1.0
1.5
2.0
2.5
3.0

c = 0.08
c = 0.01
c = .08
.06
.04
.02

THEIS CURVE

10^{-3} 10^{-2} 10^{-1} 10^0 10^1 10^2 10^3 10^4 10^5

$\tau_y = \frac{4Tt}{r^2S_y}$

$\xi = \frac{r}{D}\sqrt{\frac{3K_v}{K_H}} = \frac{r}{B}\sqrt{3}$

$c = \frac{Q}{2\pi TK_H D^2}$

Figure 21a. Dimensionless average drawdown versus dimensionless time (equation 3.54b)

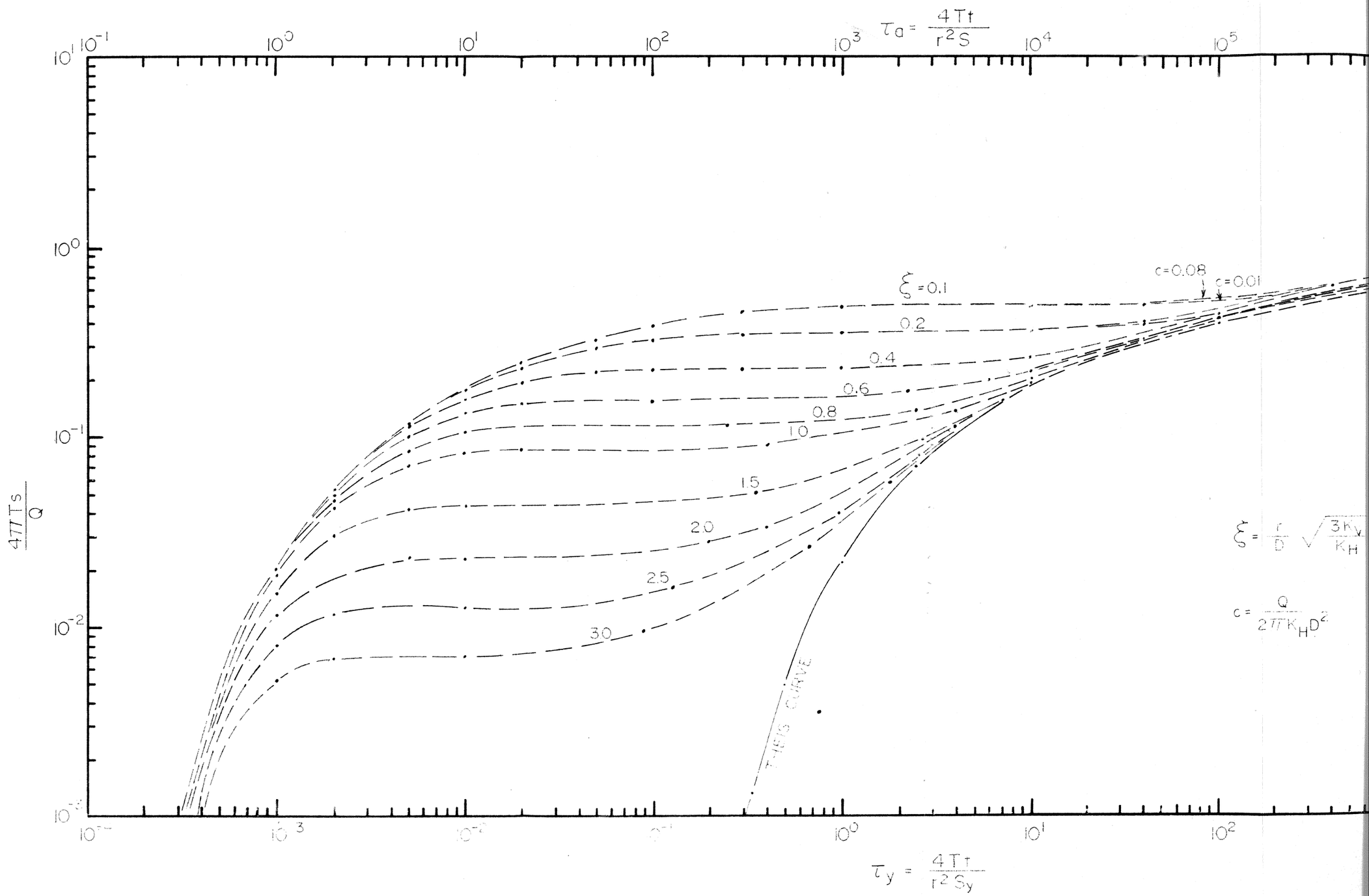
$\tau_a = \frac{4Tt}{r^2S}$
10^{1} 10^{-1} 10^{0} 10^{1} 10^{2} 10^{3} 10^{4} 10^{5}
10^{0}
10^{-1}
10^{-2}
10^{-3}
$\frac{4\pi Ts}{Q}$
ξ = 0.1
0.2
0.4
0.6
0.8
1.0
1.5
2.0
2.5
3.0
c=0.08
c=0.01
EARTH'S CURVE
$\xi = \frac{r}{D}\sqrt{\frac{3K_V}{K_H}}$
$c = \frac{Q}{2\pi K_H D^2}$
10^{-3} 10^{-2} 10^{-1} 10^{0} 10^{1} 10^{2}
$\tau_y = \frac{4Tt}{r^2 S_y}$

end up with a mathematical model similar in form to the one solved by Barenblatt, et al. (1960) for the motion of a liquid in fissured rocks. Its solution can be written as

$$s^{\circ\prime} = \frac{Q}{4\pi T} \int_0^\infty 2 \frac{J_0(\xi,x)}{x} \left[1 - \exp\left(\frac{-\alpha t x^2}{x^2+1}\right)\right] dx \qquad (3.55)$$

Now using equation (3.47) we can solve for f as

$$f = \frac{Q}{4\pi T} \int_0^\infty 2\frac{J_0(\xi,x)}{x} \left[1 - \frac{1}{x^2+1} \exp\left(\frac{-\alpha t x^2}{x^2+1}\right)\right] dx \qquad (3.56)$$

This is identical to equation (3.50) with G = 0 or S = 0, obtained by the first method of solution. The procedure used in the first solution can be followed to obtain an equation analogous to (3.53), for free surface drawdown, and then equation (3.54) can be used to solve for average drawdown.

REDUCTION TO THE SOLUTION OF LINEARIZED HORIZONTAL MODEL IN h^2

At sufficiently large time, which is determined by Boulton (1954) for the time factor $\tau = K_v t/S_y D > 5$, the value of integrals in equation (3.55) and (3.56) will be largely determined in the range of small x. Then equation (3.55) and (3.56) approximate to

$$f = s^{\circ\prime} = \frac{Q}{4\pi T} \int_0^\infty 2 \frac{J_0(\xi,x)}{x} \left[1 - \exp(-\alpha t x^2)\right] dx \qquad (3.57)$$

Rewritten in terms of $y = x\xi$ and $T_y = T t/r^2 S_y$, this becomes

$$f = s^{\circ\prime} = \frac{Q}{4\pi T} \int_0^\infty 2J_0(y)\left[1 - \exp(-T_y y^2)\right] dy/y$$

from Neuman (1972, p. 1035), it can be written

$$f = s^{\circ\prime} = \frac{Q}{4\pi T} \int_u^\infty \exp(-y) \frac{dy}{y} = \frac{Q}{4\pi T} W(u) \tag{3.58}$$

which is the Theis solution for $s^{\circ\prime}$.

Now, from equation (3.41), we have

$$s^\circ/D = (1 - (1 - W(u)c)^{1/2}) \tag{3.59}$$

which is the solution to the linearized horizontal model in h^2 (equation (3.12)).

At sufficiently large time, $\tau_y = 10^3$ (see figure 21b), the free surface drawdown and average drawdown practically coincide. Then equation (3.54a) can be written in terms of average drawdown as

$$\frac{4\pi Tf}{Q} = \frac{4\pi Ts}{Q} - \frac{4\pi T}{Q} \frac{s^2}{2D}$$

or by equation (3.58), as

$$\frac{4\pi Ts}{Q} = \frac{4\pi K_H D^2}{Q} (1 - (1 - W(u)c)^{1/2}) \tag{3.60}$$

which is also the solution for the linearized horizontal model in h^2, the Jacob correction.

C. Correlation and discussion

In section 3.8 we concluded that the linearized vertical flow models are valid only at early time for most practical purposes, whereas the nonlinear horizontal model and the linearized horizontal

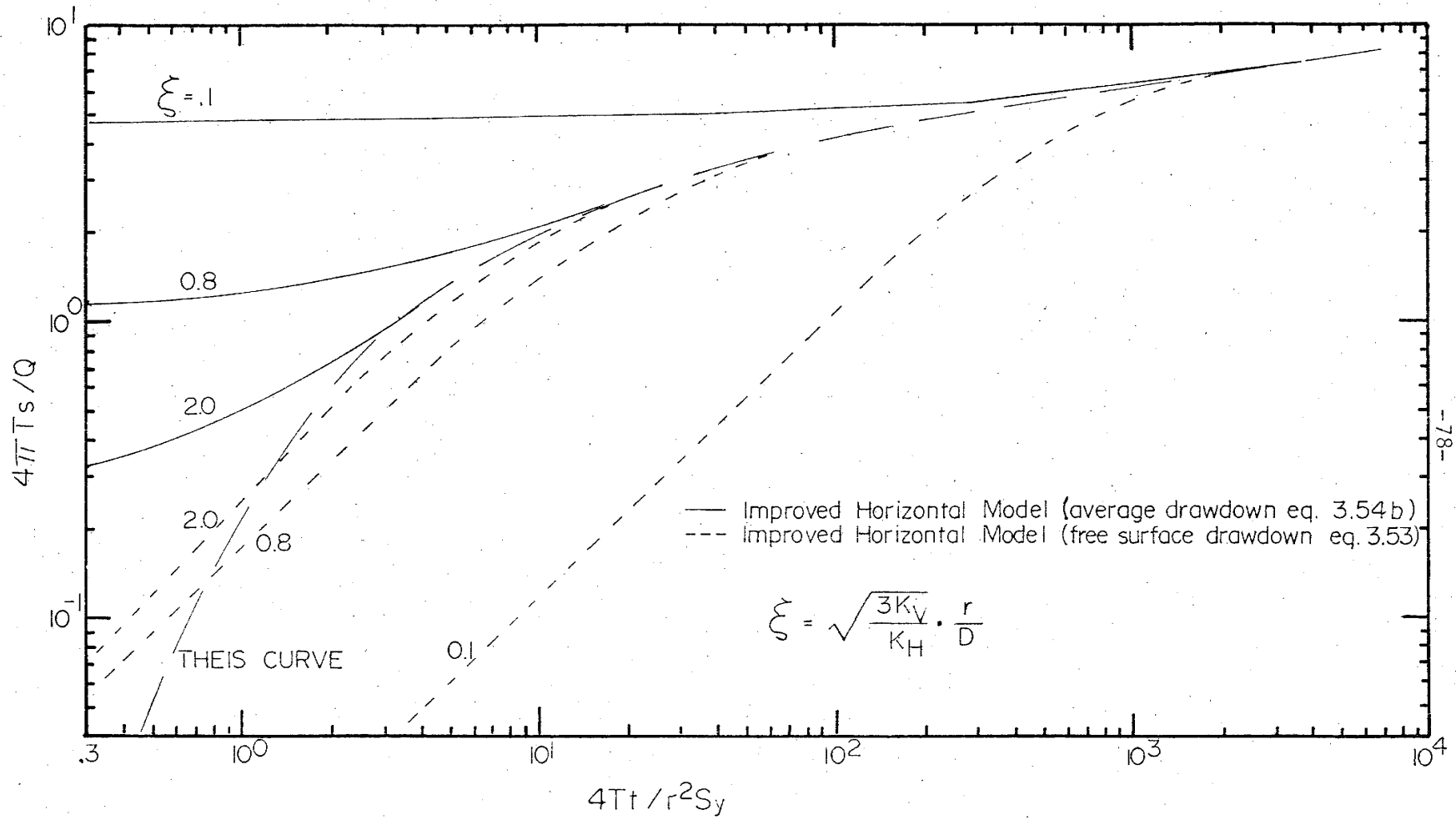

Figure 21b. Comparison between the average and the free surface drawdowns predicted by the improved horizontal flow model

model in h^2 are valid only at large time. Consequently we attempted in section 3.9 to provide a model combining the effects of vertical flow and thinning of the flow zone; see table 1 for a comparison of the models.

Now we will analyze the results of the proposed model to see how it handles the two limiting cases, i.e., the effects of vertical flow at early time and the flow zone thinning at large time.

To check how the improved horizontal model approximates the vertical flow component, we compared its results for small drawdown with those of the vertical model by Neuman (1972). Figure 22 shows that for all practical purposes the approximation to vertical flow is adequate. For clarity the results are tabulated in table 4.

Figure 23 shows a comparison of the improved horizontal model and vertical flow model by Boulton (1954) for free surface drawdown. The vertical flow effects are approximated fairly well for large values of ξ, but for small ξ the difference between the two models is very significant.

Streltsova (1972) and Streltsova, et al.(1973) approximated the vertical flow effects by assuming that the specific rate of the vertical flow varies linearly with the difference between the average head $\bar{\phi}$ and free surface head h. We used essentially the same assumption to incorporate the vertical flow component into the improved horizontal flow model. The main difference is that Streltsova assumed a constant saturated thickness, or small drawdown, whereas we make this assumption only in the storage term. (This is not very significant for the problem

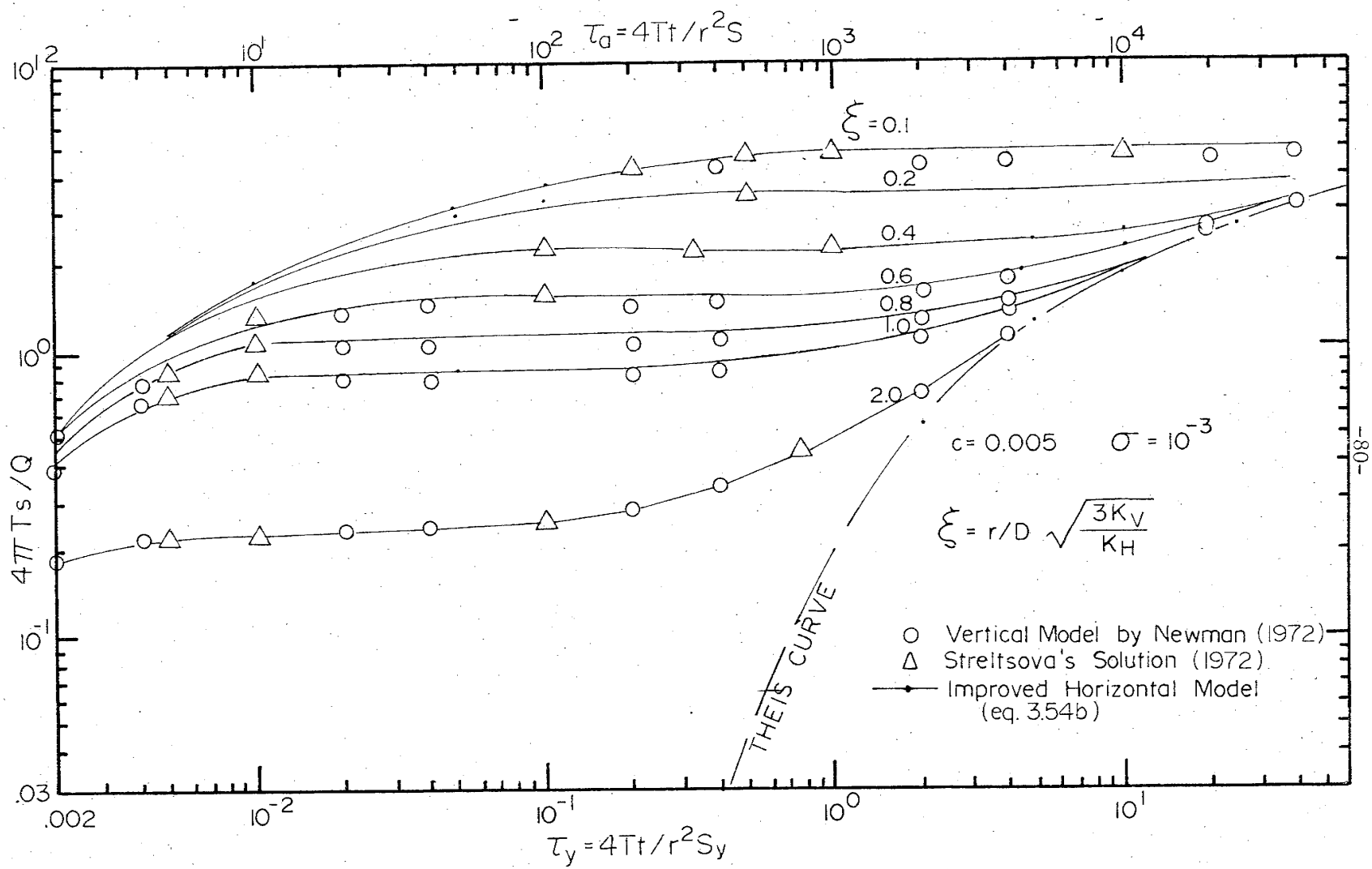

Figure 22. Comparison between the results of the improved horizontal model (equation 3.54b), Streltsova's solution (1972) and the results of the vertical flow model by Neuman (1972) for average dimensionless drawdown

Table 4. Comparison between dimensionless average drawdown ($4\pi Ts/Q$) obtained by the improved horizontal flow model and the vertical flow model by Neuman (1972) for small drawdown.

$$\% \text{ difference} = \frac{\frac{4\pi Ts}{Q}(\text{Improved horizontal model}) - \frac{4\pi Ts}{Q}(\text{Neuman, 1972})}{\frac{4\pi Ts}{Q}(\text{Neuman, 1972})} \times 100$$

$\xi = 2.0$				$\xi = 1.0$			
τ_y	$W(\xi,u)$	S_D	% difference	τ_y	$W(\xi,u)$	S_D	% difference
2×10^{-3}	0.184	0.188	-2.2	2×10^{-2}	0.841	0.794	5.9
4×10^{-2}	0.239	0.355	-2.1	4×10^{-1}	0.910	0.852	5.7
2×10^{-1}	0.283	0.385	-0.4	4×10^{0}	1.356	1.335	1.6
4×10^{0}	1.11	1.107	0.3	4×10^{1}	3.140	3.144	0.0
	$\xi = 0.8$				$\xi = 0.6$		
2×10^{-3}	0.466	0.405	15.0	2×10^{-3}	0.504	0.4439	13.5
2×10^{-2}	1.121	1.0312	8.7	2×10^{-2}	1.493	1.3418	11.3
2×10^{-1}	1.13	1.069	5.7	2×10^{-1}	1.555	1.4374	8.2
2×10^{0}	1.31	1.2748	2.8	2×10^{0}	1.69	1.583	6.8
2×10^{1}	2.5	2.516	-0.6	2×10^{1}	3.508	2.5827	-2.9
				4×10^{1}	3.1523	3.169	-0.5
	$\xi = 0.1$						
4×10^{0}	4.87	4.492	8.4				
4×10^{1}	4.96	4.665	6.3				
4×10^{2}	5.67	5.635	0.62				

where $S_D = 4\pi Ts/Q$ is the dimensionless drawdown by Neuman.

$W(\xi,u) = 4\pi Ts/Q$ is the dimensionless drawdown predicted by the improved horizontal flow model and $\tau_y = 4Tt/r^2S_y$

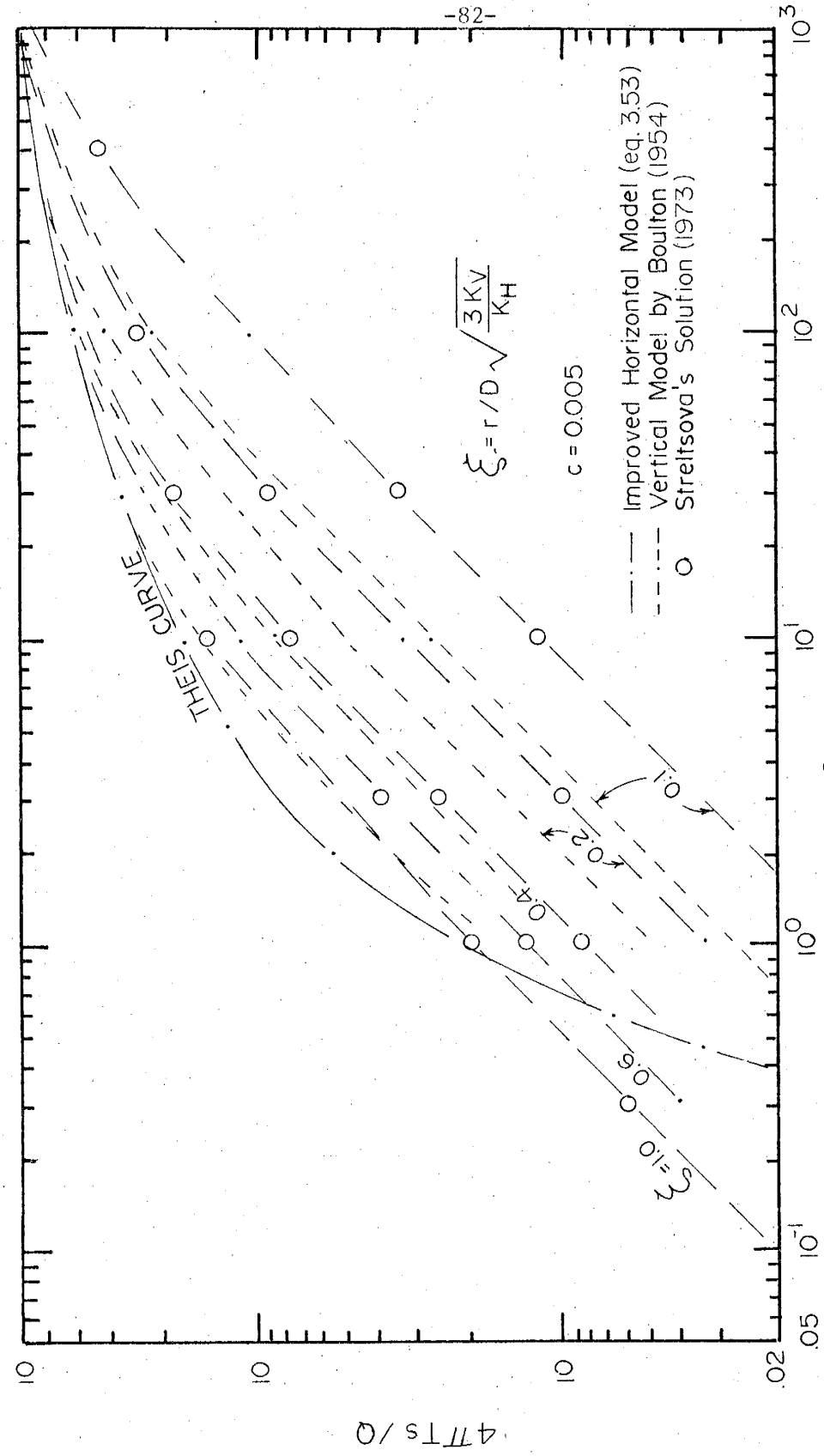

Figure 23. Comparison of free surface drawdown obtained by improved horizontal model (equation 3.53), vertical model by Boulton (1954) and Streltsova's solution (1973)

at hand; see section 3.3.) Hence the results of the two models should coincide for very small drawdown, as is the case in figures 22 and 23.

From this we can conclude that the difference between Streltsova's model and the improved horizontal model (as c approaches zero) on one hand, and the vertical model by Neuman or Boulton on the other, lies in the fact that the first two models represent only an approximation of the vertical flow rather than the exact vertical flow component. The assumption that $\alpha = 3K_v/S_y h(r,t) \approx$ a constant should not make any difference in the comparison to Boulton or Neuman's solution because both models have assumed that $h(r,t) \approx D$ (very small drawdown is taking place).

Streltsova, et al. (1973) claim that the difference between their results and Boulton's (1954) for free surface drawdown is due to the latter's assumption of a constant discharge, described by equation (5) of Streltsova. It can be written as

$$Q = 2\pi r K_H D \frac{\partial \overline{\phi}}{\partial r} = \text{const} \qquad \text{as } r = r_w \to 0$$

They describe a flux, due to the fall of the free surface, as

$$Q^\circ = 2\pi r k D \frac{\partial h}{\partial r}$$

(equation (11) of Streltsova)

which, since

$$\overline{\phi} = \frac{1}{\alpha} \frac{\partial h}{\partial t} + h$$

reduces to

$$Q^\circ = Q(1 - e^{-\alpha t}) \qquad \text{(equation (13) of Streltsova)}$$

However Boulton did not describe the flux by equation (5) of Streltsova; he used the following equation:

$$Q = 2\pi r k D \frac{\partial \phi}{\partial r} \qquad \text{(equation 8 of Boulton)}$$

where $\phi = \phi(r,z,t)$ is the actual head, not the average head. Obviously the equations used by Streltsova and Boulton to describe the flux are not comparable, except that both equations have been linearized and are valid only for small drawdown. For finite drawdown we have found that the flux should be of the form of equation (3.49),

$$Q^\circ = Q(1 - e^{-\alpha t})$$

where $Q = 2\pi r K \frac{\partial}{\partial r} (h\overline{\phi} - h^2/2)$

To check how the improved horizontal model handles flow zone thinning, we compared it with the nonlinear horizontal model by Kriz, et al.(1966). Figure 24 shows that for all values of c the two solutions practically coincide. This is expected, since in section 3.9B we theoretically reduced the solution for the proposed model to the solution of the linearized horizontal model in h^2, and in section 3.3 we showed that the nonlinear horizontal model and the linearized horizontal model in h^2 practically coincide.

So far we have concluded that the improved horizontal model approximates vertical flow and the flow zone thinning fairly well for all practical purposes. This model provides us with a new case or

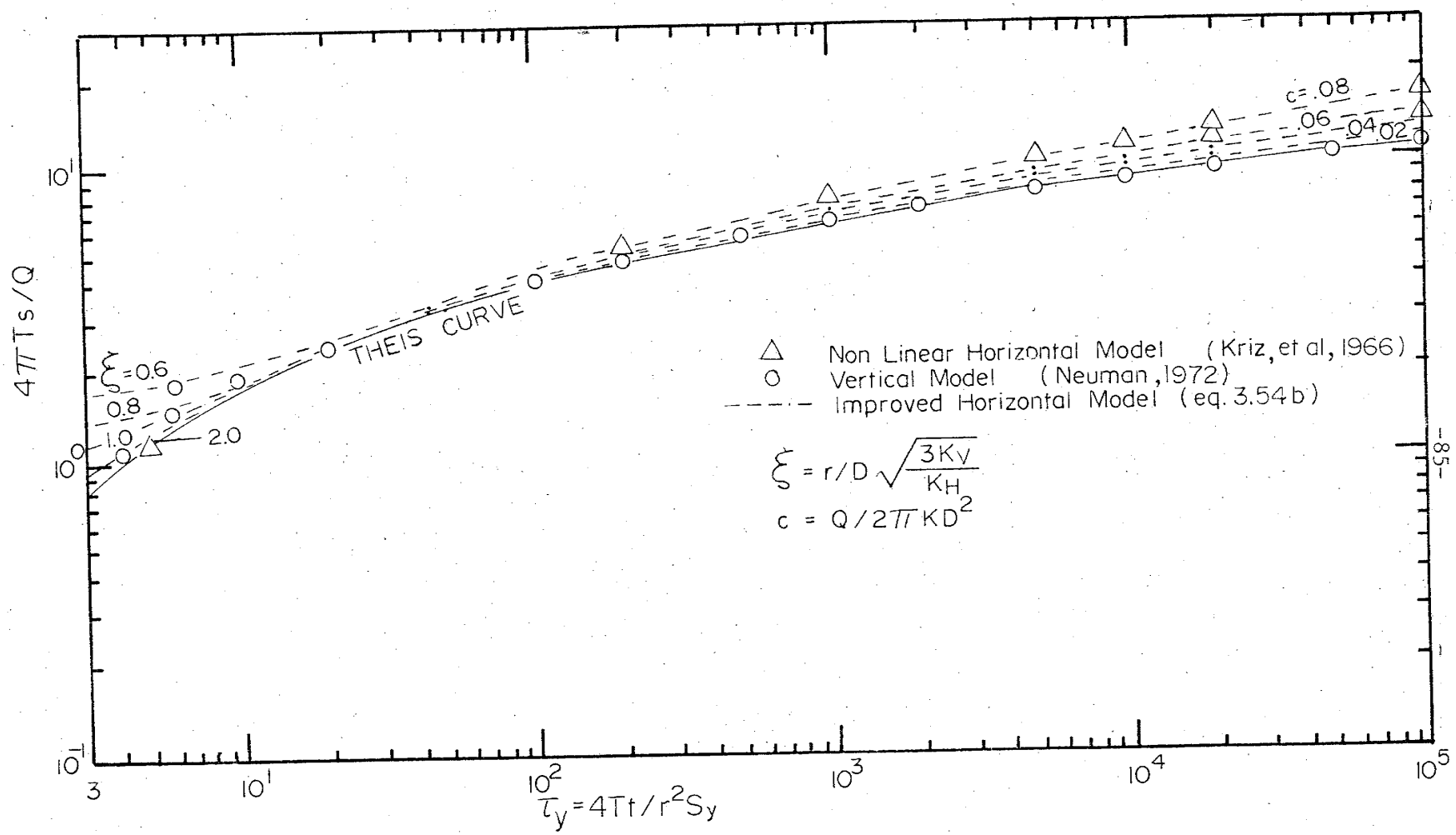

Figure 24. Comparison between the results of the improved horizontal model, nonlinear horizontal model by Kriz, et al. (1966) and the vertical model (Neuman, 1972)

zone, called the transition zone, where the effects of vertical flow and flow zone thinning interact. As illustrated in figure 25, the significance of this zone is a function of the parameters c and ξ. The figure shows that the period of time occupied by the horizontal segment of the time-drawdown curve becomes less as c increases. As c approaches zero this horizontal segment occupies a longer period of time, as is also the case with the results of Boulton (1954), Dagan (1967a) and Neuman (1972). Thus these solutions should be considered as particular examples of a more general solution that takes into account the flow zone thinning as well as the vertical flow effects.

D. Equation for Numerical Simulations

Ideal boundary conditions and water-bearing characteristics are rarely if ever found in nature; thus, analytical approaches, when applied to groundwater systems often become oversimplified. Most aquifers are heterogeneous and anisotropic with irregular boundaries. An adequate simulation of these complex systems, however, can be accomplished using digital computer solutions of a mathematical model. This provides a means for predicting the effects of future groundwater development.

Most of the mathematical models existing in literature (Prickett, et al.(1971), Pinder, et al. (1968) and Brutsaert, et al. (1972)) are subject to the Dupuit-Forchheimer assumptions and should be used with these limitations in mind. Cooley (1974) used the linearized vertical flow model, which is valid only for a small drop of the water table.

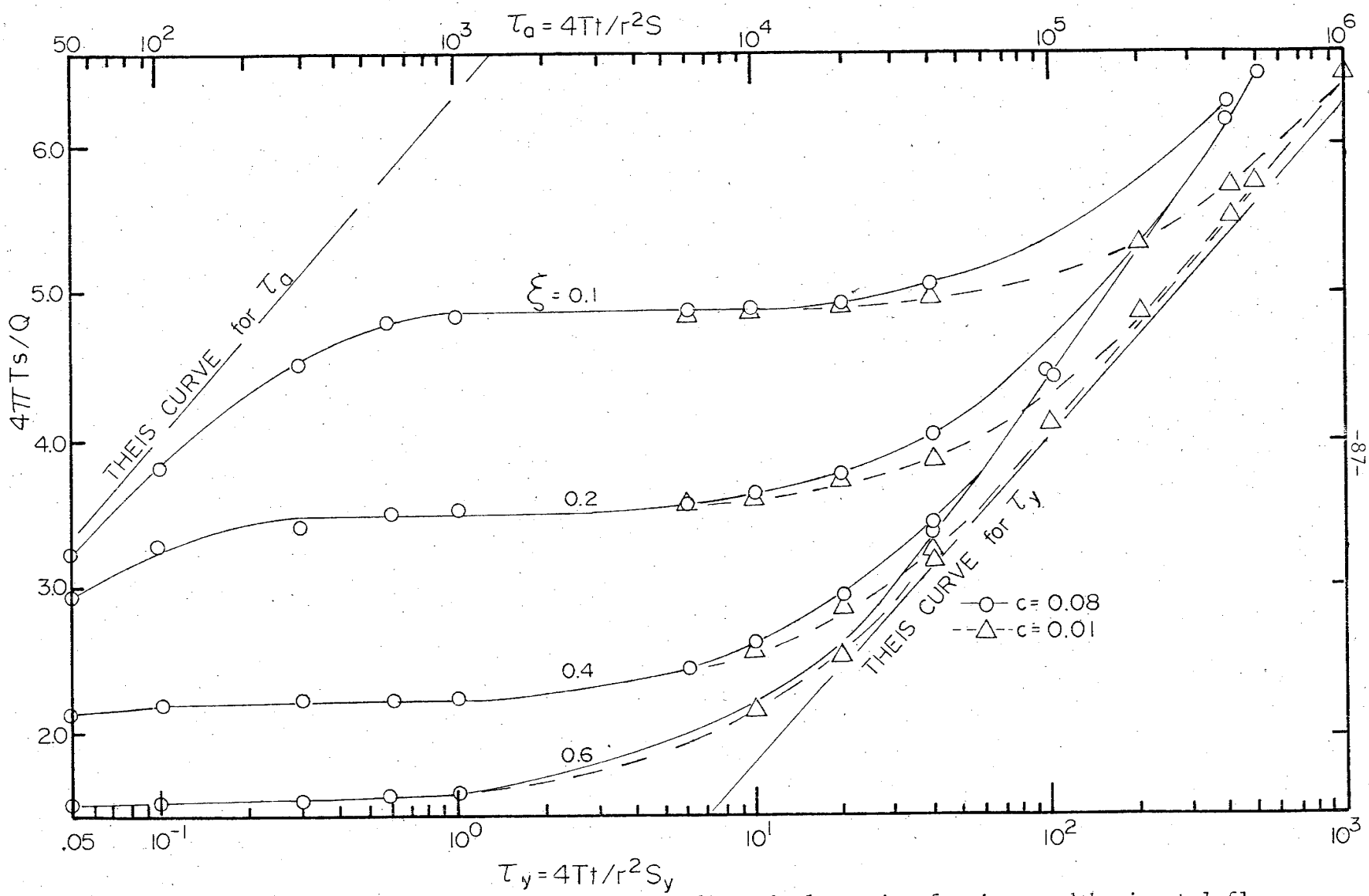

Figure 25. Dimensionless average drawdown versus dimensionless time for improved horizontal flow model (equation 3.54b)

The analysis in section 3.9B leading to equation (3.27) can be generalized for a nonhomogeneous medium and a source term as follows

$$\frac{\partial}{\partial x}\left(K_x \frac{\partial \phi^{*2}}{\partial x}\right) + \frac{\partial}{\partial y}\left(K_y \frac{\partial \phi^{*2}}{\partial y}\right) = Q + S_y \frac{\partial h}{\partial t} + S_s \frac{\partial \phi^{*2}}{\partial t} \qquad (3.61)$$

where Q = net rate of withdrawal per unit area

$$\phi^{*2} = h\bar{\phi} - h^2/2$$

This equation contains two unknowns. To solve it numerically a second equation, from equation (3.30)

$$\frac{\partial h}{\partial t} = \frac{3K_z}{S_y}\left(\frac{\phi^{*2}}{h^2} - \frac{1}{2}\right) \qquad (3.62)$$

can be used. Substituting this into equation (3.61) gives

$$\frac{\partial}{\partial x}\left(K_x \frac{\partial \phi^{*2}}{\partial x}\right) + \frac{\partial}{\partial y}\left(K_y \frac{\partial \phi^{*2}}{\partial y}\right) = Q + 3K_z\left(\frac{\phi^{*2}}{h^2} - \frac{1}{2}\right) + S_s \frac{\partial \phi^{*2}}{\partial t} \qquad (3.63)$$

which can be solved iteratively with equation (3.62). Initial values of h can be used in equation (3.63) to find ϕ^* and then equation (3.62) can be used to calculate new values of h. Then the average head ($\bar{\phi}$) can be determined from

$$\bar{\phi} = (\phi^{*2} + h^2/2)/h$$

Equation (3.62) can be written in terms of ϕ^{*2} as

$$\phi^{*2} = \frac{S_y}{6K_z} h \frac{\partial h^2}{\partial t} + \frac{h^2}{2} \qquad (3.64)$$

Substituting equation (3.64) into equation (3.61) for ϕ^{*2} we get

$$\frac{\partial}{\partial x}\left(\frac{S_y}{3}\frac{K_x}{K_z}\frac{\partial h}{\partial x}\frac{\partial h^2}{\partial t}\right) + \frac{\partial}{\partial x}\left(\frac{S_y}{3}\frac{K_x}{K_z}\,h\,\frac{\partial^2 h^2}{\partial x \partial t}\right) + \frac{\partial}{\partial x}\left(K_x\frac{\partial h^2}{\partial x}\right) +$$

$$\frac{\partial}{\partial y}\left(\frac{S_y}{3}\frac{K_y}{K_z}\frac{\partial h}{\partial y}\frac{\partial h^2}{\partial t}\right) + \frac{\partial}{\partial y}\left(\frac{S_y}{3}\frac{K_y}{K_z}\,h\,\frac{\partial^2 h^2}{\partial y \partial t}\right) + \frac{\partial}{\partial y}\left(K_y\frac{\partial h^2}{\partial y}\right)$$

$$= \frac{S_y}{h}\frac{\partial h^2}{\partial t} + \frac{Q}{2} + S_s\frac{\partial h^2}{\partial t} + \frac{S_s S_y}{3K_z}\left(\frac{\partial h}{\partial t}\frac{\partial h^2}{\partial t} + h\,\frac{\partial^2 h^2}{\partial t^2}\right) \quad (3.65)$$

Even though equation (3.65) seems to be complicated because of the third order derivative, it has the advantage of solving directly for the free surface height (h). Then the average head $\overline{\phi}$ can be determined from

$$\overline{\phi} = \frac{1}{\alpha}\frac{\partial h}{\partial t} + h$$

Equation (3.63) or equation (3.65) are valid for heterogeneous, anisotropic media, and they approximate the vertical flow effects fairly well. Their most important limitations are 1) the aquifer is bounded by a horizontal bottom and 2) fully penetrating constant head (river, lake) boundary conditions (the latter is in all of the widely used models). Either one of these equations may be used as a field equation suitable for numerical simulation if vertical flow effects are of significance.

E. Application to Well Flow Analysis

To show how the proposed model can be used to determine the hydraulic properties of an anisotropic unconfined aquifer from pumping

test data, two methods are presented. Pumping and observation wells that are perforated throughout the saturated thickness are used in this analysis.

TYPE CURVE METHOD

In section 3.9B equation (3.54b) was solved for dimensionless average drawdown as a function of $\tau_y = 4Tt/r^2S_y$, ξ, and c. The results are tabulated in appendix B and plotted against values of τ_y on logarithmic paper in figure 21a. Two families of type curves were constructed analogous to those of Boulton (1963) and Prikett (1965); they will be referred to as type A and type B curves. The curves which lie to the left of the values of ξ are the type A curves and the ones to the right are the type B curves.

To describe how the type curves are used to determine the aquifer parameters, we shall follow a method similar to that used by Prickett (1965) in connection with Boulton's theory. Observed values of drawdown s^* at a given observation well are plotted on logarithmic paper against the values of time t^*. Then a matching procedure consisting of the following three steps is utilized:

(1) First superimpose the time drawdown field data on the type A curves, keeping the horizontal and vertical axes of both graphs parallel to each other. Match as much of the early-time drawdown field data to a particular type curve as possible. The value of ξ corresponding to this type curve is noted. A match point at the intersection of the major axes is selected and marked on the time drawdown field data curve. The coordinates of this match point are

s^* and $W(\xi,\tau_a,c)$ along the vertical axis and t^* and $\tau_a = 4Tt/r^2S$ along the horizontal axis. Then the transmissivity T and the elastic storage S can be calculated as

$$T = c_1 \frac{QW(\xi,\tau_a,c)}{s^*} \tag{3.66}$$

and

$$S = c_2 \frac{Tt^*}{r^2\tau_a} \tag{3.67}$$

where c_1 and c_2 are constants which depend on the units used. If cgs units are used $c_1 = 1/4\pi = 0.0796$, and $c_2 = 4$. If a gallon-day-foot system of units is used, $c_1 = 114.6$ and $c_2 = 0.5348$.

(2) Superimpose the time drawdown field data on the type B curves keeping the vertical and horizontal axes of both graphs parallel to each other. Match as much as possible of the latest time drawdown data to the type B curve. This curve should have the same value of ξ as that of the type A curve used earlier. The value of c should also be noted. A new match point is selected at the intersection of the major axes, and its coordinates s^*, $W(\xi,\tau_y,c)$, t^* and τ_y are noted. Then the transmissivity T is calculated from equation (3.61). The relationship

$$T = c_3 \frac{Q\,c}{D} \quad , \tag{3.68}$$

where $c_3 = 1/2\pi = 0.1592$ in cgs units, may also be used, but since at intermediate time the type B curves show only a slight separation for different values of the parameter c, it is recommended that the value of transmissivity be obtained by equation (3.66).

The specific yield can be calculated from

$$S_y = c_2 \frac{Tt^*}{r^2} \tau_y \tag{3.69}$$

where c_2 is the same as in (3.67)

(3) Now that we have determined the transmissivity, elastic storage and specific yield of the aquifer, we can calculate the rest of the parameters:

the horizontal permeability,

$$K_H = T/D \tag{3.70}$$

the vertical permeability,

$$K_v = \xi^2 \frac{K_H}{3} \frac{D^2}{r^2} \tag{3.71}$$

and finally the specific storage,

$$S_s = S/b \tag{3.72}$$

SEMILOGARITHMIC METHOD

Figure 26 shows a plot of $W(\xi,\tau_y,c)$ versus τ_y on semilogarithmic paper. Three segments of this curve can be identified. The late drawdown data tend to fall on a curve that approaches a straight line as c approaches zero; the intermediate data tend to fall on a horizontal line, whereas the third segment or the early data show nearly a straight line. Equation (3.60), rewritten as

10^0 10^1 10^2 10^3 10^4 10^5 10^6 10^7 10^8

$\tau_a = 4Tt/r^2S$

$\xi = 0.1$

THEIS CURVE for τ_a

$\epsilon = 0.08$

$\epsilon = 0.01$

0.2

0.4

0.6

0.8

1.0

2.0

THEIS CURVE for τ_y

10^{-3} 10^{-2} 10^{-1} 10^0 $\tau_y = 4Tt/r^2S_y$ 10^1 10^2 10^3 10^4 10^5

Figure 26. Dimensionless average drawdown versus dimensionless time for improved horizontal flow model (equation 3.54b)

$\tau_a = 4Tt/r^2S$

$\frac{4\pi Ts}{Q}$

8.0
7.0
6.0
5.0
4.0
3.0
2.0
1.0
0

10^{-1} 10^{0} 10^{1} 10^{2} 10^{3} 10^{4} 10^{5}

THEIS CURVE for τ_a

$\xi = 0.1$

0.2

0.4

0.6

0.8

1.0

2.0

THEIS CURVE for τ_y

10^{-4} 10^{-3} 10^{-2} 10^{-1} 10^{0} $\tau_y = 4Tt/r^2S_y$ 10^{1} 10^{2}

$$s = \frac{Q}{2\pi T} \frac{2}{c} (1 - (W(u) \times c)^{1/2}) \qquad (3.73)$$

describes the late drawdown data. Jacob (1950) showed that, after sufficiently large time has elapsed for a given distance,

$$W(u) = 2.303 \log_{10} 2.25\ Tt/r^2 S_y \qquad (3.74)$$

Substituting this value of W(u) in equation (3.73), we get

$$s = \frac{Q}{4\pi T} \frac{2}{c} (1 - (1 - 2.303 \times c \log_{10} 2.25\ Tt/r^2 S_y)^{1/2}) \qquad (3.75)$$

This shows that the late drawdown data do not fall on a straight line, but on a curve which is a sensitive function of c. Thus, semilogarithmic method cannot be used unless the observed drawdown has been corrected for the flow zone thinning (Jacob correction).

ANALYSIS OF PUMPING TEST DATA

Neuman (1975, pp. 338-341) described a pumping test performed in the Vallee de la Garonne, Gironde, France. The aquifer was pumped for 48 hours and 50 minutes at an average rate of 53 m^3/h; its initial saturated thickness was 8.24m. He calculated the aquifer parameters at r = 10 m and 30 m using both the type curve and the semilogarithmic methods. His results will be compared with the results we obtained for the same pumping test.

In figure 27, circles show the variation of time-drawdown field data at r = 10 m. The solid lines are traces of the type curve that fits with the field data, and the squares are the match

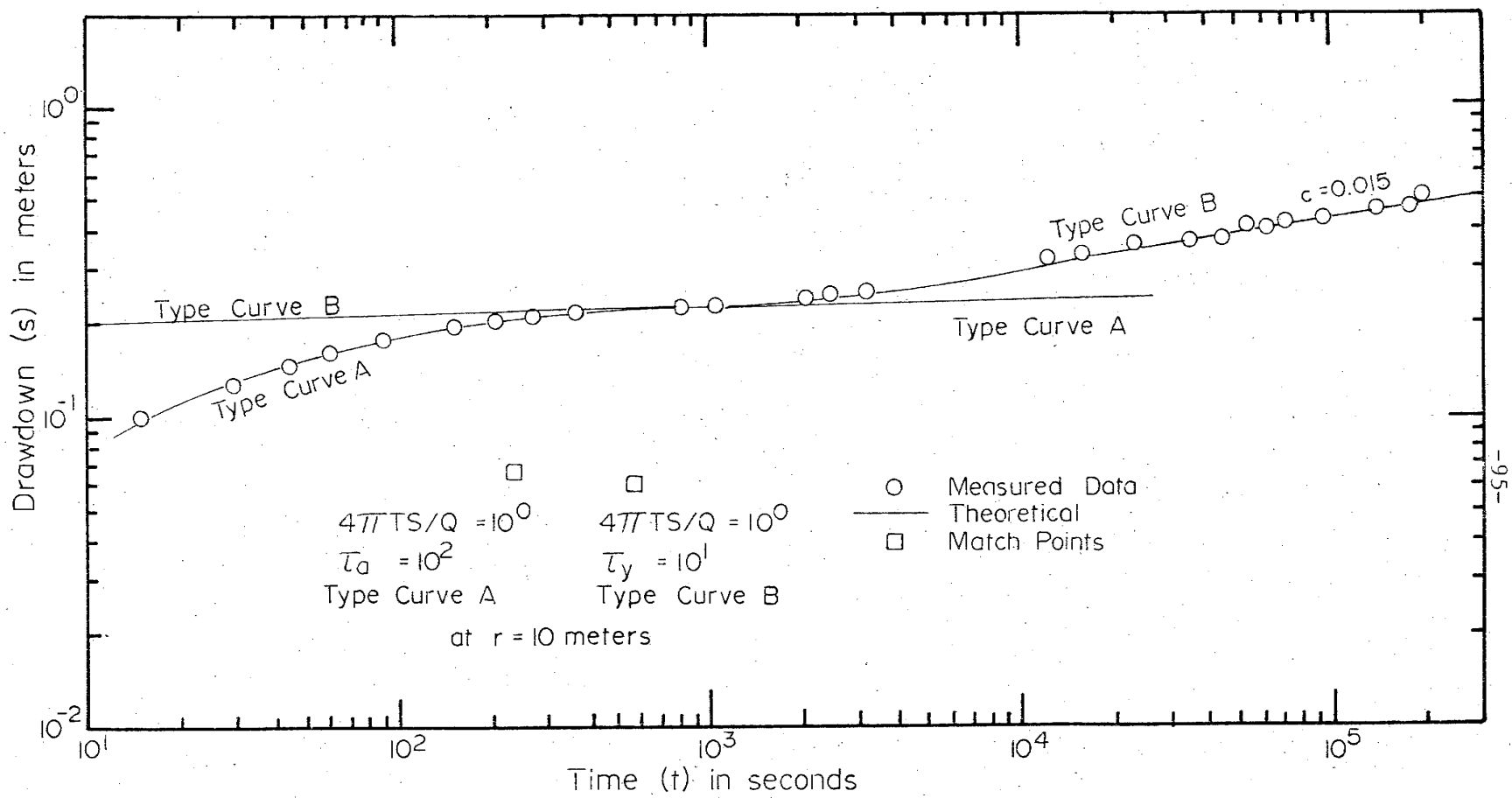

Figure 27. Logarithmic plot of drawdown versus time at Saint Pordon de Conques

points. The coordinates of the match point for the observation well 10 m away and the type A curve for $\xi = 0.2$ are $W(\xi,\tau_a,c) = 1$, $\tau_a = 100$, $s^* = 0.065$ m, and $t^* = 230s = 0.064$ h. Hence according to equations (3.66) and (3.67),

$$T = \frac{(0.0796)(53)(1)}{(0.065)} = 64.9 \text{ m}^2/\text{h}$$

and

$$S = \frac{(4)(64.9)(0.064)}{(100)(100)} = 1.65 \times 10^{-3}$$

The coordinates of the match point that corresponds to the same observation well and the type B curve for $\xi = 0.2$ are $W(\xi,\tau_y,c) = 1$, $\tau_y = 10$, $s^* = 0.06$ m, $t^* = 570s = 0.1583$ h and $c = 0.015$. Now equations (3.66) and (3.67) give

$$T = \frac{(0.0796)(53)(1)}{0.06} = 70.3 \text{ m}^2/\text{h}$$

and

$$S_y = \frac{(4)(70.3)(0.1583)}{(100)(10)} = 4.5 \times 10^{-2}$$

Now that we know T, we can also calculate $c = 53/2(70.3)(8.24) = 0.0146$; a value of 0.015 was obtained by curve matching. Using the type A curve Neuman calculated $T = 65.9$ m^2/h and $S = 1.45 \times 10^{-3}$; using the type B curve, $T = 70.3$ m^2/h and $S_y = 3.9 \times 10^{-2}$.

We used equations (3.70-3.72) to obtain the rest of the aquifer parameters.

$$K_H = 70.3/8.24 = 8.5 \text{ m/h}$$

$$K_v = \frac{(0.2)^2\ (8.53)(8.24)^2}{(3)(100)} = 7.8 \times 10^{-2}\ \text{m/h}$$

and finally,

$$S_s = 1.65 \times 10^{-3}/8.24 = 2.0 \times 10^{-4}\ \text{m}^{-1}.$$

Since the late data give a better fit with the type curves than the early data, we chose the value of $T = 70.3\ m^2/h$ to calculate horizontal permeability.

The results obtained using the improved horizontal flow model and those obtained by Neuman (1975) are practically identical without the corrected drawdown. However, this is the case only because the drawdown is small compared to the initial saturated thickness ($s/D = 0.06$).

When the drawdown is a large fraction of the initial saturated thickness it must be corrected before applying the linearized vertical flow model method by Neuman (1975). This can be demonstrated by using the results of Jacob (1963) for T and S_y for an aquifer near Wichita, Kansas (Wenzel, 1942). Their test lasted for 18 days of continuous pumping at 1,000 gpm. The average initial thickness of saturated material was 28.8 feet, and after the 18 day period of pumping it was 22.3 feet. Jacob found that $T = 129{,}000$ gpd per ft^2 and $S_y = 0.47$ using the observed drawdown, whereas the corrected drawdown in the same observation wells gives $T = 154{,}000$ gpd per ft^2 and $S_y = 0.35$. To simulate drawdown, we use the value $T = 154{,}000$ gpd per ft^2 to calculate the parameter $c = Q/2\pi KD^2 = 0.056$ and then we calculate the drawdown from the theoretical results of the improved horizontal flow model for $c = 0.056$ and $\xi = 1.0$ and 0.1. The

calculated drawdowns were then corrected for the flow zone thinning using the Jacob correction (Jacob, 1963). Using the above values of T, S_y and ξ we also calculated the drawdown from the linearized vertical flow model (Neuman, 1972). Figures 28a and 28b show the calculated drawdown and the corrected drawdown for $\xi = 1$ and 0.1 respectively. Obviously the calculated drawdown from Neuman, 1972 and the corrected drawdown (obtained from the improved horizontal flow model) are practically identical. They produce a straight line at large times and a horizontal line at intermediate times; the calculated drawdown from the improved horizontal flow model shows a curve at large time and a horizontal line at intermediate time.

The straight line portion of the drawdown in figures 28a and 28b was used to calculate T and S_y; we found that $T \approx 154{,}000$ gpd per ft^2 and $S_y = 0.35$. Correcting the drawdowns at intermediate time does not seem to be important for $\xi = 1.0$ (figure 28a), whereas for $\xi = 0.1$ (figure 28b) the correction is very significant. It was not possible to determine the rest of the aquifer parameters K_v and K_v/K_H, using Neuman's semilogarithmic method (Neuman, 1975) because of the limited values for $T_{y\beta}$ and $1/\beta$ given by Neuman.

We conclude from this discussion that the semilogarithmic method recommended by Neuman, 1975, is a very practical method and should be used to determine the aquifer parameters provided that we correct the observed drawdowns for the flow zone thinning (Jacob, 1963) at large time as well as at intermediate time. The correction is especially important at intermediate time for observation wells close to the pumping well. This method eliminates the subjective curve matching

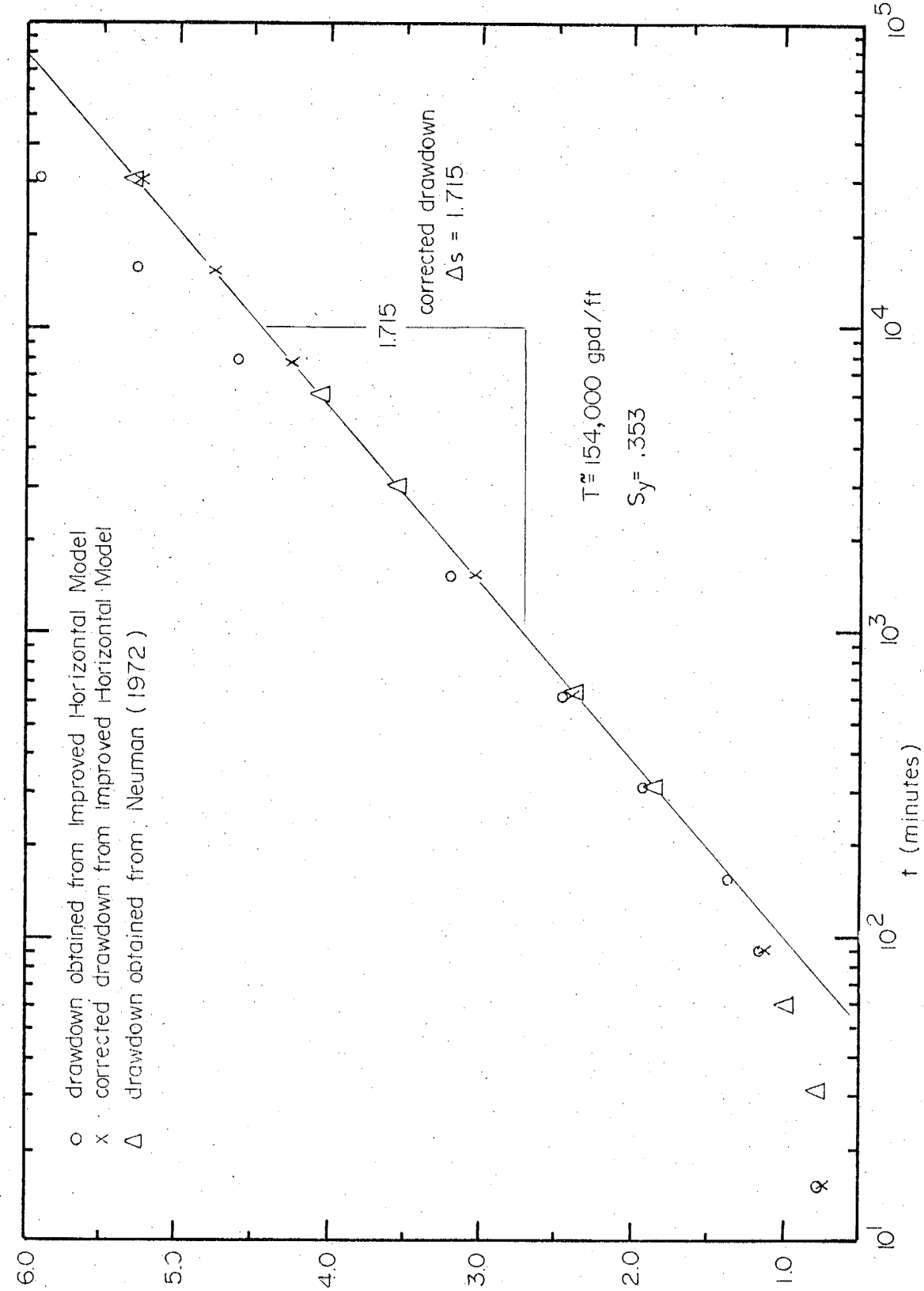

Figure 28a. Semilogarithmic plot of time versus drawdown ($\xi = 1.0$)

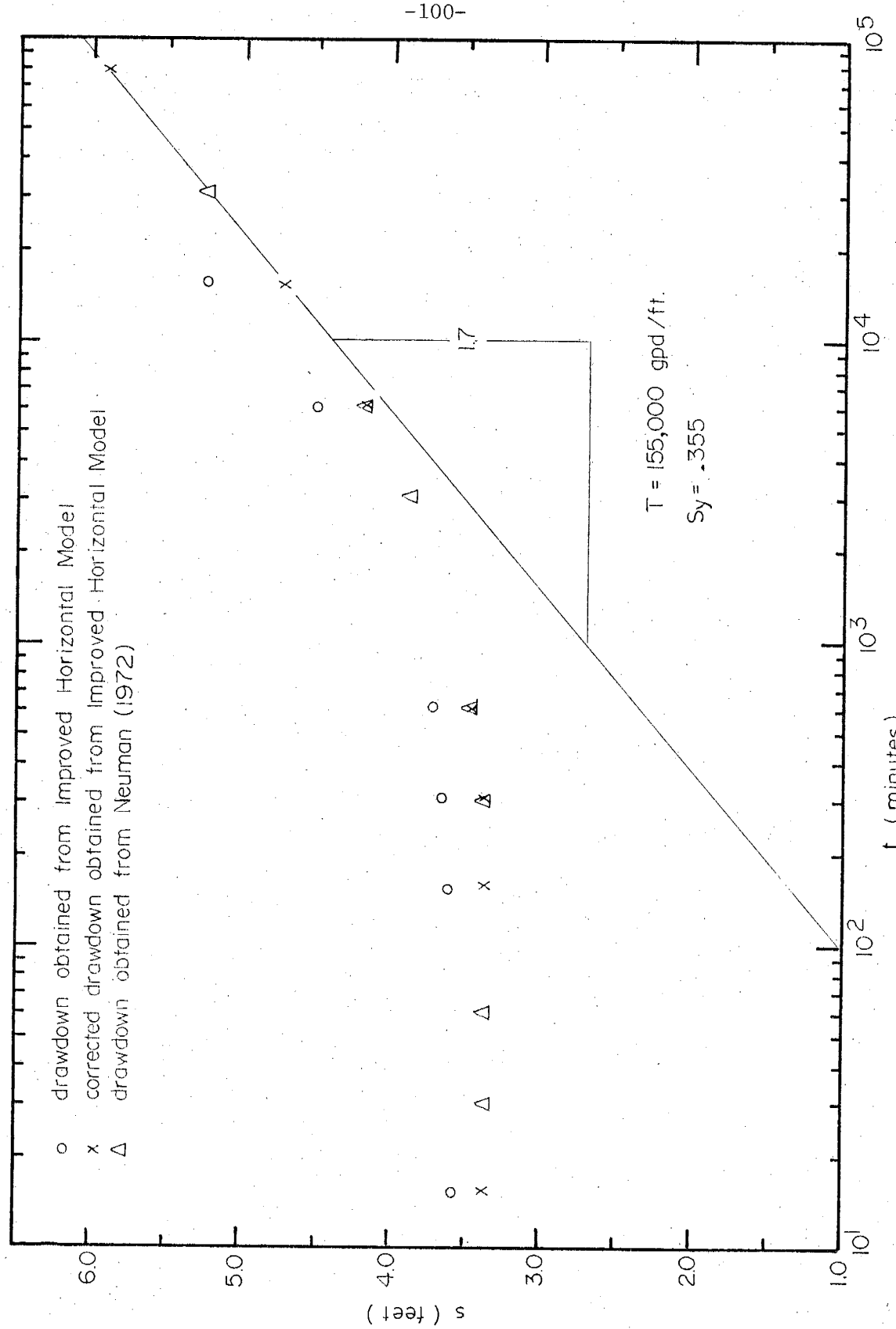

Figure 28b. Semilogarithmic plot of time versus drawdown ($\xi = 0.1$)

involved in the type curve method.

3.10 Summary and Conclusion

The problem of axisymmetric flow to a fully penetrating pumping well has been analyzed using the nonlinear and the linearized horizontal flow models, the potential flow model and the linearized and the nonlinear variably saturated models. The following conclusions have been reached:

1) The parameter s/D can serve as a criterion for determining the effects of the flow zone thinning. The larger the value of this parameter, the larger the effects. The critical value is s/D = 0.2 with an error of less than 10%. The linearized horizontal model in h^2 (Jacob correction) approximates the flow zone thinning fairly well for all values of s/D.

2) The parameter $r/B = \sqrt{K_V/K_H}\ (r/D)$ can serve as a criterion in determining the importance of vertical flow effects. The smaller the value of this parameter, the larger will be the effects of the vertical flow. The critical value is r/B = 4.0.

3) The unsaturated zone can be neglected provided that $h_{cr}/D \leq 0.07$ and deep observation wells ($z/D \leq 0.5$) or fully penetrating observation wells are being used. For shallow observation wells there is about a 30% error at dimensionless time $K_V t/S_y D \leq 1 \times 10^{-1}$, but later this error decreases rapidly.

4) The nonlinear horizontal flow model and linearized horizontal model in h^2 are valid provided that $h_{cr} \leq 0.07$ and $r/B = \sqrt{K_V/K_H}\ (r/D) \geq 4.0$.

5) The horizontal flow model has been improved by a correction developed to account for the combined effects of vertical flow and flow zone thinning. A new field equation suitable for numerical simulations, combining the effects of flow zone thinning and vertical flow, has also been obtained.

6) The semilogarithmic method (Neuman, 1975) is a very practical method and should be used to determine the aquifer parameters provided that the observed drawdown is corrected for the flow zone thinning (Jacob correction).

CHAPTER 4

Theoretical Models for flow to Parallel Drains

4.1 Introduction

When natural drainage is inadequate, irrigated agricultural lands in arid or semiarid climates, and substantial groundwater discharge areas in humid climates often undergo water table rises, creating water-logged lands. To improve drainage, parallel drains such as drainage ditches or tile drains may be utilized. This research is limited to shallow horizontal aquifers underlain at uniform depth by an impermeable boundary. Only fully penetrating parallel open ditches (figure 29) will be considered.

Various models (Table 5) will be analyzed systematically in investigating the significance of the assumptions and approximations involved in the horizontal model in order to establish its validity and limitations.

4.2 Horizontal Flow Model

Equation (2.23) is the basic partial differential equation in horizontal flow models (for an aquifer bounded by an impervious horizontal bottom). Neglecting the infiltration term and the elastic storage of the aquifer, we can rewrite this equation in one dimension as

$$K_H \frac{\partial}{\partial x} \left(h \frac{\partial h}{\partial x}\right) = S_y \frac{\partial h}{\partial t} \qquad (4.1)$$

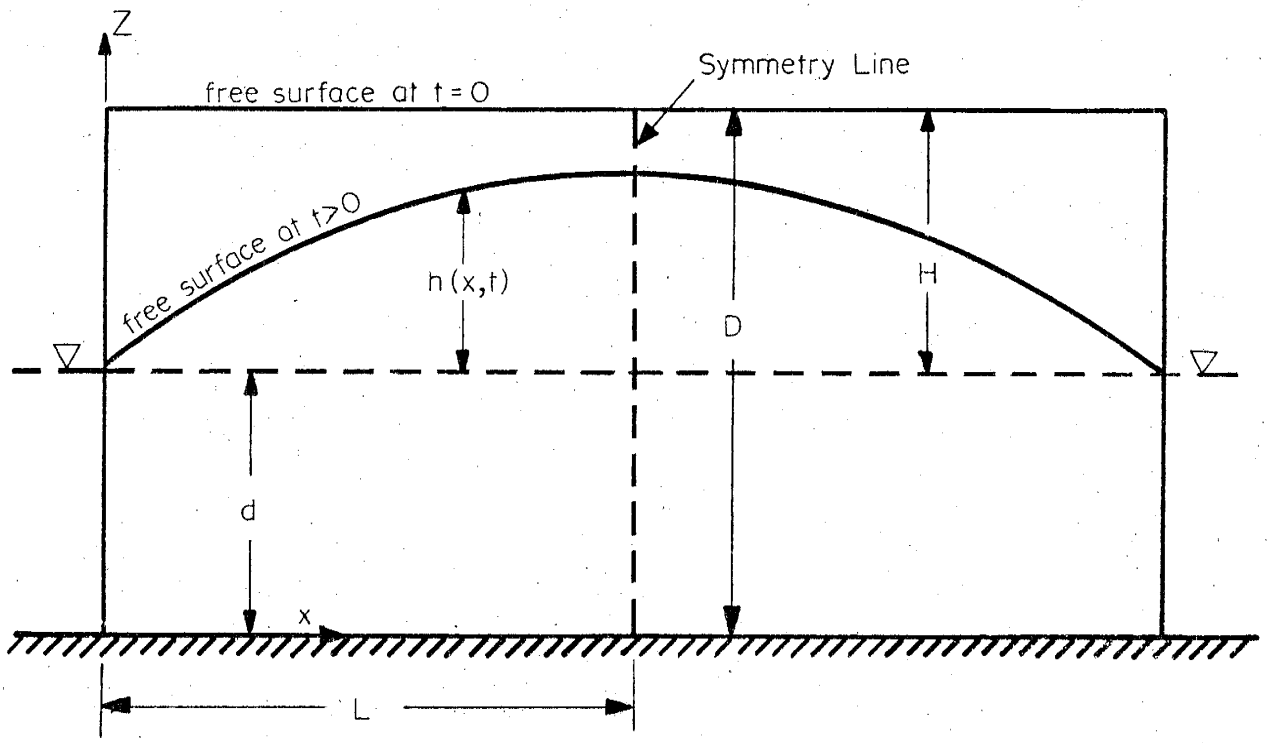

Figure 29. Drainage ditches

Table 5. Different theoretical models and their limitations, considered in flow to parallel drains, $h = h(r,t)$ is the height of the phreatic surface above a datum and D is the initial saturated thickness.

Theoretical Model	Assumptions			Author
	Vertical flow	Flow zone thinning ($h \neq$ constant)	Unsaturated zone	
Horizontal Flow Model:				
linear in h	no	no	no	Dumm(1954)
linear in h^2	no	yes ($h \approx D$ in storage term)	no	Werner (1957)
nonlinear	no	yes	no	Boussinesq (1904) Van Schilfgaarde (1963) Moody (1966) Verma (1969)
Potential Flow Model:				
nonlinear	yes	yes	no	Verma (1969)
Variably Saturated Flow Model:				
nonlinear	yes	yes	yes	Verma (1969)

This is nonlinear in h, and no general analytical solution is available. However, for specific boundary conditions, Boussinesq (1904) solved the problem exactly for the case when the drains penetrate to the impervious layer of a shallow aquifer and the saturated thickness at the drains, d = 0 (see figure 29). The solution, subject to the conditions

$$h = H \quad \text{at } x = L \quad \text{and } t = 0$$

$$h = 0 \quad \text{at } x = 0 \quad \text{and } t \geq 0 \tag{4.2}$$

and $$\frac{\partial h}{\partial x} = 0 \quad \text{at } x = L \quad \text{and } t \geq 0$$

can be written at x/L = 1 as

$$h/H = \frac{1}{1.115\,(K_H Dt/S_y L^2) + 1} \tag{4.3}$$

The results are shown graphically in figure 30.

All of the solutions will be analyzed at x/L = 1, a point midway between the drains. If this point can be drained, every other point will also be drained.

When the saturated thickness d below the drains is not zero, equation (4.3) is invalid because the second boundary condition of equation (4.2) can no longer be satisfied. To avoid this difficulty it is necessary to linearize equation (4.1), following the same procedure as in section 3.2.

A. Linearized Model in h

Dumm (1954) and Maasland (1959) used the linearized form of

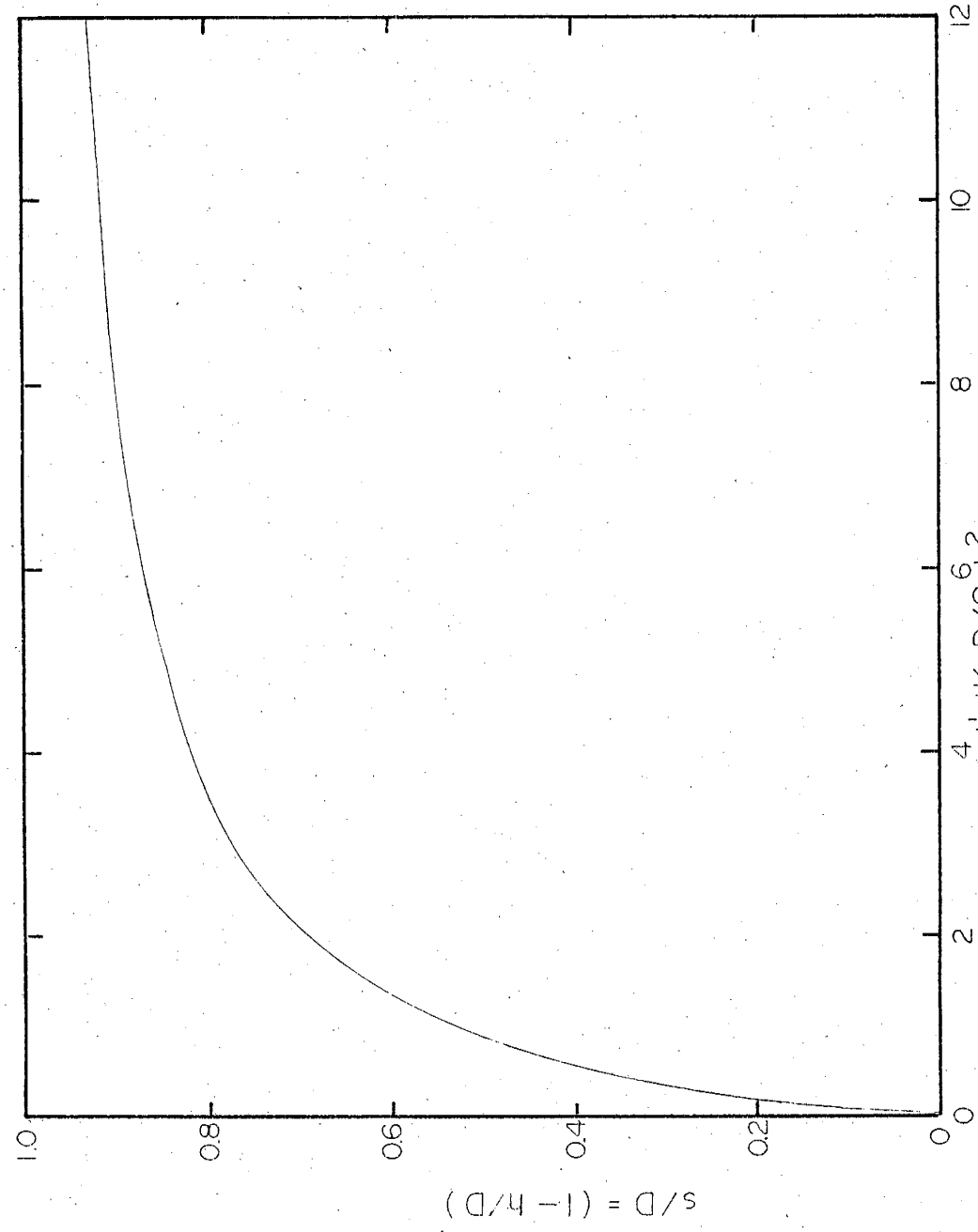

Figure 30. Dimensionless drawdown versus dimensionless time corresponding to Boussenisq (1904)

equation (4.1), written as

$$\bar{h} K_H \frac{\partial h}{\partial x} = S_y \frac{\partial h}{\partial t} \tag{4.4}$$

where $\bar{h} = d + H/2$. For an initially flat water table, the boundary and initial conditions are

$$\begin{aligned} h &= d + H = D && \text{for } 0 < x < L && \text{and } t = 0 \\ h &= d && \text{for } x = 0 && \text{and } t > 0 \\ \frac{\partial h}{\partial x} &= 0 && \text{for } x = L && \text{at } t > 0 \end{aligned} \tag{4.5}$$

Using Fourier series, the solution of equations (4.4) and (4.5) is

$$h/H = \frac{4}{\pi} \sum_{n=1,3,5\ldots}^{\infty} (1/n)\, e^{-n^2\pi^2\alpha t/4L^2} \sin n\pi x/2L \tag{4.6}$$

When $x = L$ this becomes

$$h/H = \frac{4}{\pi} \sum_{n=1,3,5\ldots}^{\infty} \frac{e^{-n\pi^2\alpha t/4L^2}}{n} \sin n\pi/2 \tag{4.7}$$

where $\alpha = K_H(d + H/2)/S_y$

B. Linearized Model in h^2

Werner (1957) linearized equation (4.1) to the form

$$K_H \frac{\partial^2 h^2}{\partial x^2} = \frac{S_y}{h} \frac{\partial h^2}{\partial t} \tag{4.8}$$

or

$$\frac{\partial^2 h^2}{\partial x^2} = \frac{1}{\alpha} \frac{\partial h^2}{\partial t} \tag{4.9}$$

The solution to equation (4.9) and (4.5) at x = L is

$$h/H = \left[\frac{4}{\pi} \sum_{n=1,3,5\ldots}^{\infty} e^{-n^2\pi^2\alpha t/4L^2} \sin n\pi/2\right]^{1/2} \qquad (4.10)$$

The results of the linearized horizontal models in h and in h^2 for various depths are shown graphically in figure 31.

C. Nonlinear Model

Van Schilfgaarde (1963) attempted to solve the nonlinear equation (4.1) subject to the following initial and boundary conditions:

$$\begin{aligned} &h = D \quad \text{at } x = L \quad \text{and } t = 0 \\ &h = d \quad \text{at } x = 0 \quad \text{and } t \geq 0 \\ &\frac{\partial h}{\partial x} = 0 \quad \text{at } x = L \quad \text{and } t \geq 0 \end{aligned} \qquad (4.11)$$

Equations (4.11) and (4.1) describe a problem similar to the one solved by Boussinesq, except that the saturated thickness d below the drains is not zero. A solution of equation (4.1) can be written as

$$h/H = \frac{1}{1 + (4.5/4)A^2\, t'} \quad \frac{1}{1 + (8/9A^2\, t')} \quad \frac{d}{H} \qquad (4.12)$$

where $t' = K_H Dt/S_y L^2$

and A is an incomplete beta function which can be approximated by

$$A^2 = 1 - (d/D)^2$$

This solution fails to satisfy the second boundary condition

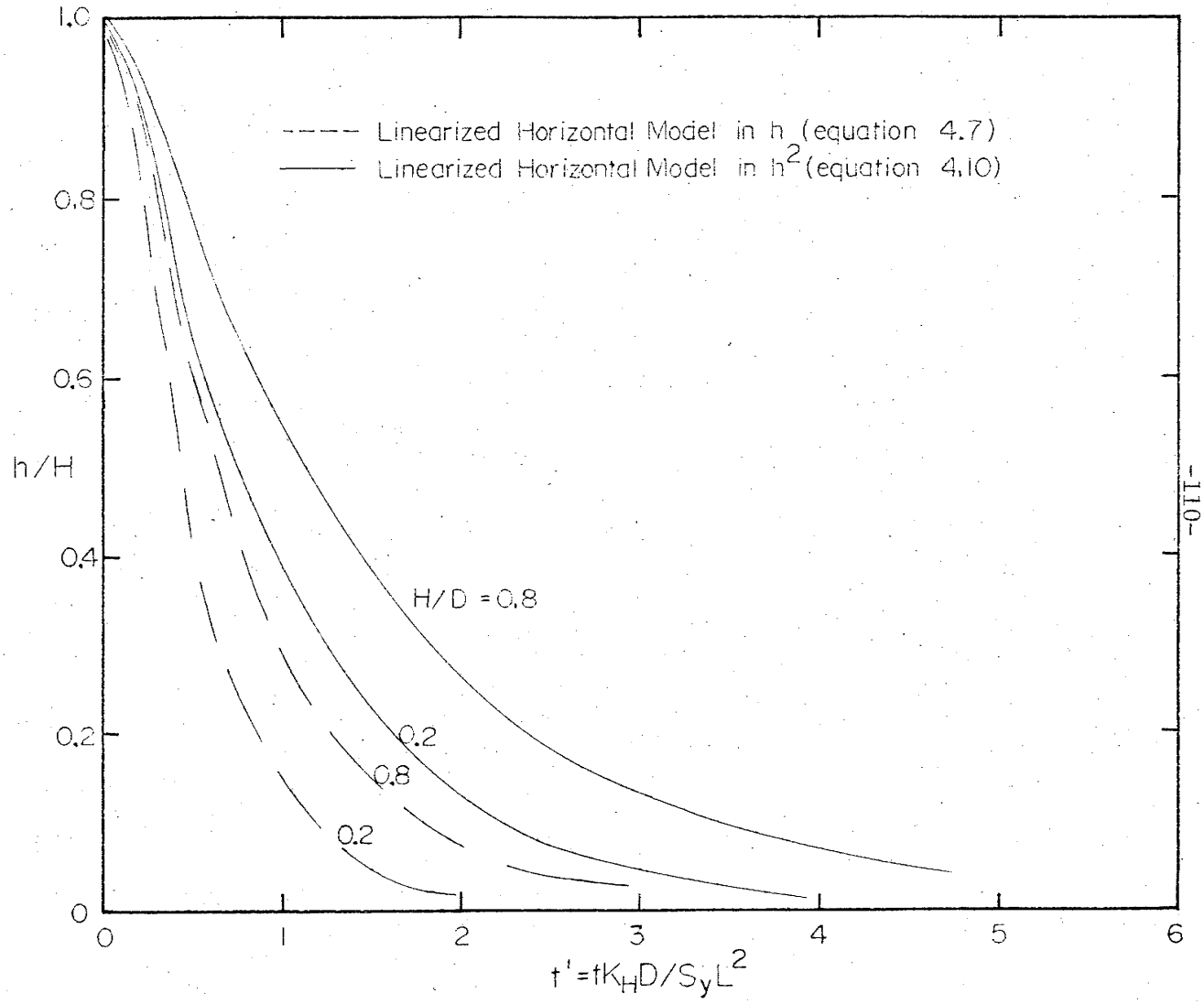

Figure 31. Dimensionless height of the water table versus dimensionless time

(equation 4.11). Van Schilfgaarde got around this problem by considering the drawdown process as a sequence of small steps. Then he substituted the expression for A into equation (4.11) and solved for t, getting

$$t = 8S_y L^2 (H - h)(d + H)/9K_H H(2d + H)(d + H)$$

This represents the time increment t required for the drawdown $s = H - h$. The total drawdown is the summation of the successive drawdown increments Δs; as these become small the summation reduces to the integral

$$t = (8S_y L^2/9K_H) \int_h^H \frac{dh}{h(2d + h)} \qquad (4.14)$$

or

$$t = (4S_y L^2/9K_H) \ln \frac{H(2d + h)}{h(2d + H)}$$

This can be written in terms of h at $x/L = 1$ as

$$h/H = \frac{d}{H} \frac{2}{(2d/H + 1)\, e^{2.25t'd/D} - 1} \qquad (4.15)$$

The results of (4.15) are shown in figure 32.

Moody (1966) solved the same problem (equations (4.1) and (4.11)) numerically for a series of drain positions ranging from a location near the water table to a location on the barrier. He produced a table listing the maximum phreatic surface height, the discharge to the drains, and the volume of water removed. This is in dimensionless form and covers the entire range of possible drain positions between

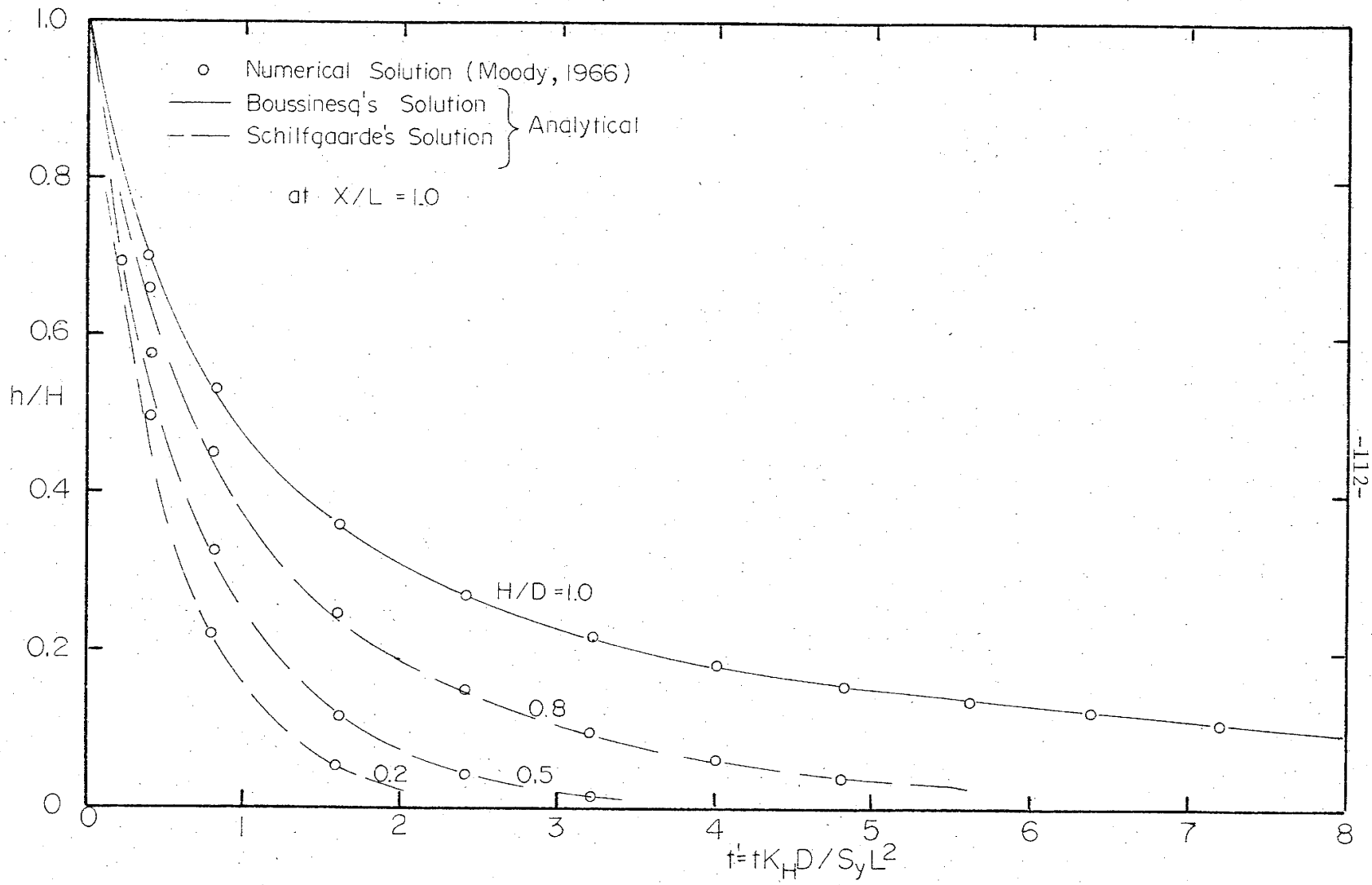

Figure 32. Dimensionless height of the water table versus dimensionless time predicted by the nonlinear horizontal flow model

the water table and the barrier. Some of his results are shown in figure 32.

Verma (1969) solved the same problem numerically, assuming an initially flat water table.

4.3 Correlation of the Horizontal Flow Models

All of the models in section 4.2 are based on the Dupuit assumptions (1) that all streamlines in a system of gravity flow are horizontal, and (2) that the velocity along these streamlines is proportional to the slope of the free surface but independent of depth.

After these assumptions the resulting equation is still nonlinear and not easy to solve analytically for most practical problems. Hence several different methods of linearization have been used to arrive at a simple analytical solution. In this section we will correlate the different models representing different linearizations with the nonlinear model.

Figures 33a, 33b and 33c show a comparison of the results of the nonlinear model (Moody, 1966) and the linearized horizontal models in h and h^2, as a function of the ratio of drainable depth H to total saturated thickness D. In figure 33a, the results of the nonlinear and linearized horizontal model in h for H/D = 0.2 practically coincide, but for higher values of H/D (figures 33b and 33c) the discrepancy between the models is very significant. On the other hand, a comparison of the linearized horizontal model in h^2 and the nonlinear model shows a significant difference for all values of

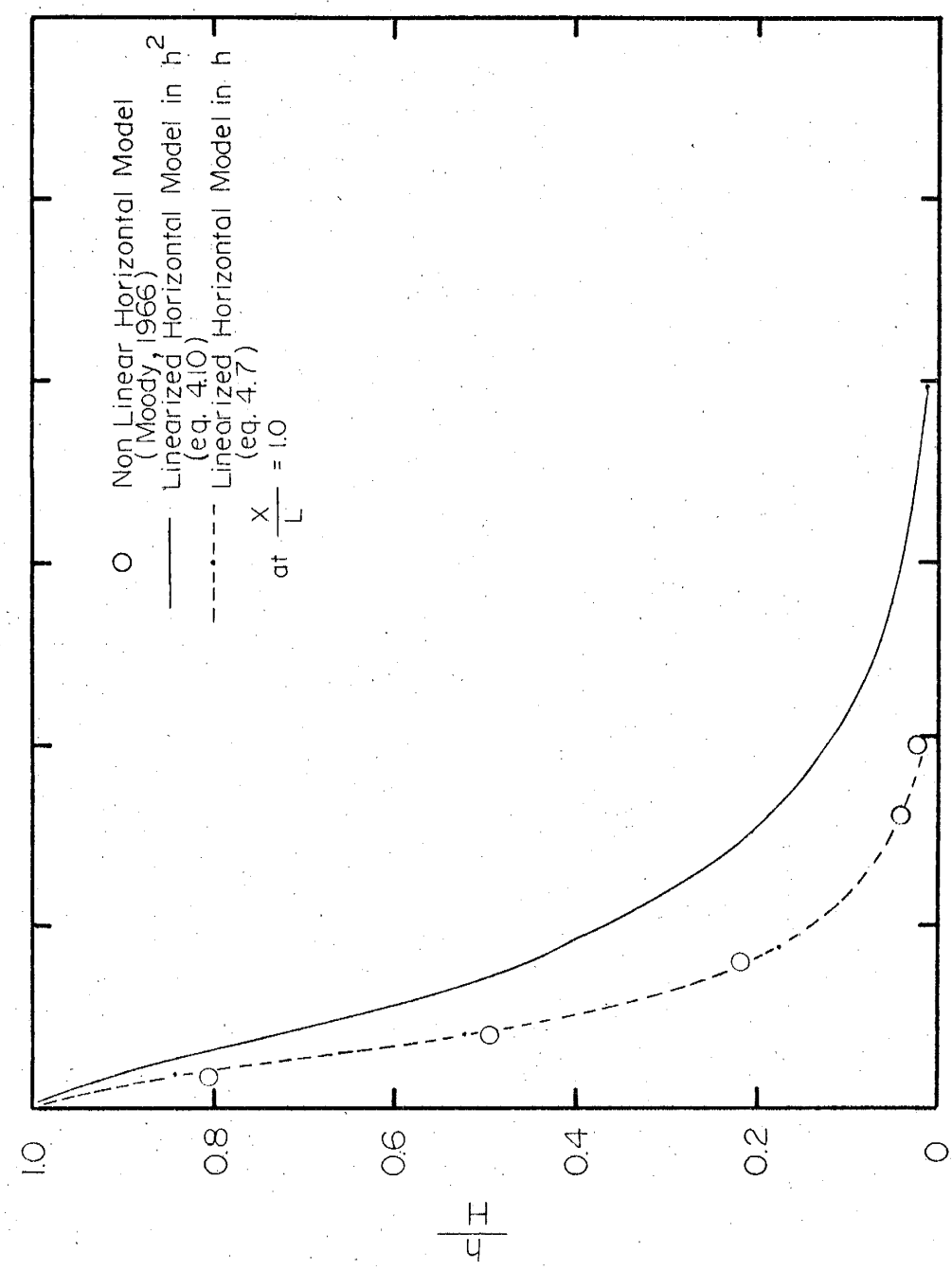

Figure 33a. Comparison between the results of the nonlinear and linearized horizontal model in h and h^2 for H/D = 0.2

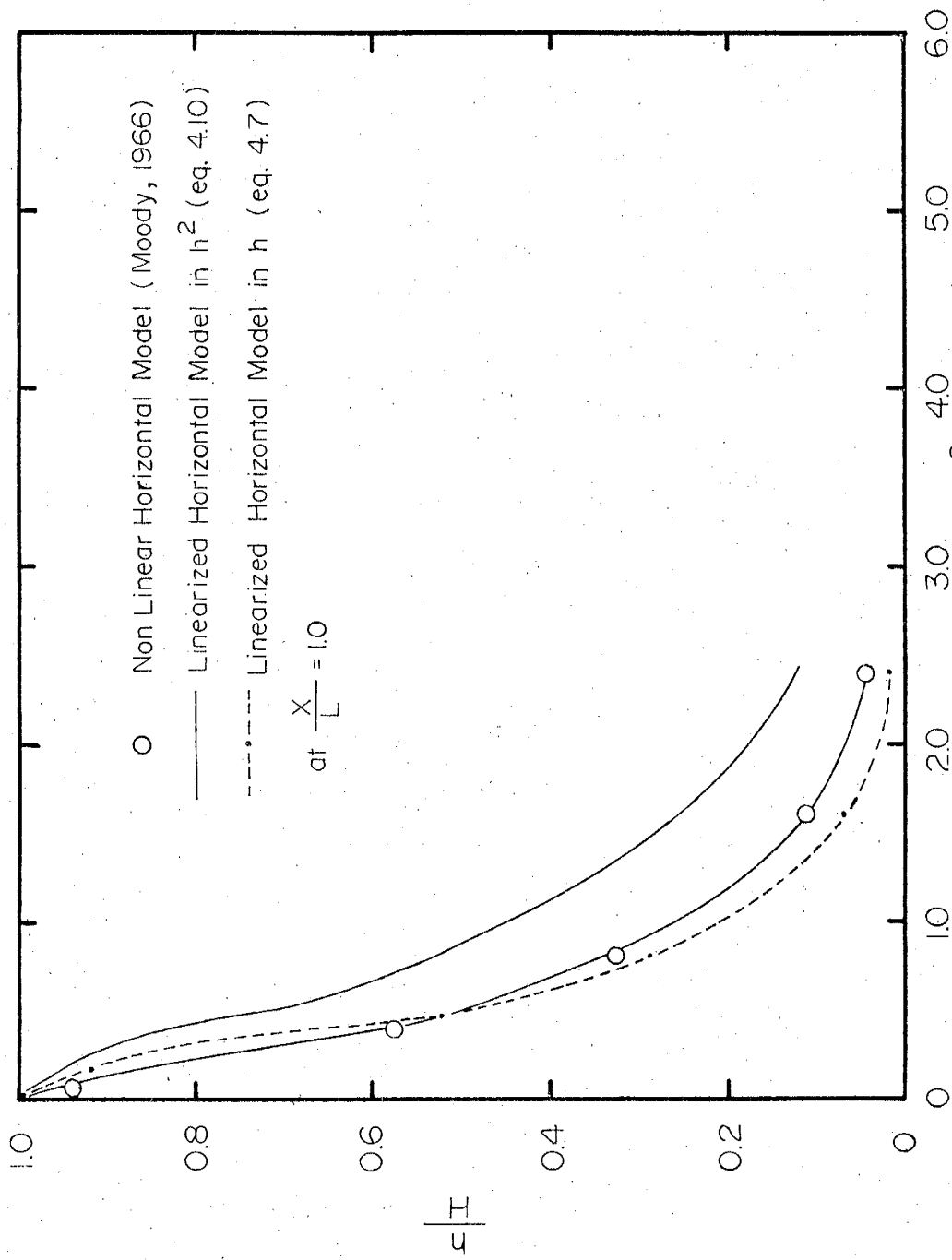

Figure 33b. Comparison between the results of nonlinear and linearized horizontal model in h and h^2 for H/D = 0.5

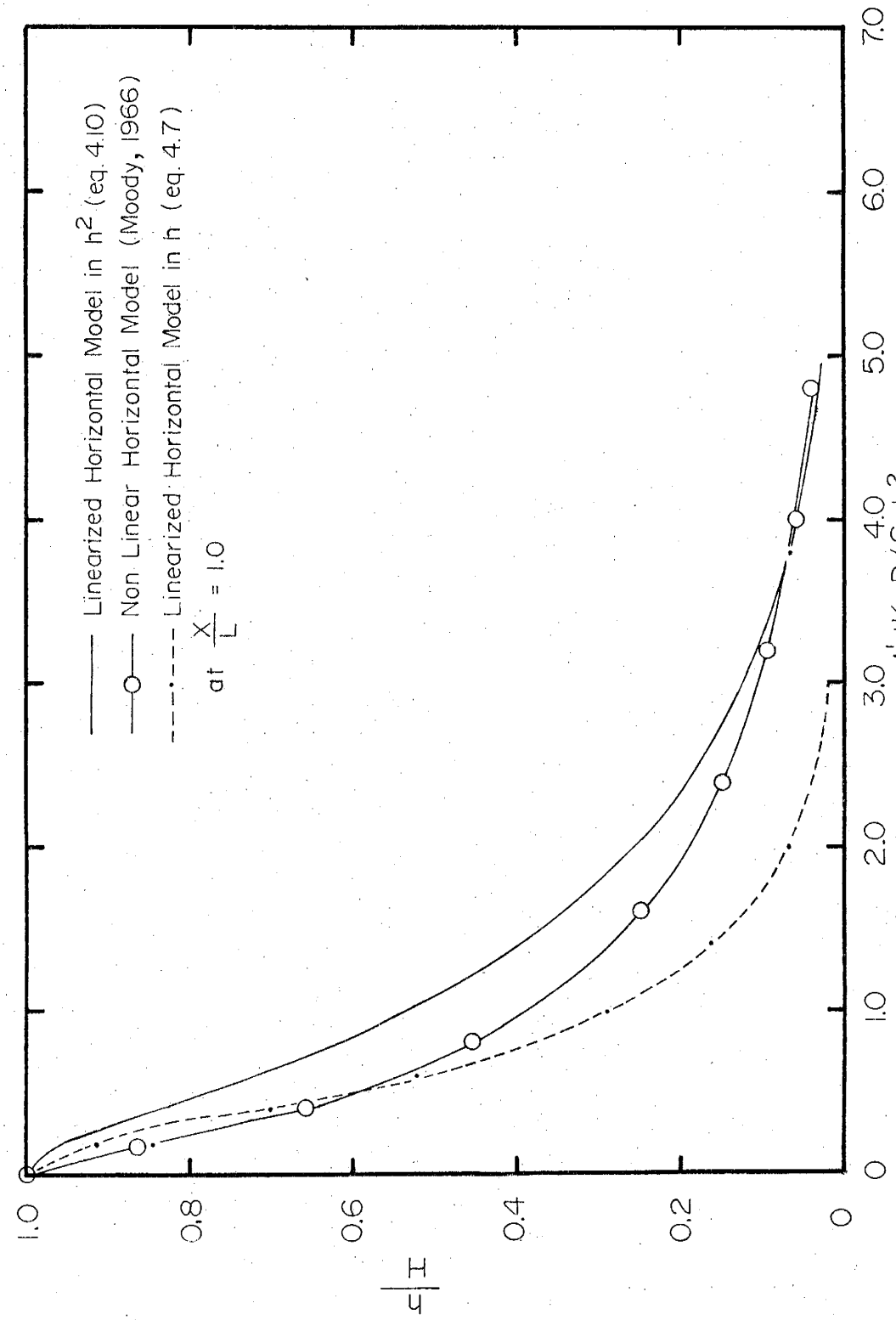

Figure 33c. Comparison between the results of the nonlinear and linearized horizontal models in h and h^2 for H/D = 0.8

H/D. (The nonlinear model predicts a faster drop of the water table.) The results of the linearized horizontal models in h and h^2 depend very strongly on the choice of $\tilde{h}$. If instead of the assumption that $\tilde{h} = d + H/2$ we assume that $\tilde{h} = d$ (figure 34a), the nonlinear model predicts a faster drop of the water table than either linearized model. The discrepancy between the nonlinear model and the linearized model in h is less pronounced than that between the linearized model in h^2 and the nonlinear model. If $\tilde{h} = d + H = D$ the linearized models in h and h^2 are no longer dependent on H/D (see equation 4.7). Figure 34b shows that the disagreement between the linearized model in h^2 and the nonlinear model (Moody, 1966) for $H/D \geq 0.5$ is less than that between the linearized model in h and the nonlinear model. The linearized model in h^2 overemphasizes the thinning of the flow zone, while the linearized model in h underemphasizes it. The latter functions best for $H/D \leq 0.5$ and $\tilde{h} = d$ (figure 34a).

Figure 34c compares the numerical solution by Verma (1969) (using his results) for an initially flat water table to the numerical solution by Moody (1966) and exact solution by Boussinesq(1904) for a parabolic water table. At early time there is a small deviation between the solutions due to their particular initial conditions; as time increases, it diminishes and the three solutions coincide.

Figure 32 compares results of the analytical solutions by Boussinesq (1904) for $d = 0$ and Schilfgaarde (1963) for $d \neq 0$ to those of the numerical solution (Moody, 1966) to the nonlinear horizontal model. The numerical and analytical solutions for $d = 0$ ($H/D = 1$) are identical; the solutions for $d \neq 0$ ($H/D < 1$) are slightly different

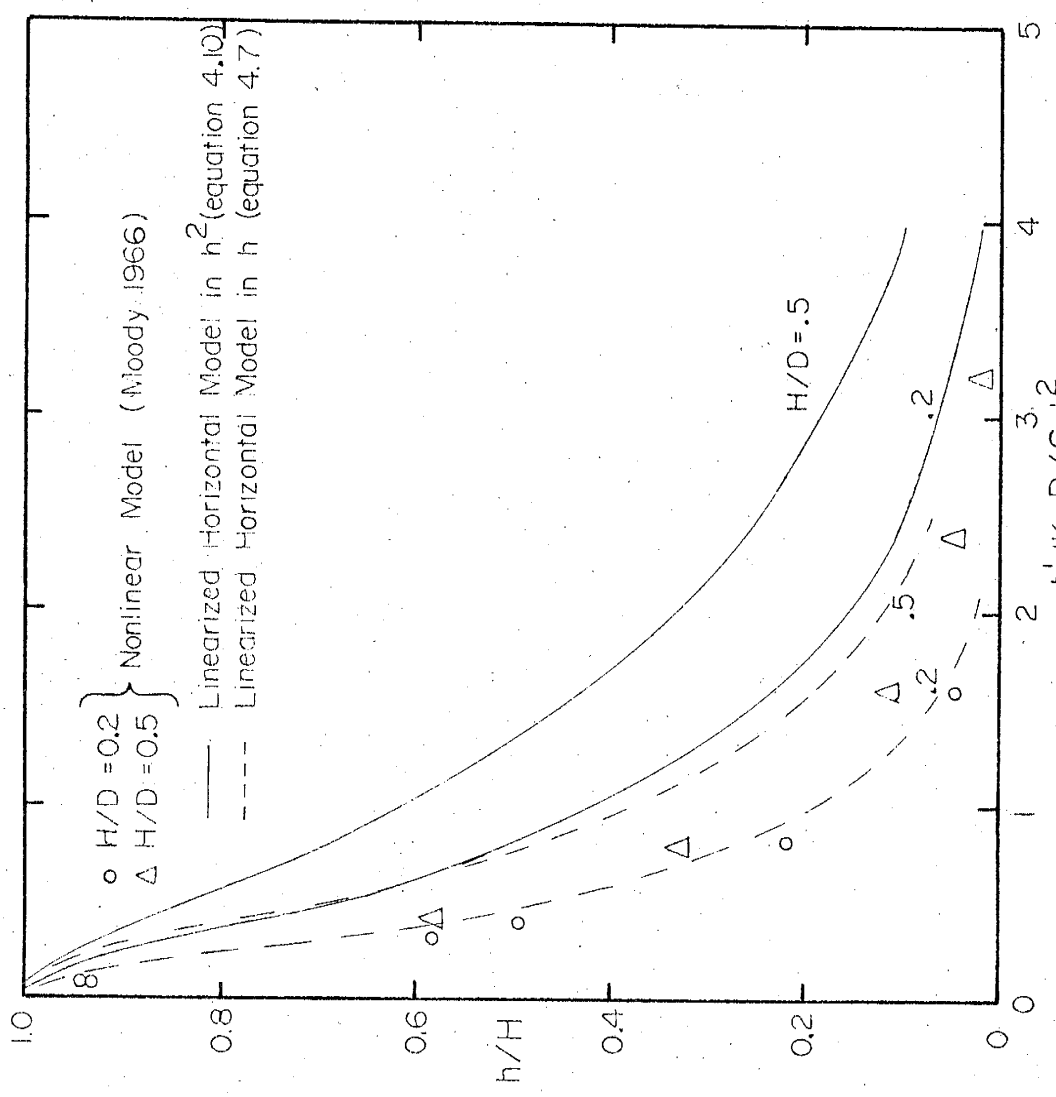

Figure 34a. Comparison between the results of the nonlinear and linearized horizontal model in h and h^2 for $\tilde{h} = d$

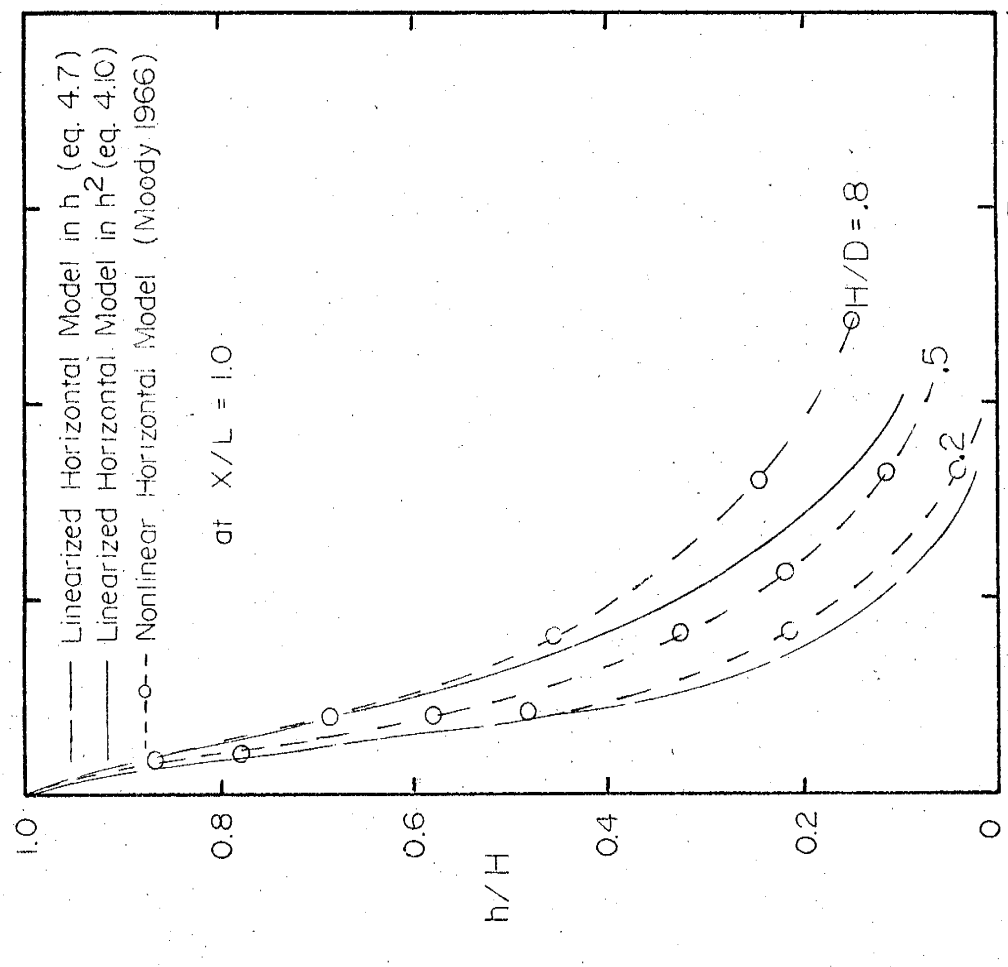

Figure 34b. Comparison between the results of the nonlinear and linearized horizontal models in h and h^2 for $\bar{h} = H + d$

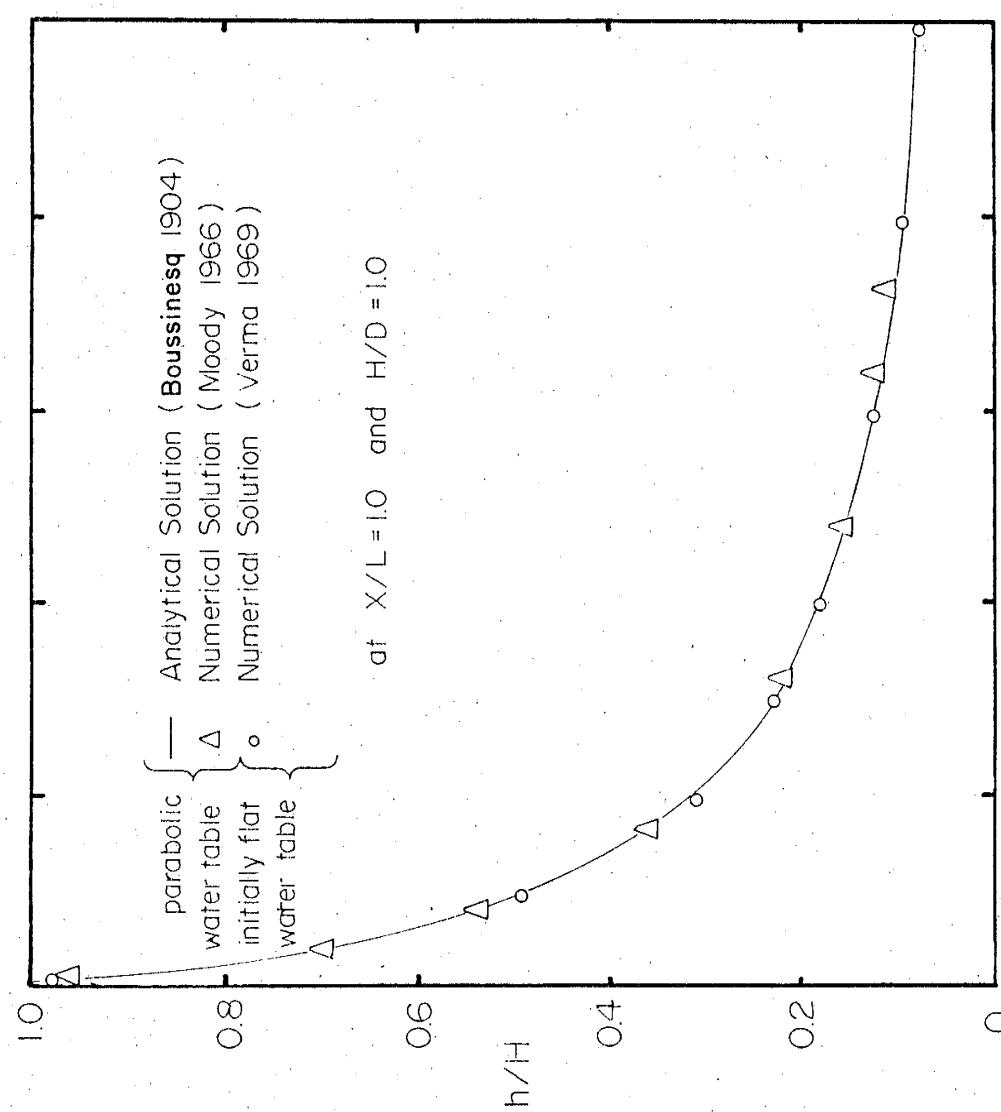

Figure 34c. Comparison between the analytical and numerical solution for the nonlinear horizontal flow model.

at early time, but coincide at large time.

The effects of nonlinearity are small only if the ratio of the drainable depth H to the total saturated thickness D is less than or equal to 0.2. Thus the linearized horizontal model in h is a good approximation to the nonlinear horizontal flow model provided that $H/D \leq 0.2$. The solution obtained by Van Schilfgaarde seems to approximate the nonlinearity effects or the flow zone thinning fairly well, but it is only valid for this specific problem.

4.4 Potential Flow Model

In section 4.2 we assumed that the vertical flow effects are insignificant and can be neglected; now we will investigate this assumption.

Equations (2.7a) and (2.13) with appropriate boundary and initial conditions describe the potential flow model for the problem illustrated in figure 29. Equation (2.13), the free surface boundary condition, is nonlinear and difficult to solve analytically. However, several investigators have linearized the problem to find an analytical solution. Kirkham (1964) and Dagan (1964) solved the problem for flow to tile drains; Gelhar (1974) used a stochastic approach in solving the potential flow model for a partially penetrating stream.

Verma (1969) used numerical techniques to solve the nonlinear potential flow problem. The difficulty in arriving at a numerical solution in this case arises from the fact that the upper boundary of the domain of flow is changing with time. Verma calculated the position of the free surface at successive intervals of time by

applying the forward finite difference approximations of equation (2.13). Then he solved the Laplace equation by using a successive over-relaxation iterative scheme with the new free surface being the upper boundary of the flow domain at each interval of time. He reported that the error in the results of the numerical solution should not be larger than 2.5×10^{-3}.

Verma (1969) tabulated his results for dimensionless head and rate of outflow to the stream. In his analysis the emphasis is on the rate of outflow. His results (drop of the phreatic surface) offer us an opportunity to investigate the vertical flow effects by comparing them to the results of the horizontal flow model.

Figures 35 and 36 show the drop of the free surface height at the line of symmetry as a function of time and the anisotropy parameter $\eta = L/D \sqrt{K_V/K_H}$. In both cases, H/D = 1 and H/D = 0.5, the potential flow model predicts a faster drop (which becomes increasingly rapid for smaller values of η) of the phreatic surface than does the horizontal model.

4.5 Correlation of the Horizontal and Vertical Flow Models

The difference between the nonlinear horizontal model and the nonlinear vertical model lies mainly in the effects of the vertical flow and seepage face. To investigate these effects, two solutions to the vertical flow model are needed; one takes into account the seepage face, and the other does not. For the problem at hand the second solution does not exist. However, the difference between the two models at $x/L = 0.0$ and $t > 0$ is due mainly to the seepage face effects.

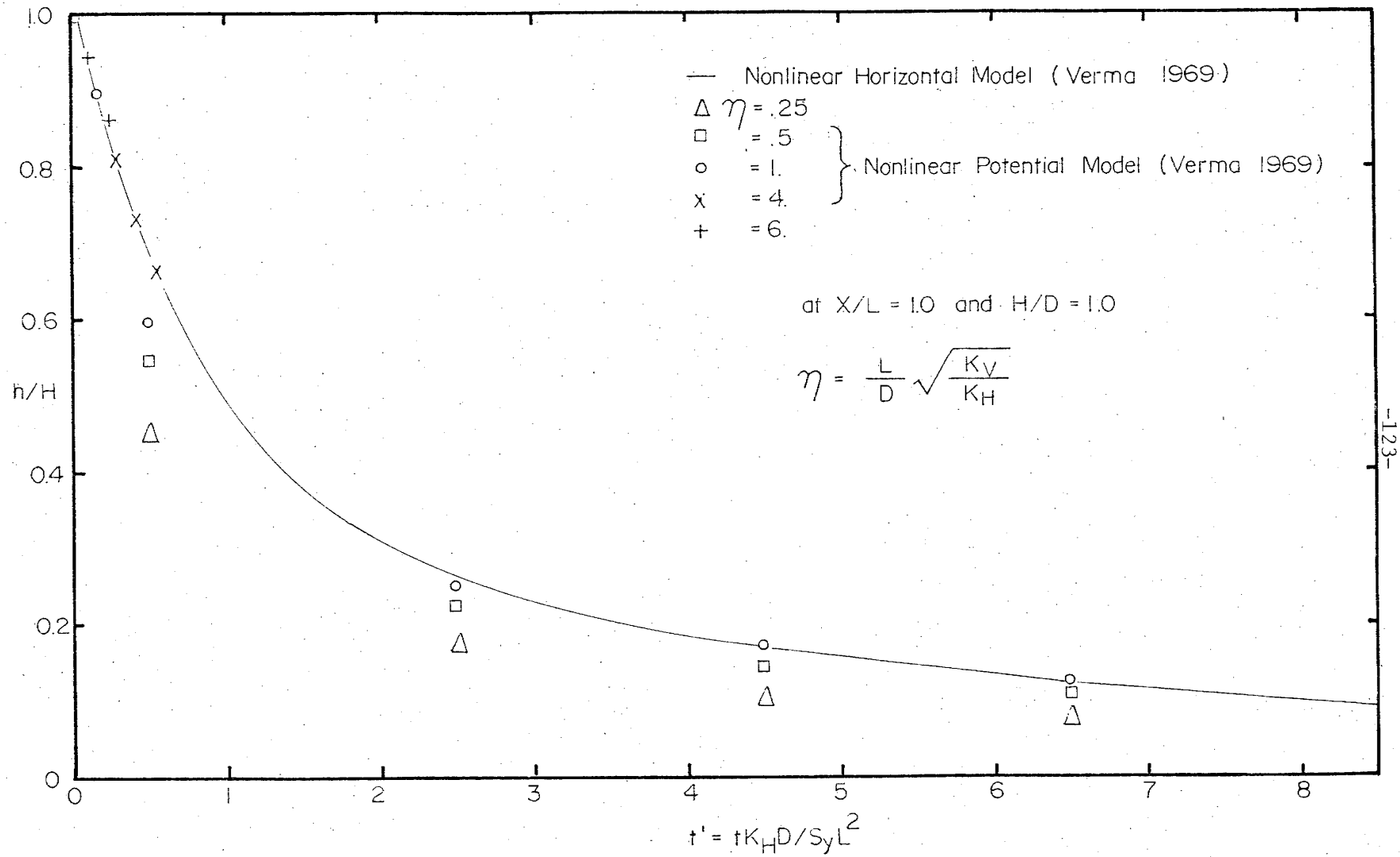

Figure 35. Comparison between the results of the nonlinear horizontal model and the nonlinear potential model for H/D = 1

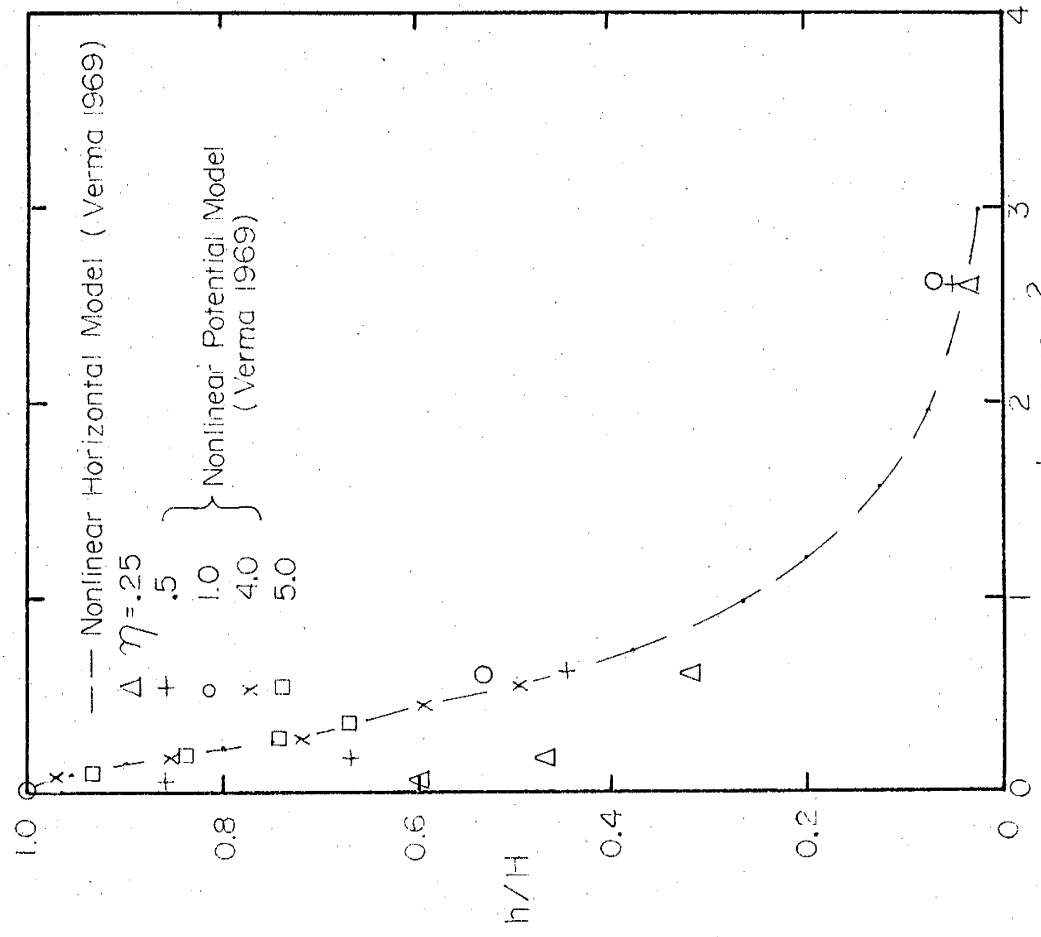

Figure 36. Comparison between the results of the nonlinear horizontal model and the nonlinear potential model for H/D = 0.5

For all values of t greater than zero and x/L = 0.0, the dimensionless height of the free surface predicted by the nonlinear horizontal model is the same as the height of water in the ditch. (It is zero for H/D = 1 and 0.5 for H/D = 0.5.) The dimensionless free surface height predicted by the vertical flow model is 0.218 for $t' = K_H Dt/S_y L^2 = 0.5$, x/L = 0.0 and H/D = 1.0. It is zero for t' = 2.5, and 0.5 for t' = 0.5, x/L = 0.0 and H/D = 0.5 (the same as that predicted by the horizontal model). Thus the seepage face effects are significant for large values of H/D only at early time.

Figures 35 and 36 contrast the results (at x/L = 1) of the nonlinear horizontal model and those of the nonlinear potential model; the difference between these two is due mainly to vertical flow effects.

At $\eta = L/D \sqrt{K_v/K_H} \geq 4$ the vertical flow effects are insignificant, and the solutions for the two models practically coincide. For small values of η, the potential flow model predicts lower head or higher drawdown than the horizontal model. A quantitative evaluation of the difference between the models for various values of η is given in Table 6. The table shows that the vertical flow effects are very significant, especially for H/D = 1 and small η, but their significance decreases for smaller values of H/D.

The vertical flow effects are also a function of time. For H/D = 0.5 they decrease with an increase in time; for H/D = 1, at early time they increase and at large time they decrease.

The parameter η, analogous to $r/B = r/D \sqrt{K_v/K_H}$ in the well flow problem, characterizes the importance of vertical flow effects. In section 3.5 we showed that these effects can be neglected provided

Table 6. Comparison of dimensionless height of the water table determined by nonlinear horizontal model and nonlinear potential flow model at x/L = 1.

$$\% \text{ error} = \frac{\frac{h+d}{D}\ (\text{N.L. Horizontal Model}) - \frac{h+d}{D}\ (\text{N.L. Potential Model})}{\frac{h+d}{D}\ (\text{N.L. Potential Model})} \times 100$$

H/D = 1

$t' = K_H Dt/S_y L^2$	η = 0.25	0.5	1.0
0.3	45.0	16.0	9.7
1.0	50.0	23.1	5.5
2.0	47.6	17.0	0.0
6.0	56.2	13.6	0.0

H/D = 0.5

$t' = K_H Dt/S_y L^2$	η = 0.25	0.5	1.0
0.3	25.2	11.2	1.2
0.5	21.7	5.7	0.0
1	10.7	2.5	-2.4
2	4.2	1.9	-0.0

+ sign indicates overestimate

- sign indicates underestimate

that $r/B \geq 4.0$; this is also the value of η at which the vertical flow effects can be neglected in the problem at hand.

4.6 Variably Saturated Model (Exact Theory)

In sections 4.2 and 4.4 it was assumed that effects of the unsaturated zone are small and can be neglected; now we will investigate this assumption.

Equation (2.5) describes the unsaturated and saturated zones as one continuous system. Its solution requires a unique relationship between the unsaturated hydraulic conductivity K and the moisture content θ. In solving the problem of flow to a stream, Verma (1969) used the equation and appropriate boundary conditions along with the relationship between K and θ suggested by Brutsaert (1967), equation (3.19). He made use of the combined explicit-implicit scheme. For most of his study the dimensionless time increment Δt^* ($t^* = tK_H/S_yD$) was initially of the order of 2.5×10^{-4} and increased gradually to 5×10^{-2}. The dimensionless space increments $\Delta x/D$ and $\Delta z/D$ both had the value of 0.125. The number of nodes was $1/\Delta z$ in the vertical direction and $(L/\Delta x)+1$ in the x direction. In another case, Verma began with a Δt^* of 2.5×10^{-6} which gradually increased to 5×10^{-4}, $\Delta x/D$ and $\Delta z/D$ both had values of 0.05. He reported no noticeable difference between the results of the two cases. Using the values from the latter case, he found that the error encountered with the finite difference numerical scheme should be less than 2.5×10^{-3}.

Verma (1969) tabulated most of his results for rate of outflow and dimensionless head at the free surface. He was concerned mainly with

the rate of outflow to a stream. We will use his results for dimensionless head at the free surface to investigate the effects of the unsaturated zone.

Figures 37 and 38 show values for the height of the phreatic surface as determined by the variably saturated model for H/D = 1 and H/D = 0.5. For larger values of h_{cr}/D the drop of the phreatic surface is faster. (This is more pronounced for H/D = 1 than for H/D = 0.5.) Physically this is expected, because smaller values of h_{cr}/D indicate small capillary forces and drainage due mainly to gravity forces (as is the case with the potential flow model); a large value of h_{cr}/D means strong enough capillary forces to hold a significant quantity of water within the interstices of the porous medium. Thus, drainage may actually take a very long time.

4.7 Correlation of Models

Dimensionless drop of the phreatic surface as a function of time, as predicted by the variably saturated model, the potential flow model, and the nonlinear horizontal model for the same values of η, H/D, and h_{cr}/D, is shown in figures 37 and 38. Examination of these figures for the unsaturated zone effects reveals that the variably saturated model predicts a faster drop of the phreatic surface than the potential model. The discrepancy between the results of the two models at x/L = 1.0 and η = 1 is presented quantitatively in table 7; the unsaturated zone effects are fairly small and practically insignificant for h_{cr}/D = 0.07 and H/D = 0.5, but for H/D = 1.0 and the same value of h_{cr}/D the difference between the two models increases, suggesting that contributions

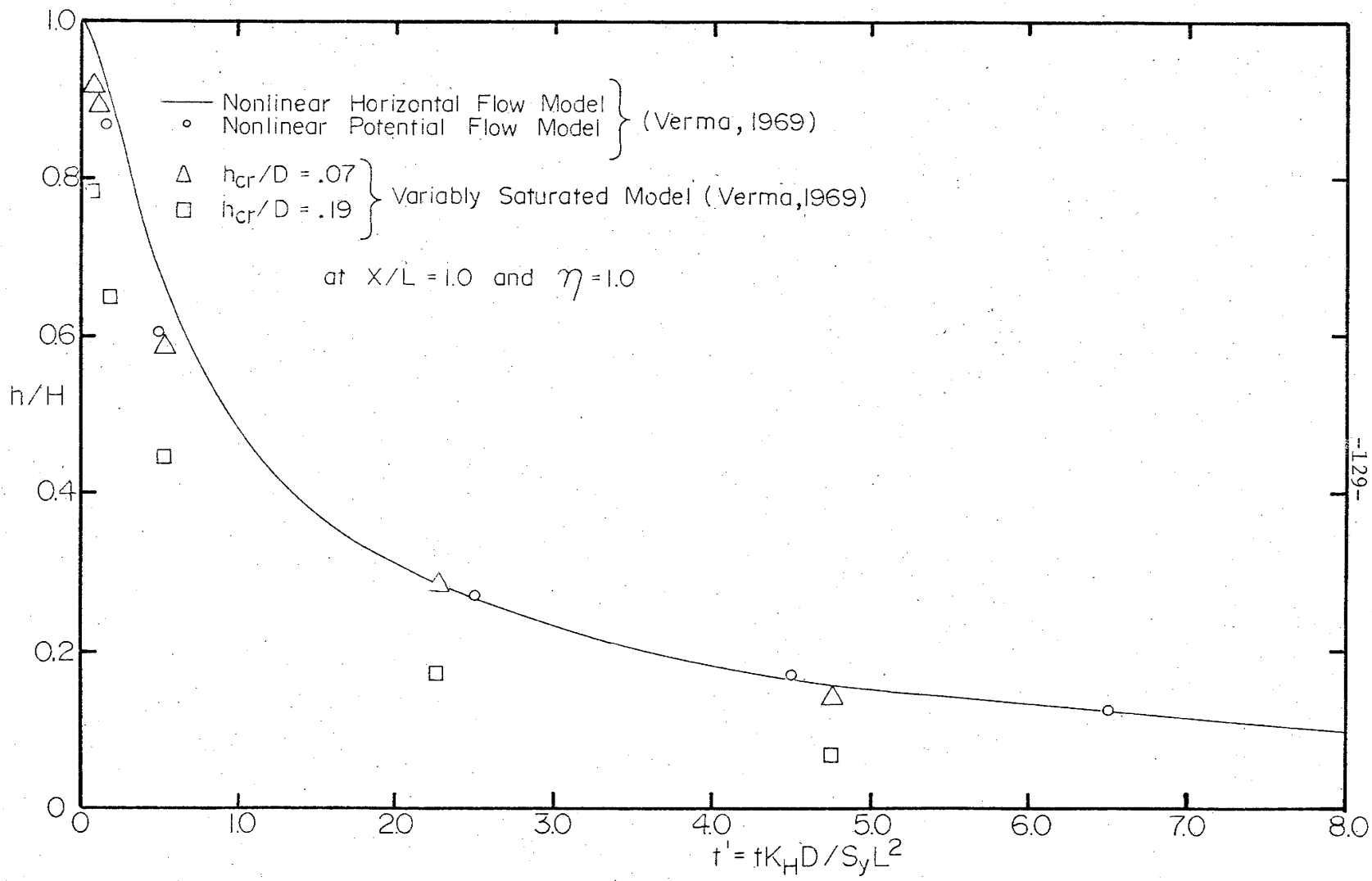

Figure 37. Comparison between the results of the variably saturated model, nonlinear potentia model and nonlinear horizontal model for H/D = 1.0

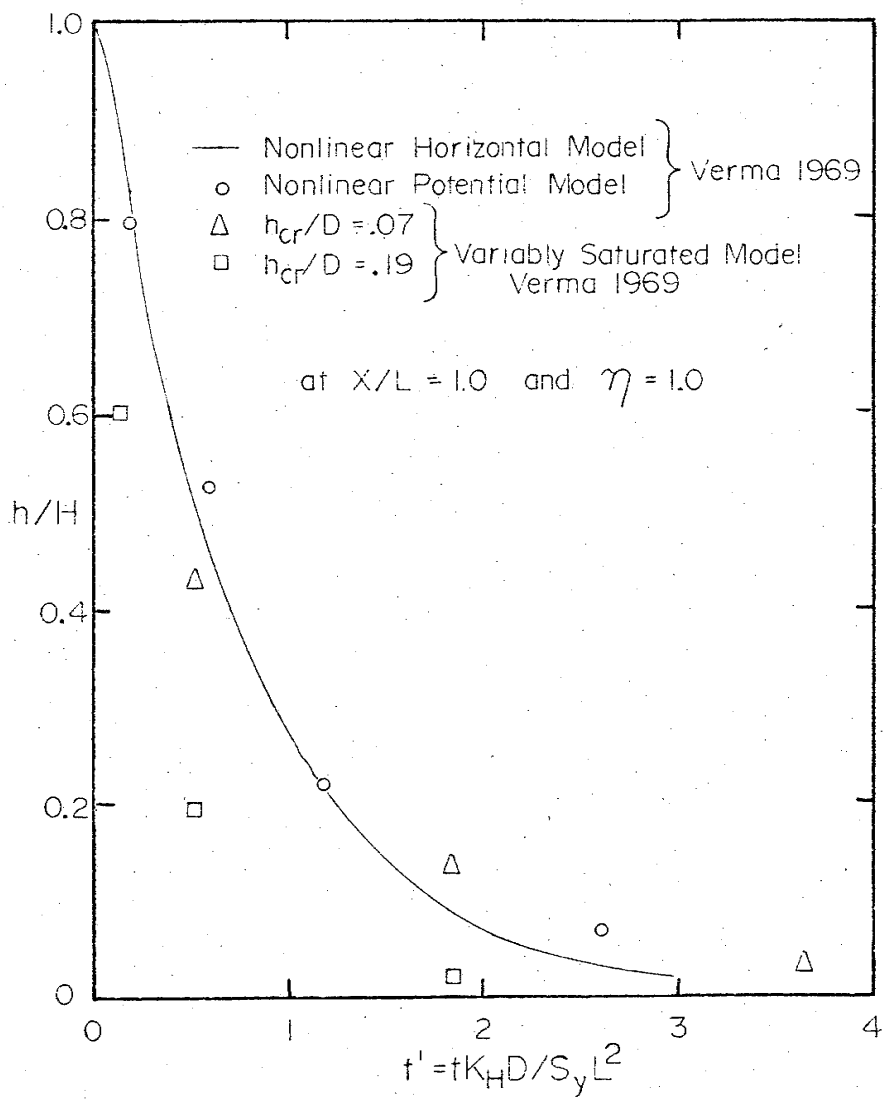

Figure 38. Comparison between the results of variably saturated model, nonlinear potential flow model and nonlinear horizontal model for H/D = 0.5

Table 7. Comparison of dimensionless height of the water table determined by variably saturated model and potential flow model for $\eta = 1$ and $x/L = 1.0$

$$\% \text{ error} = \frac{\frac{h+d}{D} \text{ (potential flow model)} - \frac{h+d}{D} \text{ (variably saturated flow model)}}{\frac{h+d}{D} \text{ (variably saturated flow model)}} \times 100$$

H/D = 1.0

$t' = tK_H D/S_y L^2$	% error in h/H obtained by potential flow model	
$h_{cr}/D =$	0.07	0.19
0.5	3.25	27.174
2.5	5.0	70.6
4.5	12.0	115.4

H/D = 0.5

$t' = tK_H D/S_y L^2$	$h_{cr}/D =$	0.07	0.19
0.19		7.9	15.6
0.69		3.6	23.0
1.69		-1.6	9.0

- sign indicates underestimate

+ sign indicates overestimate

from the unsaturated zone become significant.

The value of $h_{cr}/D = 0.07$ describes Webster soil of 38% clay, 31% silt and 31% sand, with a depth D to the impervious layer of about 3.55 meters. To emphasize the role of the unsaturated zone, a value of $A^{1/\lambda}/D = 0.355$, equivalent to $h_{cr}/D = 0.19$, was used by Verma (1969). The difference between the variably saturated model and the potential flow model is given in table 7 and figures 37 and 38. For $H/D = 1.0$, the unsaturated zone effects are very significant and an error of about 115% is encountered. These effects decrease with a decrease in H/D ratio; for $H/D = 0.5$ and error of 23% or less is encountered. Thus the unsaturated zone effects can only be neglected provided that $h_{cr}/D \leq 0.07$ and $H/D \leq 0.5$, where for $H/D = 1$, and the same value of h_{cr}/D there is about 12% error.

For the well flow problem (section 3.8), we showed that the unsaturated zone effects can be neglected provided that $h_{cr}/D = 0.067$ and deep observation wells are being used. It is interesting to note that the critical values of h_{cr}/D for both problems are fairly close, even though we started with a completely saturated medium in the drainage problem. In general, a value of $h_{cr}/D \leq 0.07$ can safely be chosen as the condition under which the unsaturated zone can be neglected, provided that $H/D \leq 0.5$ and deep observation wells are being used.

These correlations apply to the results of the nonlinear horizontal model shown in figures 37 and 38, except that in this model we neglected the unsaturated zone as well as the vertical flow effects. In section 4.6 we showed that the vertical flow effects can be

neglected provided that $\eta \geq 4.0$. Consequently we can say that the nonlinear horizontal model is valid provided that $\eta \geq 4$ and $h_{cr}/D \leq 0.07$. For actual application of this problem within the above limitations Moody's (1966) solution to the nonlinear horizontal model can be used (his results are tabulated for a large range of H/D values).

CHAPTER 5.

Theoretical Models for Artificial Groundwater Recharge

5.1 Introduction

Artificial recharge of unconfined aquifers is usually accomplished with the use of spreading ponds or long narrow pits, irrigation of open lands, and spraying over forested regions. Rise of the groundwater table occurs under and in the immediate vicinity of the recharge basins. The practicing engineer must be able to predict changes of the water table with reasonable accuracy.

The phenomena of rise and movement of the water table resulting from the recharge of an unconfined aquifer is governed by Darcy's equation and the equation of continuity. If the unsaturated zone is neglected and the medium is homogeneous, equation (2.7a) is the governing equation, with appropriate boundary and initial conditions. The conditions at the free surface are nonlinear and very intractable. To overcome this difficulty, various techniques have been applied to simplify the problem. The simplifications consist mainly of the Dupuit assumptions leading to what we call the horizontal model (see section 2.2E). Because of their simplicity these models are widely used.

The difficulty in analyzing the limitations of the horizontal flow model is that the literature for the problem (figure 39) is not complete; also all of the existing solutions assume complete saturation (see Table 8). Hence our final conclusions about the

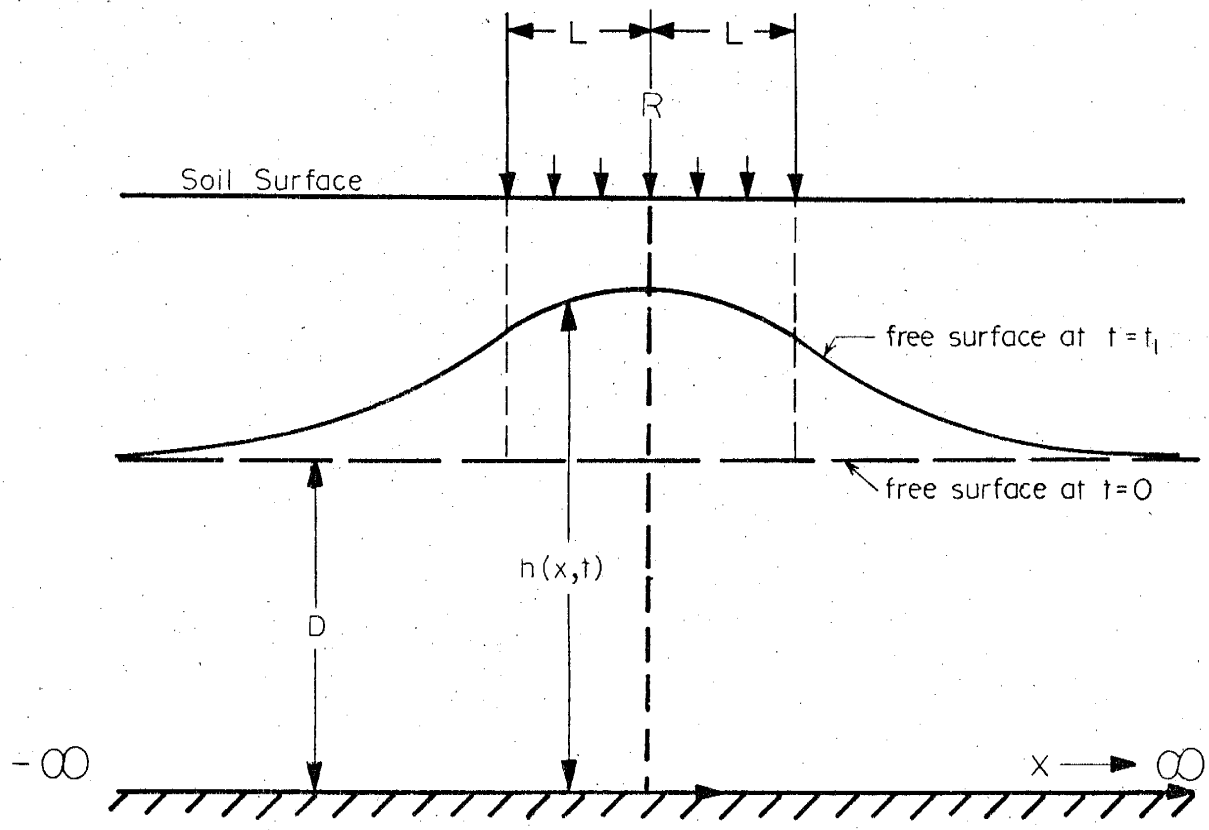

Figure 39. Ground water mound

validity and limitations of the horizontal model in artificial groundwater recharge will be incomplete. We can however analyze the significance of the vertical flow effects that are neglected in the horizontal model.

5.2 Horizontal Flow Models

In section 2.2 we derived the basic partial differential equation according to the horizontal flow model theory. Equation (2.23) describes the free surface of a transient groundwater mound in a region subject to artificial recharge. It is nonlinear and no general analytical solution is available.

A. Linearized Model in h

If the height of the groundwater mound is assumed small compared to the initial saturated thickness, and if $S \ll S_y$, a linearized version of equation (2.23) in one dimension may be written as

$$\frac{\partial h}{\partial t} = \frac{DK_H}{S_y} \frac{\partial^2 h}{\partial x^2} + \frac{R(x)}{S_y} \tag{5.1}$$

where

$$R(x) = R, \quad |x| \leq L$$

$$= 0, \quad |x| \geq L$$

Now if

$$s_r = h - D$$

and

$$\alpha = DK_H/S_y$$

Table 8. Different theoretical models and their limitations, considered in artificial groundwater recharge problem, $h = h(r,t)$ is the height of the phreatic surface above a datum and D is the initial saturated thickness.

Theoretical Model	Assumptions			Author
	Vertical Flow	Flow Zone Thinning ($h \neq$ constant)	Unsaturated Zone	
Horizontal flow model:				
linear in h	no	no	no	Polubarinova-Kochina (1962)
linear in h^2	no	yes ($h \approx D$ in storage term)	no	Hantush (1967)
nonlinear	no	yes	no	Amar (1973)
Potential flow model:				
linearized phreatic surface	yes	no	no	Dagan (1967) Hunt (1970)
nonlinear phreatic surface	yes	yes	no	Amar (1973) Singh (1972)
Variably saturated flow model:				
nonlinear	yes	yes	yes	no solution available

equation (5.1) becomes

$$\frac{\partial s_r}{\partial t} = \alpha \frac{\partial^2 s_r}{\partial x^2} + \frac{R(x)}{S_y} \tag{5.2}$$

This should be solved subject to the following boundary and initial conditions (see figure 39):

$$s_r \to 0 \quad \text{as} \quad |x| \to \infty$$
$$\text{and} \quad s_r(x, t=0) = 0 \tag{5.3}$$

Equations (5.2) and (5.3) have been solved by Polubarinova-Kochina (1962); the solution in dimensionless form is

$$s_r' = 1/2 \{t' \operatorname{erf}(\frac{1 - x'}{2\sqrt{t'}}) + \frac{(1 - x')\sqrt{t'}}{\sqrt{\pi}} e^{-(1 - x')^2/4t'}$$
$$- \frac{(1 - x')^2}{2} [1 - \operatorname{erf}(\frac{1 + x'}{2\sqrt{t'}})] + t' \operatorname{erf}(\frac{1 + x'}{2\sqrt{t'}})$$
$$+ \frac{(1 + x')\sqrt{t'}}{\sqrt{\pi}} e^{-(1 + x')^2/4t'} - \frac{(1 - x')^2}{2} [1 - \operatorname{erf}(\frac{1+x'}{2\sqrt{t'}})]\} \tag{5.4}$$

for $|x'| \leq 1$

and

$$s_r' = 1/2 \{t' \operatorname{erf}(\frac{1 + x'}{2\sqrt{t'}}) + \frac{(1 + x')\sqrt{t'}}{\sqrt{\pi}} e^{-(1+x')^2/4t'}$$
$$- \frac{(1+x')^2}{2} [1 - \operatorname{erf}(\frac{1+x'}{2\sqrt{t'}})] - t' \operatorname{erf}(\frac{x'-1}{2\sqrt{t'}})$$
$$- \frac{(x'-1)\sqrt{t'}}{\sqrt{\pi}} e^{-(1-x)^2/4t'} + \frac{(x'-1)^2}{2} [1 - \operatorname{erf}(\frac{x'-1}{2\sqrt{t'}})]\} \tag{5.5}$$

for $|x'| \geq 1$

where $s_r' = s_r/DP$, $P = RL^2/K_H D^2$, $x' = x/L$, $t' = tK_H D/S_y L^2$

and $\operatorname{erf}(w) = \frac{2}{\sqrt{\pi}} \int_0^w e^{-\lambda^2} \, d\lambda$

Equations (5.4)and (5.5) were evaluated numerically, and the results are shown in figure 40.

B. Linearized Model in h^2

Hantush (1967), Polubarinova-Kochina (1962) and other investigators applied another method of linearization, solving for h^2 instead of h. Following Hantush's derivation, let $Z = h^2 - D^2$ in equation (2.23); it can then be written as

$$\frac{S_y}{K_H h} \frac{\partial Z}{\partial t} = \frac{\partial^2 Z}{\partial x^2} + \frac{2R}{K_H}$$

Replacing h with an average value $\tilde{h}$ transforms this to

$$\frac{\partial Z}{\partial t} = \alpha \frac{\partial^2 Z}{\partial x^2} + \frac{2\tilde{h}R}{S_y} \tag{5.6}$$

where $\alpha = K_H \tilde{h}/S_y$

Equation (6.5) is subject to the following boundary and initial conditions:

$$\begin{aligned} Z(x,t) &= 0 \qquad \text{at } t = 0 \\ Z(x,t) &= 0 \qquad \text{at } x = \pm B \end{aligned} \tag{5.7}$$

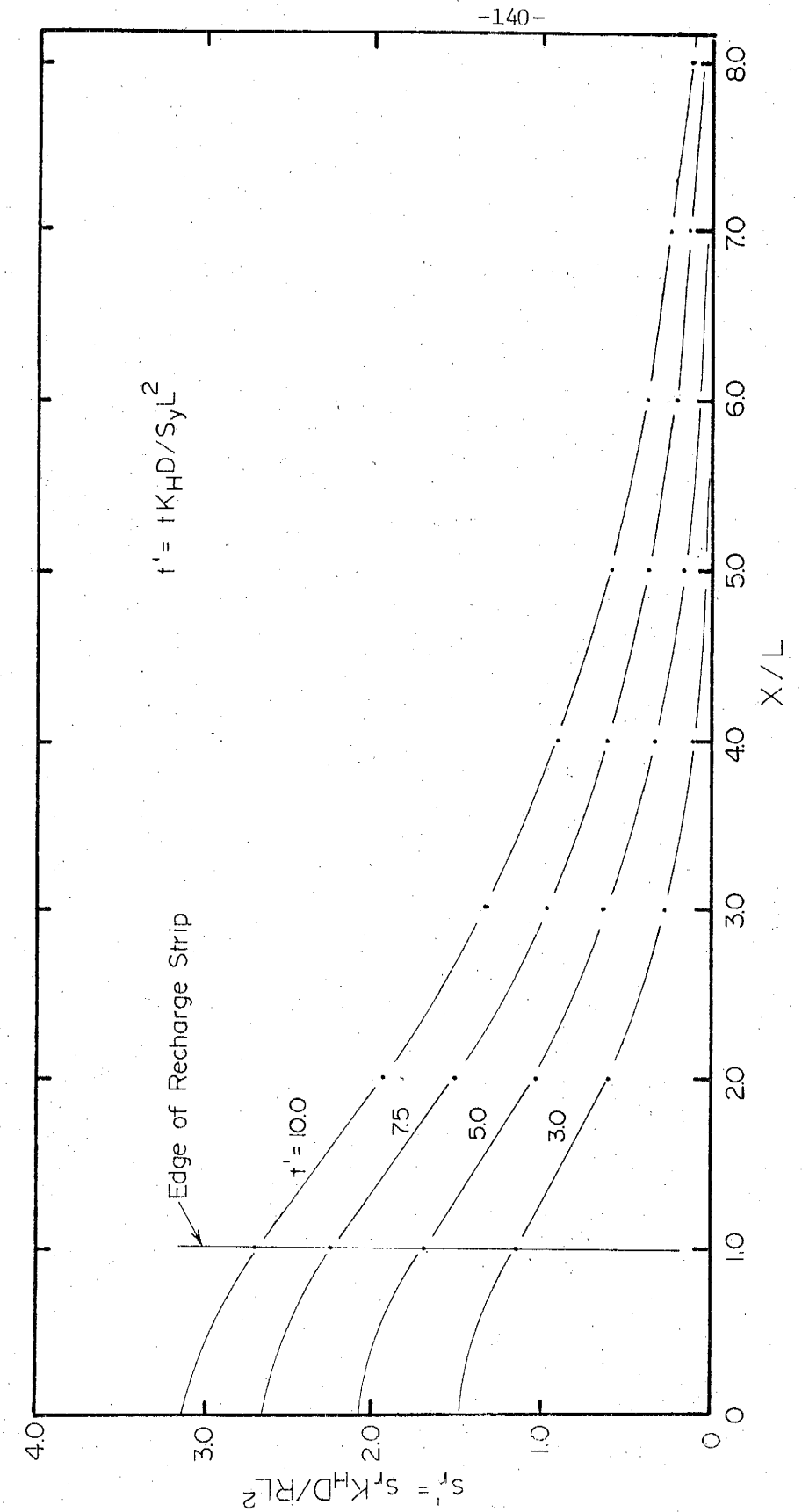

Figure 40. Dimensionless rise of the water table versus dimensionless distance predicted by the linearized horizontal model in h (equation 5.4)

Hantush (1967) solved this for a finite and an infinite domain, i.e. when $|B| \to \infty$. The solution for the finite domain is

$$Z(x,t) = \frac{32B^2D}{S_y\alpha\pi^3}\left\{\sum_{n=1}^{\infty}\frac{1}{(2n-1)^3}\left(1 - e^{-\alpha(2n-1)\pi^2 t/4B^2}\right)\right.$$

$$\left. x \sin((2n-1)\pi L/2B)\cos((2n-1\pi x/2B)\right.$$

or in dimensionless form,

$$s_r' = \frac{1}{P}\left[1 + \frac{32PB'^2}{\pi^3}\sum_{n=1}^{\infty}\frac{1 - e^{-(2n-1)^2\pi^2 t'/4B^2}}{(2n-1)^3}\sin((2n-1)\pi/2B')\right.$$

$$\left. x \cos((2n-1)\pi x'/2B')\right]^{1/2} - \frac{1}{P} \qquad (5.8)$$

where $B' = B/L$ and $P = RL^2/K_H D^2$

The solution for an infinite domain is

$$s_r' = \frac{1}{P}\sqrt{1 + Ps_{r_o}'(x',t')} - 1/P \qquad (5.9)$$

where s_{r_o}' is the solution to the linearized model in h (equations (5.4) and (5.5) for $|x'| \leq 1$ and $|x'| \geq 1$, respectively). The results of equation (5.9) are shown in figure 41. In figure 42, to demonstrate the effects of the boundary, the infinite and finite domain ($B' = B/L = 17$) solutions are compared. They are identical up to $x/L = 10$, where the finite domain solution starts to show a lower rise of the water table; overall, however the difference is insignificant.

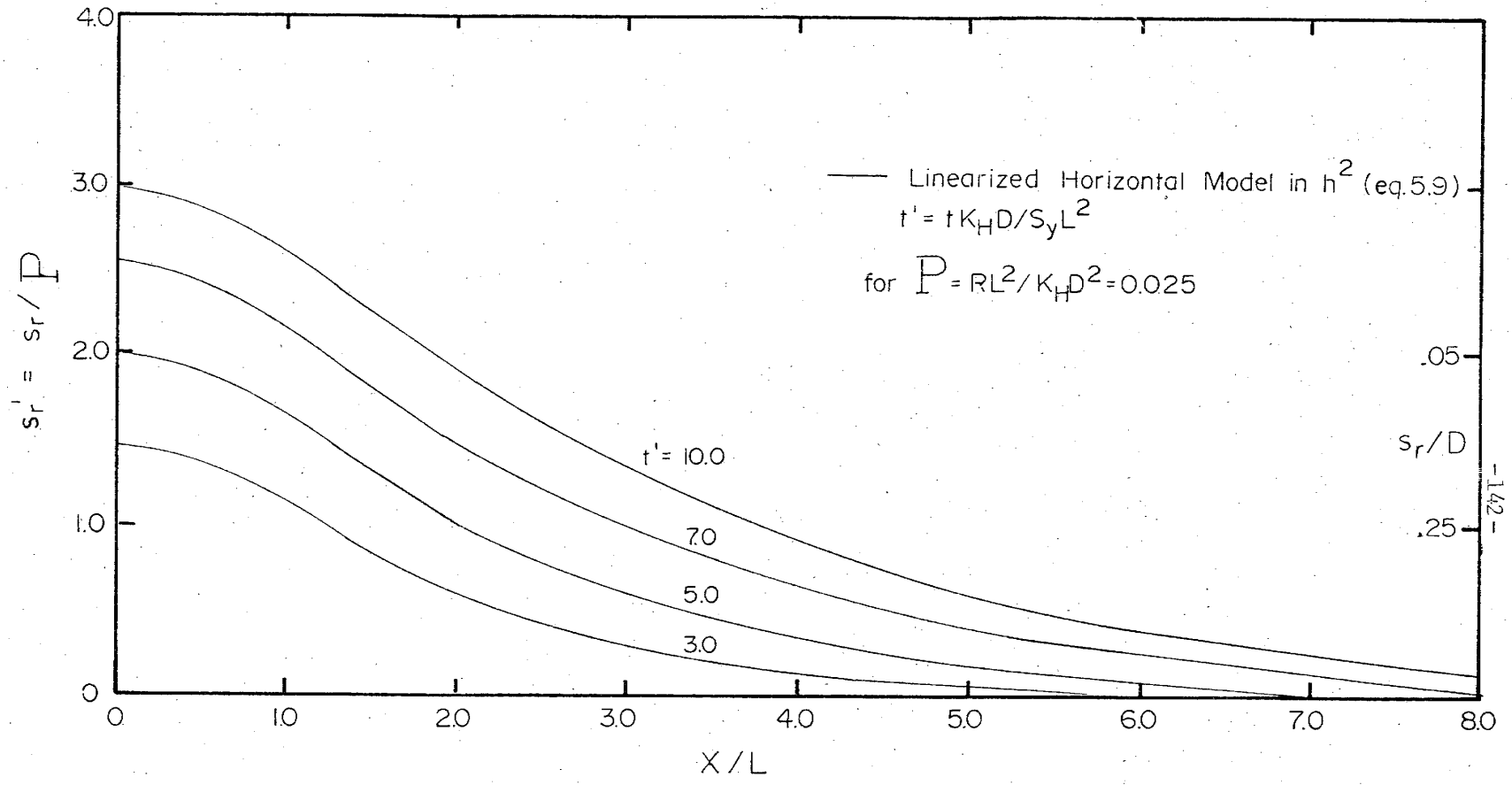

Figure 41. Dimensionless rise of the water table versus dimensionless distance predicted by the linearized horizontal model in h^2

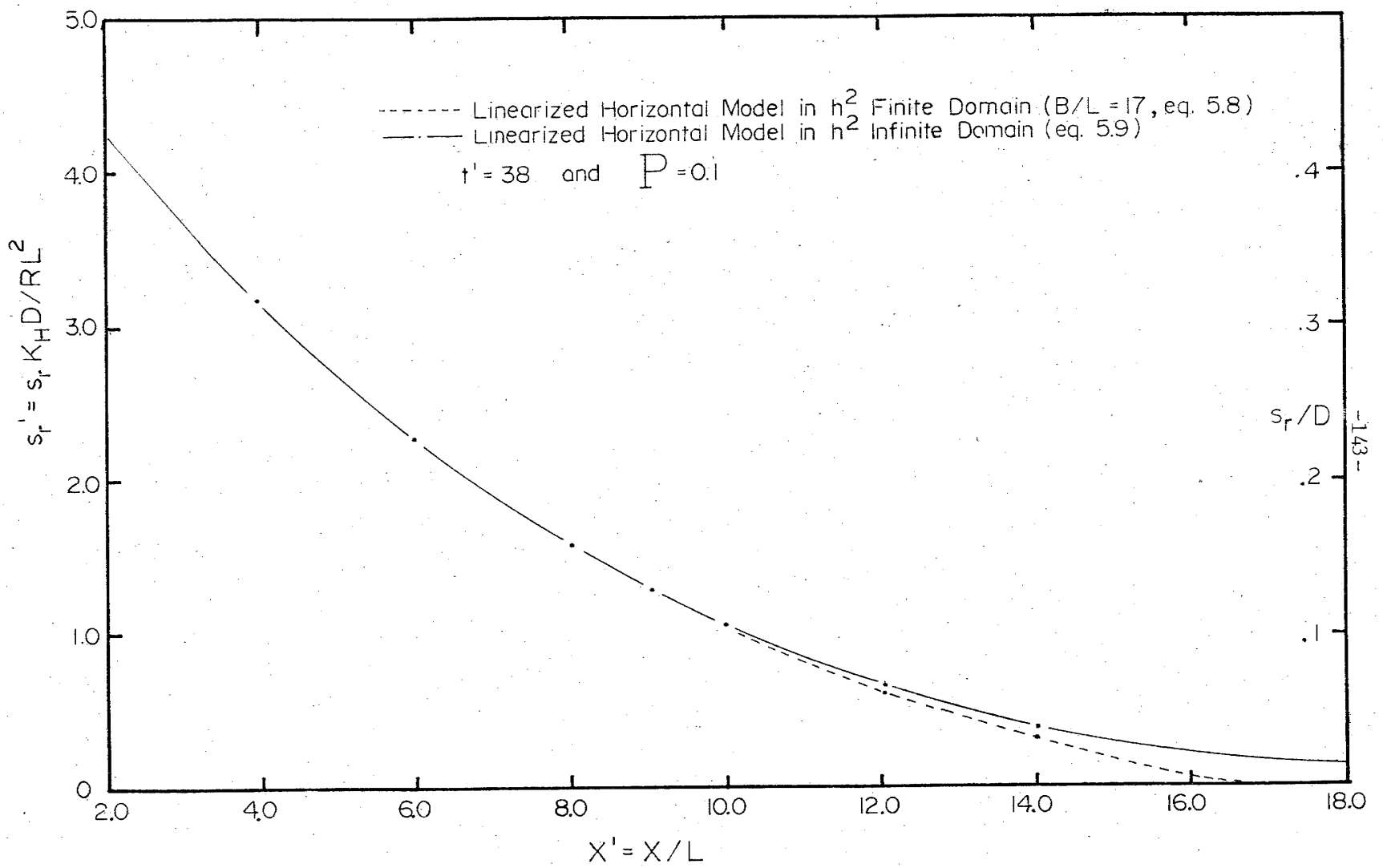

Figure 42. Dimensionless rise of the water table versus dimensionless distance

C. Nonlinear Horizontal Model

Amar (1973) numerically solved equation (2.23) (with the compressibility term omitted) and appropriate boundary and initial conditions. He used both the explicit and implicit finite difference formulations. We used his computer program for the explicit finite difference approximation to obtain the rise in the phreatic surface height. A dimensionless time increment ($\Delta t'$) equal to 1.25×10^{-3} and space increment ($\Delta x/L$) equal to 5×10^{-2} were used. However, this method of solution has the disadvantage that if Δx is chosen rather small in the interest of accuracy, the permissible $\Delta t'$ (note that the limit imposed on $\Delta t'$ is proportional to $(\Delta x)^2$) turns out to be so small that about an hour of the computer (IBM 360/44) time is required to complete a problem. The results obtained using Amar's computer program for the nonlinear horizontal model are compared with those of the linearized models in h and h^2 in figures 43a and 43b.

5.3 Correlation of the Horizontal Flow Models

The solution curves shown so far have been for the linearized horizontal models in h and h^2 and the nonlinear horizontal model. Figure 44 shows a significant difference between the linearized horizontal model in h and the linearized model in h^2; this increases with an increase in time and the nonlinearity parameter $P = RL^2/K_H D^2$. In figures 43a and 43b the three horizontal models are compared for values of P of 0.2 and 0.0759; the linearized horizontal model in h predicts a higher rise of the water table than the nonlinear model, which in turn predicts a higher rise than the linearized model in h^2.

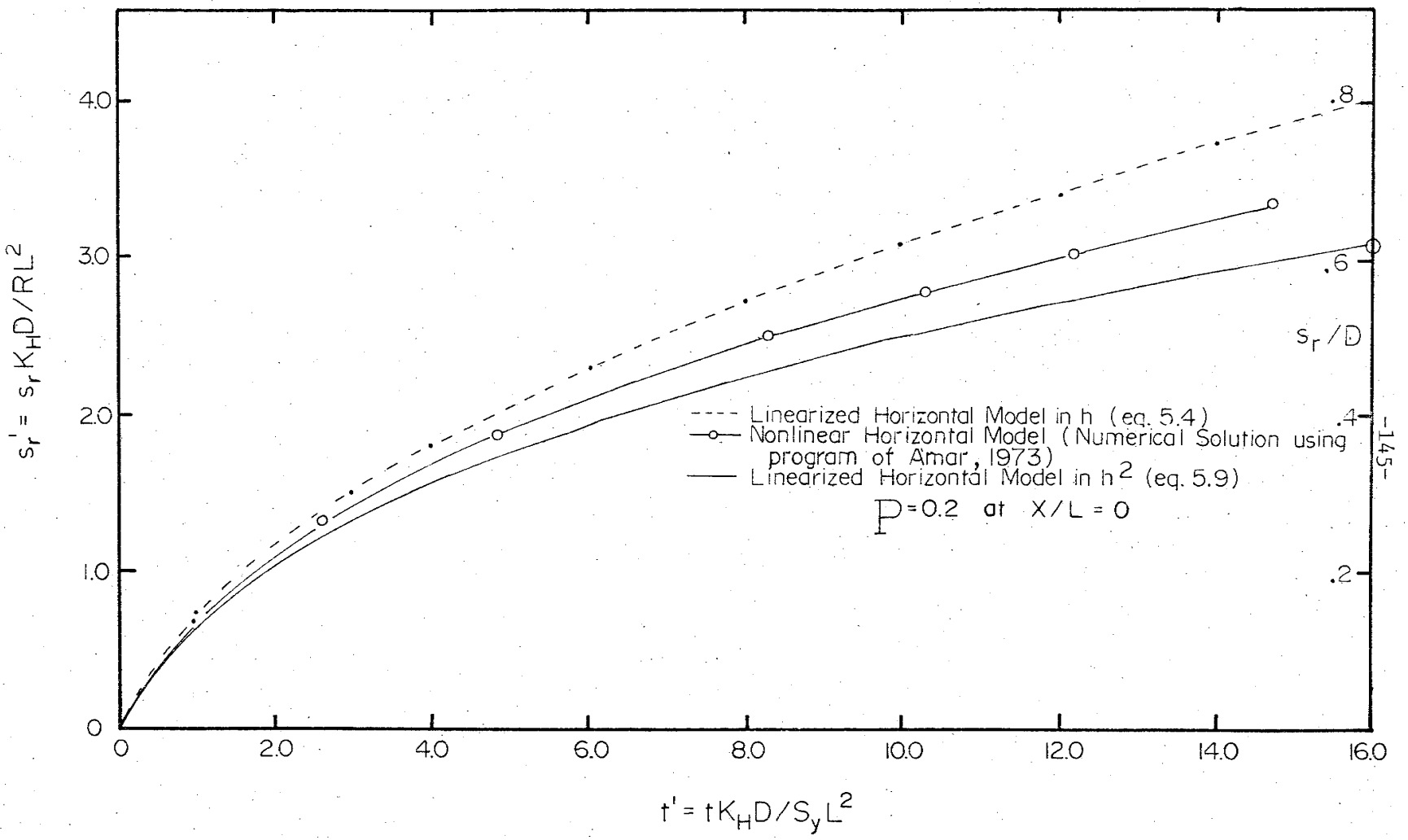

Figure 43a. Comparison between the nonlinear and linearized horizontal model in h and h^2 for P = 0.2

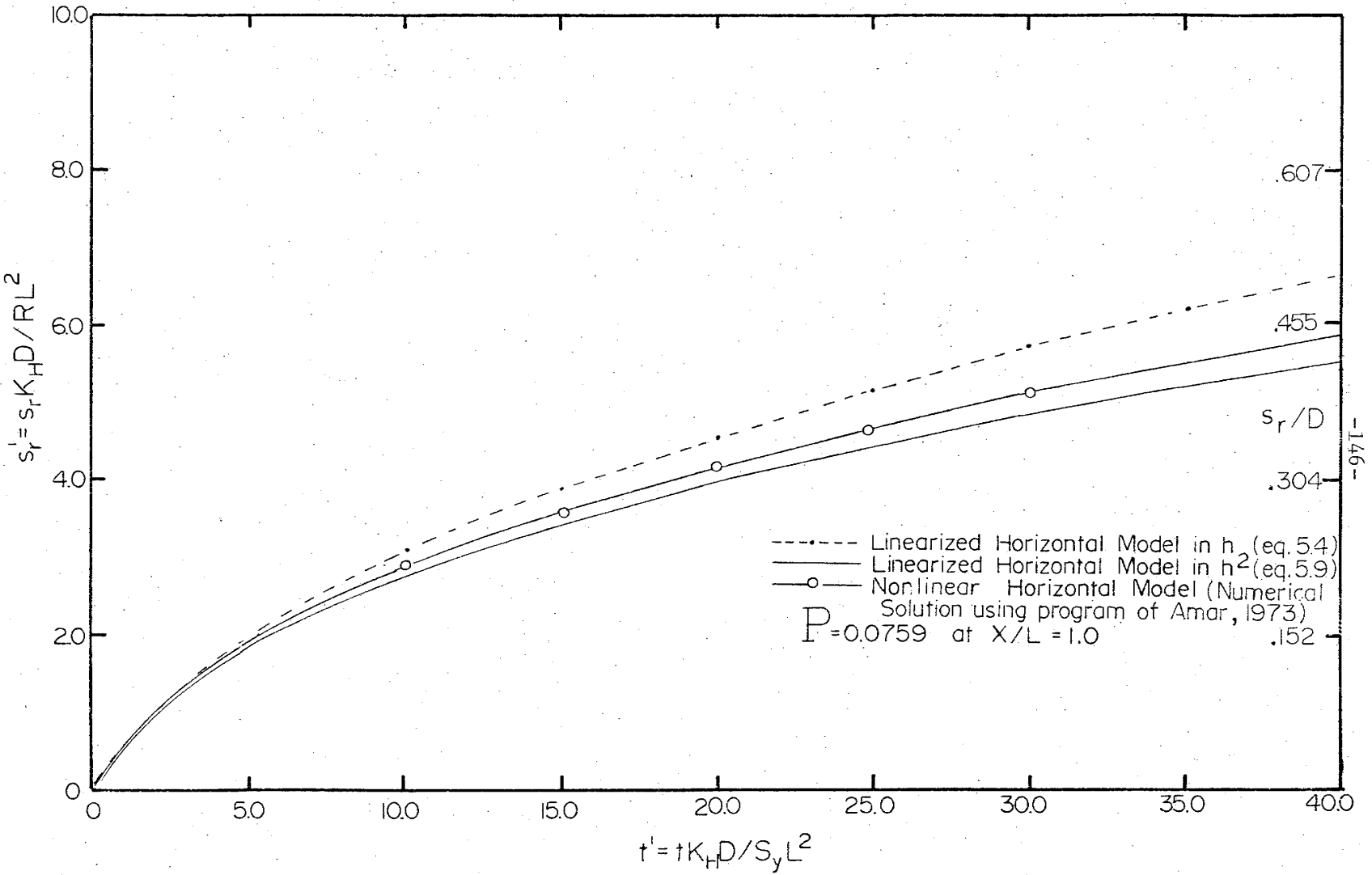

Figure 43b. Comparison between the nonlinear and linearized horizontal model in h and h^2 for P = 0.0759

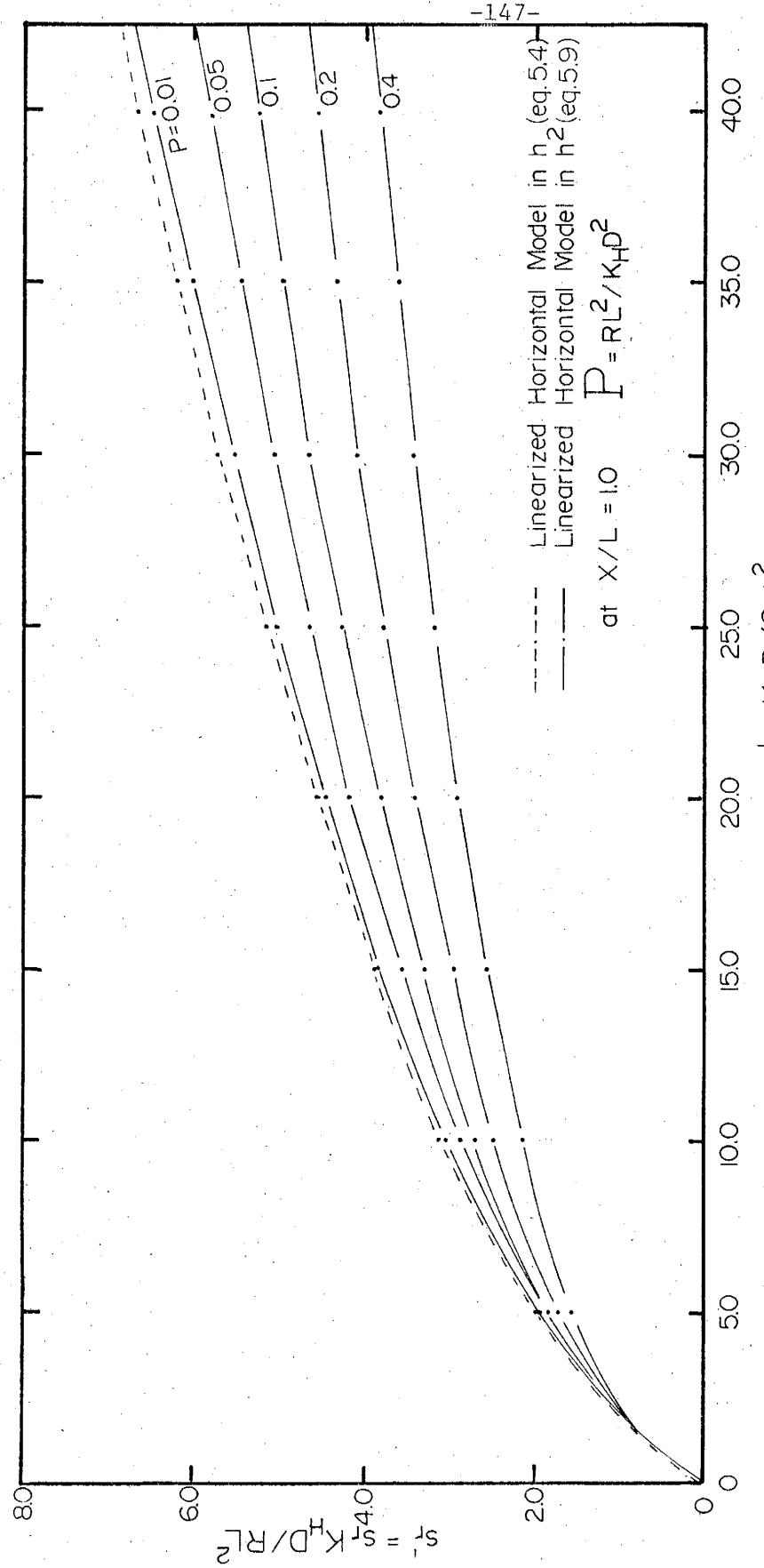

Figure 44. Comparison between the linearized horizontal flow models in h and h^2

Figure 45 shows that, for P = 0.2 and $s_r/D = 0.6$, the difference between dimensionless rise of the water table at x/L = 0 predicted by the nonlinear model and that predicted by the linearized model in h^2 is about 10%; for P = 0.0759 and the same s_r/D, the difference is less than 9%. It is obvious from this that the linearized model in h^2 does not approximate the exact horizontal flow model for the problem of recharge as adequately as it does for the well flow problem (see figure 6). Nevertheless, the linearized horizontal model in h^2 approximates the nonlinearity effects for most practical purposes ($s_r/D \leq 0.5$) with an error of less than 10%.

5.4 Potential Flow Model

According to potential theory, equation (2.7a) is the governing equation for flow through a porous medium under incompressible, saturated and homogeneous conditions. The free surface boundary condition is described by a nonlinear partial differential equation containing a time derivative. This can be used to determine the height of the phreatic surface after the other terms in the equation are known. Since it is nonlinear no general analytical solution is available.

A. Linearized Model

Assuming that the rise of the groundwater mound is small compared to the initial saturated thickness and neglecting the seepage face, the linearized potential flow model can be described as follows:

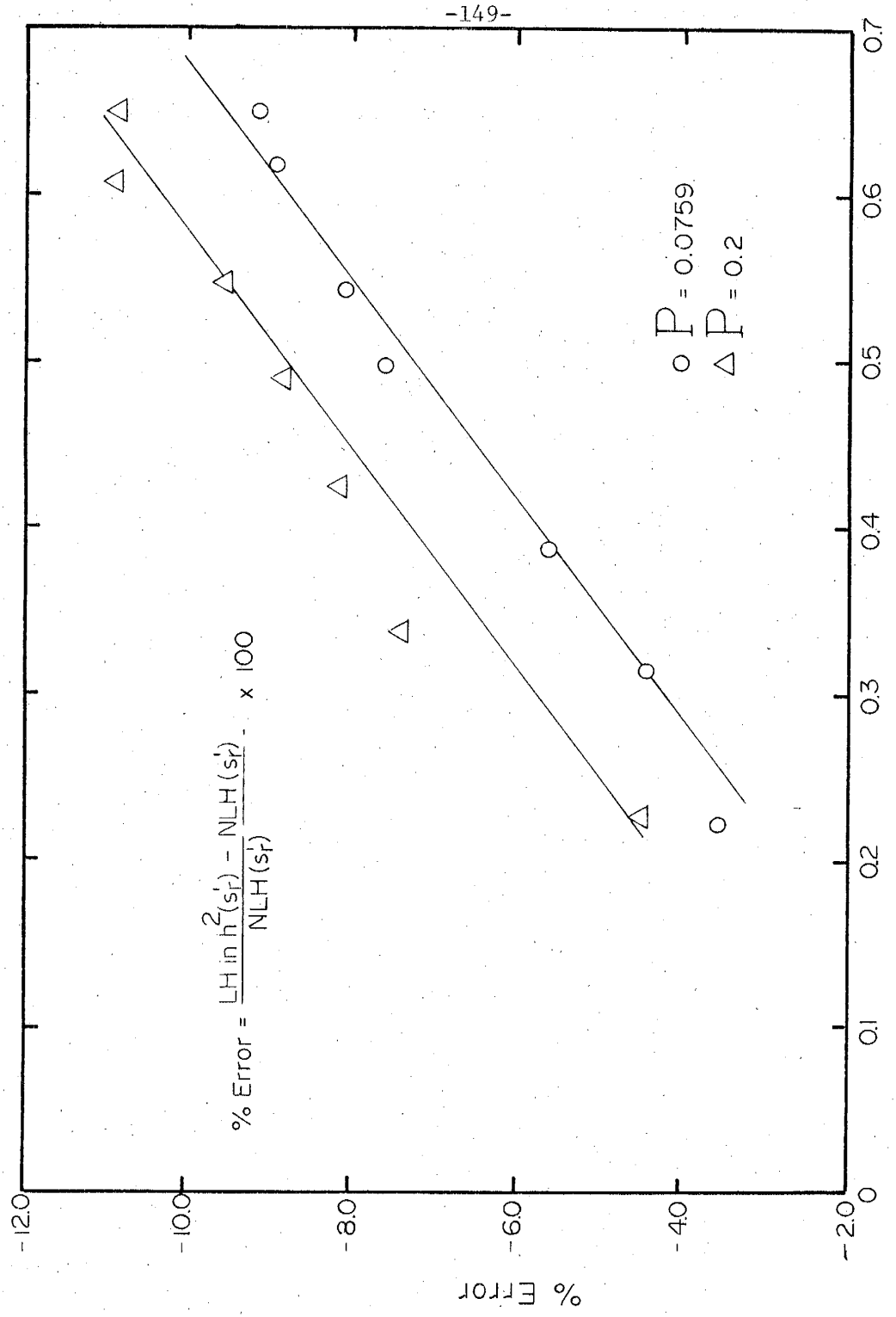

Figure 45. Error in the rise of the free surface as a function of (s_r'/D) based on the linearized horizontal model in h^2

$$K_H \frac{\partial^2 \phi}{\partial x^2} + K_v \frac{\partial^2 \phi}{\partial z^2} = 0 \qquad (5.10)$$

$$\phi(x,z,t = 0) = 0$$

$$\frac{\partial \phi}{\partial z} = 0 \quad \text{on } z = -D$$

$$\frac{\partial \phi}{\partial x} = 0 \quad \text{on } x = 0 \qquad (5.11)$$

$$\phi(x \to \infty, z, t) = 0$$

$$\frac{S_y}{K_v} \frac{\partial \phi}{\partial t} = \frac{R}{K_v} - \frac{\partial \phi}{\partial z} \qquad \text{on } z = 0 \qquad (5.12)$$

By letting $X = \sqrt{K_v/K_H}\ x$ in equation (5.10), we get

$$\frac{\partial^2 \phi}{\partial X^2} + \frac{\partial^2 \phi}{\partial z^2} = 0 \qquad (5.13)$$

Also let $\ell = L\sqrt{K_v/K_H}$

Equations (5.11), (5.12) and (5.13) are analogous to the equations obtained by Dagan (1967) and Hunt (1970), who used perturbation techniques and assumed an isotropic medium ($K_v = K_H = K$). Their solutions are identical (equation (26) of Dagan's paper and equation (31) of Hunt's paper), and can be written in the transformed form (for anisotropic medium) as

$$s'_r = \frac{s_r}{D}\frac{K_H D^2}{RL^2} = \frac{2}{\pi}\frac{1}{\eta}\int_0^{\infty} \frac{\sin\lambda \cos\lambda X'}{\lambda^2} \frac{1 - e^{-(\lambda t'\eta)} \tanh(\lambda/\eta)}{\tanh(\lambda/\eta)}\, d\lambda$$

where $\eta = \sqrt{K_V/K_H}\ L/D$, and $D' = D/\ell$

This integral was evaluated numerically using Simpson's rule (see Appendix (C) for program listing). The results are shown in figure 46 for various values of η. The figure shows that the linearized potential flow model predicts a higher rise of the phreatic surface for smaller values of η.

B. Nonlinear Model

Amar (1973) and Singh (1972) solved the nonlinear potential flow model numerically without introducing any linearization. Amar used the accelerated Liebman relaxation method to calculate the values of head at interior points of the flow domain from the known initial position of the phreatic surface and the various boundary conditions except the upper moving phreatic surface. He then determined the position of the phreatic surface at successive intervals of time by applying the forward finite difference approximation. The computer program used to solve this problem is unavailable, as are the time and space increments and the error involved in the difference approximation. His results are reproduced in figure 47. This figure shows that the nonlinear potential flow model predicts a lower rise of phreatic surface than the linearized model.

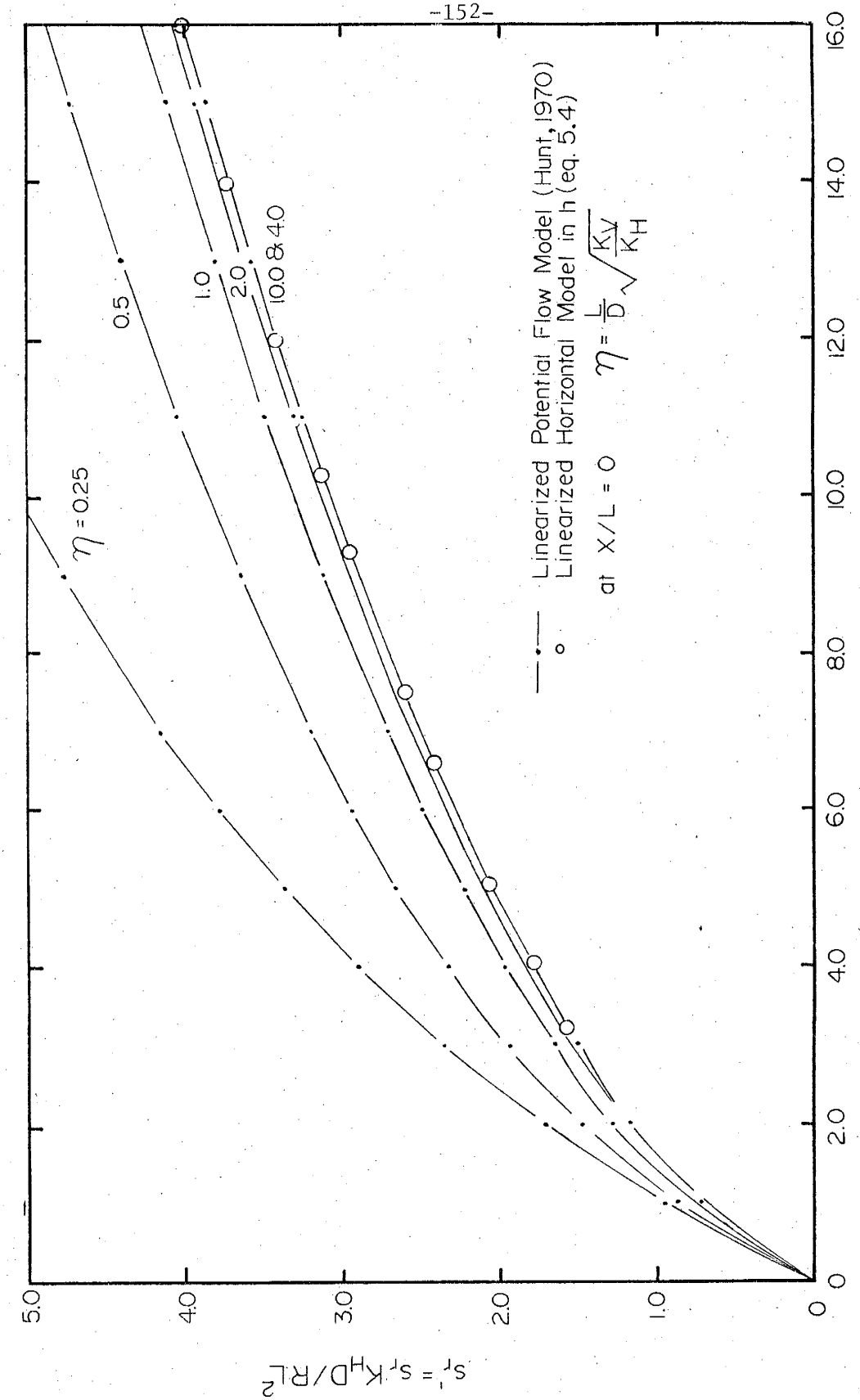

Figure 46. Comparison between the linearized potential flow model and linearized horizontal model in h

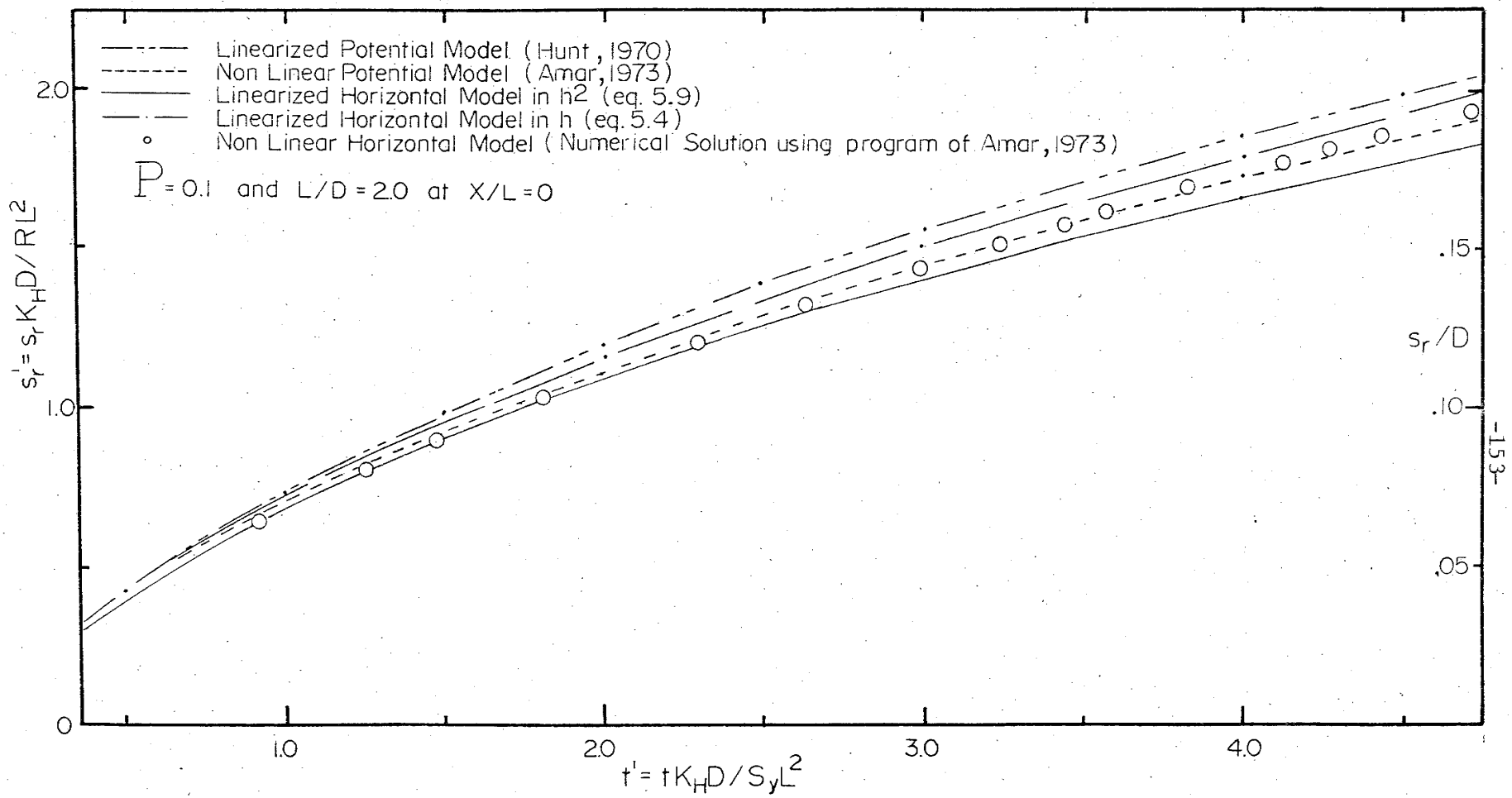

Figure 47. Dimensionless rise of the water table versus dimensionless time

5.5 Correlation of the Horizontal Flow Models and the Vertical Flow Models

Figure 46 compares the dimensionless rise of the water table obtained from the linearized potential model with that from the linearized horizontal model in h. The two solutions are practically identical for $\eta = (L/D)\sqrt{K_V/K_H} \geq 4$. For smaller values of η, the linearized potential flow model predicts a higher rise than does the linearized horizontal model in h, particularly beneath the recharge basin. Outside the recharge basin, the reverse is true; the linearized horizontal model shows a higher rise of the water table, but the difference is relatively small (see figure 48).

Figure 47 shows a comparison of the nonlinear potential flow model and the nonlinear horizontal model. The dimensionless rise of the water table predicted by the two models practically coincides for $\eta = 2$ and $P = 0.1$. In general the nonlinear horizontal and potential flow models predict a lower rise of the water than the corresponding linearized models.

From this investigation, we conclude that beneath a recharge basin the vertical flow effects are insignificant and can be neglected provided that $\eta \geq 4$ (this is the same critical value obtained in the well flow and drainage problems). Consequently the nonlinear horizontal flow model is valid provided that $\eta \geq 4$ and the unsaturated zone is small and can be neglected. The linearized horizontal model in h^2 is a fair approximation (with an error of less than 10%) for determining the rise of the water table provided that $\eta \geq 4$ and $s_r/D \leq 0.5$.

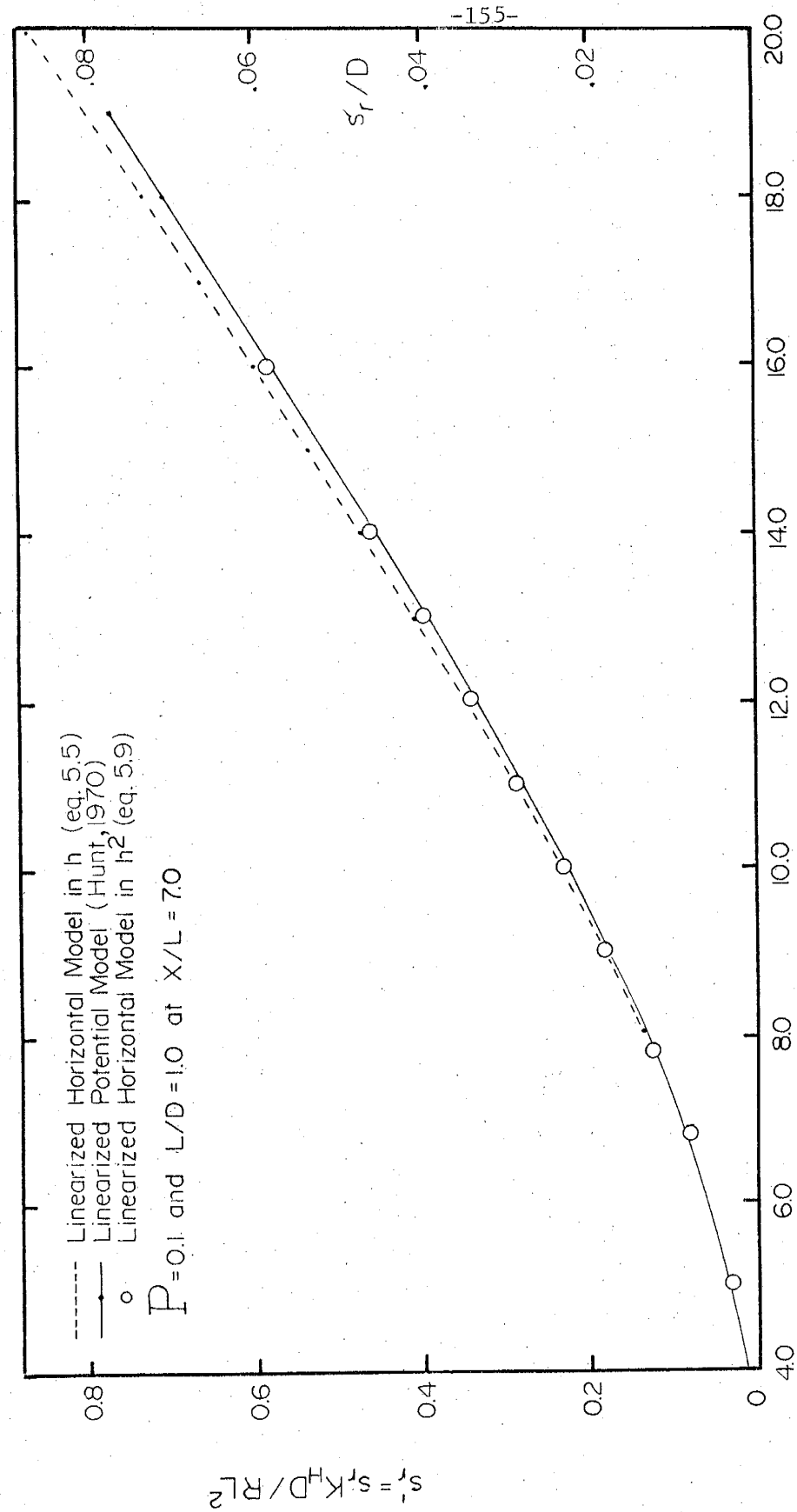

Figure 48. Dimensionless rise of the water table versus dimensionless time, outside the recharge basin

SUMMARY, CONCLUSIONS AND RECOMMENDATIONS

Axisymmetric flow toward a fully penetrating pumping well, flow to parallel drainage ditches in agricultural land, and artificial groundwater recharge in unconfined anisotropic aquifers are the problems that have been considered. Analysis of these problems was made using:

1) horizontal flow models assuming hydrostatic pressure distribution and no contribution from the unsaturated zone,
2) potential flow models (vertical flow) assuming that the unsaturated zone does not contribute to flow,
3) variably saturated models where both the saturated and partly saturated flow are taken into account (This model has not been considered in the artificial groundwater recharge problem), and
4) improved horizontal flow model, in which vertical flow effects are approximated (only for well flow).

A mathematical model for the fourth case was derived for the first time here; analogous to Boulton's (1963), the analytical solution for this model was obtained and evaluated.

Correlation and analysis of the existing analytical and numerical solutions for the first three cases as well as the solution for the fourth case made it possible to evaluate the effects and the significance of the following physical factors:

1) thinning of the flow zone,
2) vertical flow and the anisotropy of permeability

3) the unsaturated zone above the phreatic surface. These in turn made it possible to examine the validity of the horizontal flow models.

The following conclusions can be drawn from this research:

1) The variably saturated model predicts higher drawdown than do the saturated models. The ratio between the critical height or thickness of the unsaturated zone to the initial saturated thickness (h_{cr}/D) can serve as a criterion for determining whether the contribution from the unsaturated zone is important. The larger the value of h_{cr}/D, the more significant the unsaturated zone is. For values of this parameter less than 0.07 the unsaturated zone can usually be neglected. Under this condition errors in hydraulic head are less than 10% for fully penetrating or deep observation wells ($z/D \leq 0.5$). This same critical value holds in the drainage problem where the ratio of drainable depth to the initial saturated thickness (H/D) is equal to or less than 0.5. For H/D = 1, there is about a 12% error.

2) The parameters $r/B = (r/D)\sqrt{K_v/K_H}$ in well flow and $\eta = (L/D)\sqrt{K_v/K_H}$ in linear flow can serve as criteria for determining whether the effects of vertical flow and anisotropy of permeability are important. The smaller the value of r/B and η, the larger the effects are. The critical value of η and r/B above which the vertical flow effects can be neglected was found to be 4.0.

3) The parameters s/D in well flow, H/D in flow to parallel drainage ditches, and $P = RL^2/K_H D^2$ in artificial groundwater recharge can serve as criteria for determining the effects of thinning of the flow zone. The larger the value of these parameters, the larger

will be the effects of thinning of the flow zone. The critical values are $s/D = 0.2$ with an error $\leq 10\%$, $H/D = 0.2$ and $P = 0.01$ with less than 5% error.

4) The nonlinear horizontal flow model in general is valid provided that r/B and η are equal to or greater than 4.0 and h_{cr}/D is equal to or less than 0.07 (with an error of less than 10%).

5) The horizontal flow model has been improved by a correction developed to account for the vertical flow and flow zone thinning. This model has been analyzed and a transition zone (where the vertical flow and flow zone thinning interact) has been provided for the first time. A new field equation suitable for numerical simulations, combining the above effects, has also been obtained.

It is recommended that further research be conducted in the following:

1) The investigation and analysis presented here needs to be extended to more practical problems of partially penetrating stream-connected aquifers and agricultural drainage. The effects of the unsaturated zone can be very important in these problems and analytical corrections for them can be developed similar to the one by Kroszynski and Dagan, 1974, for well flow.

2) The improved horizontal flow model developed here (for the well flow problem) to account for flow zone thinning and vertical flow can be solved for agricultural drainage and artificial groundwater recharge problems.

3) The new field equations obtained in this study, combining the

vertical flow effects and the flow zone thinning, need to be tested for numerical simulations.

REFERENCES

Amar, A., 1973, "Hydrodynamics of Artificial Groundwater Recharge," Ph.D. Dissertation, Dept. of Eng., Univ. of Calif. Irvine.

Barenblatt, G.I., Zheltov, P., and Kochina, I.F., 1960, "Basic concepts in the theory of seepage of homogeneous liquids in fissured rocks," J. Appl. Math. Mech., v. 24, n. 5.

Baumann, P., 1965, "Technical developments in groundwater recharge," Advances in Hydroscience, v. 2, pp. 209-279, Academic Press, New York.

Bear, J., Zaslavsky, D., and Irmay, S., 1968, "Physical principles of water percolation and seepage," Arid Zone Research, UNESCO, 465 p.

Bear, J., 1972, "Dynamics of fluid in porous media," 764 p., American Elsevier Publishing Co.

Bianchi, W.C. and Haskell, E.E. Jr., 1968, "Field observations compared with Dupuit-Forchheimer theory for mound heights under a recharge basin, "Water Resour. Res., v. 4, n. 5, pp. 1049-1057.

Bibby, R. and Sunada, D.K., 1971, "Mathematical model of leaky aquifer," J. Irrig. and Drainage Div., Proc. Amer. Soc. Civil Eng., v.97, n.IR3.

Bittinger, M.W. and Trelease, F.J., 1960, "The development and dissipation of a groundwater mound beneath a spreading basin," (mimeo) 10 p. Paper presented at 1960 Winter meeting Amer. Soc. Agric. Eng., Memphis, Tenn.

Boulton, N.S., 1951, "The flow pattern near a gravity well in a uniform water bearing medium," J. Inst. Civil Eng., v. 36, p. 534.

Boulton, N.S., 1954, "The drawdown of the water-table under non-steady conditions near a pumped well in an unconfined formation," Proc. Inst. Civil Eng., v.3, n.3.

_____, 1963, "Analysis of data from non-equilibrium pumping tests allowing for delayed yield from storage," Proc. Inst. Civil Eng., v.26.

Boussinesq, J., 1904, "Recherches theoretiques sur l'ecoulement des nappes d'eau infiltrees dans le sol et sur le debuit des sources," J. Math. Pure Appl., v.10 (5th series), pp. 363-394.

Bouwer, H., 1964, "Unsaturated flow in groundwater hydraulics," J. Hydraulic Div., Amer. Soc. Civil Eng. Proc. Paper 4057, pp. 121-144.

_____, 1965, "Limitation of Dupuit-Forchheimer assumption in recharge and seepage," Trans. Amer. Soc. Agric. Eng., v.8, pp. 512-515.

Brutsaert, W., 1967, "Some methods of calculating unsaturated permeability," Trans. Amer. Soc. Agric. Eng., v.10, n.3, pp. 400-404.

Brutsaert, W., Breitenbach, A., and Sunada, D.K., 1971, "Computer analysis of free surface well flow," J. Irrig. and Drainage Div., Amer. Soc. Civil Eng., pp. 405-420.

Brutsaert, W. and Way, C., 1973, "A conjunctive use surface water-groundwater simulator," WRRI report no. 033, N. Mexico Water Resources Research Institute.

Cooley, R.L., 1971, "A finite difference method for unsteady flow in variably saturated porous media: Application to a single pumping well," Water Resour. Res., v.7, n.6.

Dagan, G., 1964, "Linearized solution of unsteady deep flow toward an array of horizontal drains," J. Geophys. Res., v.69, n.16, pp. 3361-3369.

_____, 1966, "The solution of the linearized equations of free surface flow in porous media," J. de Mechanique, v.5, n.2, pp. 207-215.

_____, 1967a, "A method of determining the permeability and effective porosity of unconfined anisotropic aquifers," Water Resour. Res., v.3.

_____, 1967, "Linearized solutions of free-surface groundwater flow with uniform recharge," J. Geophys. Res., v.72, n.4, pp. 1183-1193.

Davidson, J.M., Stone, L.R., Nielsen, D.R., and LaRue, M.E., 1969, "Field measurement and use of soil-water properties," Paper presented at the 5th annual meeting of the American Geophysical Union, n.443.

Davison, B., 1936, "On the steady two-dimensional motion of groundwater with a free surface," Philosophical Magazine, 5.7, v.21, n.143, pp. 881-903.

Day, P.R., and Luthin, J.N., 1956, "A numerical solution of the differential equation of flow for a vertical drainage problem," Soil Sci. Soc. Amer. Proc. v.20, n.4, pp. 443-447.

DeWiest, R.J.M., 1961, "Free surface flow in homogeneous porous medium," J. Hydraulic. div. Proc. Amer. Soc. Civil Eng., v.87, n.H44, pp. 181-221.

_____, 1965, "History of the Dupuit-Forchheimer assumptions on groundwater hydraulics," Trans., Amer. Soc. Civil Eng., pp. 508-509.

_____, 1969, "Flow through Porous Media," Academic Press.

Dumm, L.D., 1954, "New formula for determining depth and spacing of subsurface drains in irrigated lands," Agr. Engr. 35, pp. 726-730.

Dupuit, J., 1863, "Etudes theoriques et pratiques sur le mouvement des eaux," 2nd ed., Paris.

Gardner, W.R. and Miklich, F.J., 1962, "Unsaturated conductivity and diffusivity measurements by a constant flux method," Soc. Soil Sci., v.93, pp. 271-274.

Gelhar, L.W., 1974, "Stochastic analysis of phreatic aquifers," Water Resour. Res., v.10, n.3, pp. 539-545.

Glover, R.E., 1965, "Application of Dupuit-Forchheimer assumptions in groundwater hydraulics," Trans. Amer. Soc. Agric. Eng., v.8, n.4.

_____, 1974, "Transient Groundwater Hydraulics," Department of C.E., College of Eng., Colorado State Univ., 413 p.

Hantush, M.S., 1964, "Hydraulics of wells," Advances in Hydroscience 1, edited by Ven Te Chow, pp. 282-432, Academic Press, New York.

_____, 1967, "Growth and decay of groundwater mounds in response to uniform percolation," Water Resour. Res., v.3, n.1, pp. 227-234.

Hornberger, G.M., Ebert, J., and Remson, I., 1970, "Numerical Solution of the Boussinesq Equation for aquifer-stream interaction," Water Resour. Res., v.6, n.2, pp. 601-608.

Hunt, B.W., 1970, "Vertical recharge of unconfined aquifer," J. Hydraulic. Div., Proc. Amer. Soc. Civil Eng., v.97, n.HY7, pp. 1017-1030.

Irmay, S., 1966, "Solution of the nonlinear diffusion equation with a gravity term in hydrology. Symposium on water in the unsaturated zone," UNESCO, Washington, 50 p.

Isherwood, J.D., 1959, "Water table recession in tile-drained land," J. Geophys. Res., v.64, pp. 795-804.

Jacob, C.E., 1940, "On the flow of water in an elastic artesian aquifer," Trans. AGU, part 2.

_____, 1944, "Notes on determining permeability of pumping tests under water table conditions," U.S. Geol. Surv. open-file report.

_____, 1950, "Flow of groundwater," Engineering Hydraulics," edited by H. Rouse, pp. 321-386, John Wiley and Sons, New York.

_____, 1963, "Determining the permeability of water table aquifers," U.S. Geol. Surv. Water Supply Pap. 1536-I.

Jeffrey, S.H., and Swirles, B., 1956, "Methods of Mathematical Physics," University Press, Cambridge.

Jeppson, R.W., 1968, "Seepage from ditches--solution by finite differences," J. Hydraulic. Div., Proc. Amer. Soc. Civil Eng., v.94, n.HY1, pp. 259-283.

Karadi, G.M., Krizek, R.J., and Elnagyer, H., 1968, "Unsteady seepage flow between fully penetrating trenches," J. Hydrol., v.6, n.4, pp. 417-430.

Karadi, G.M., Krizek, R.J., and Rechea, M., 1970, "Critical evaluation of certain methods of unsteady groundwater hydraulics," Water Resour. Bull., v.6, n.3, pp. 424-438.

Kipp, K.L., 1973, "Unsteady flow to a partially penetrating finite radius well in an unconfined aquifer," Water Resour. Res. v.9, n.2, pp. 448-462.

Kirkham, D., 1950, "Seepage into ditches in the case of a plane water table and an impervious substratum," Trans. American Geophysical Union, v. 31, n.3, pp. 425-430.

Kirkham, D. and Gaskell, R.E., 1951, "The falling water table in tile and ditch drainage," Soil Sci. Soc. Amer. Proc., v.15, pp. 37-42.

Kirkham, D., 1966, "Steady-state theories for drainage," J. Irrig. and Drainage Div., Amer. Soc. Civil Eng. Proc., n.IR1, Paper 4707, pp. 19-39.

Kirkham, D., 1964, "Exact theory for the shape of the free water surface about a well in a semiconfined aquifer," J. Geophys. Res., v.69, n.12, pp. 2537-2549.

Kriz, G.J., 1967, "Determination of unconfined aquifer characteristics," J. Hydraulic Div. Proc. Amer. Soc. Civil Eng., n.HY2, pp. 37-47.

Kriz, G.J., Scott, V.H., and Borgy, R.H., 1966, "Analysis of parameters of an unconfined aquifer," J. Hydraulic Div., Amer. Soc. Civil Eng., pp. 49-56.

Kroszynski, U.I., and Dagan, G., 1974, "Well pumping in unconfined aquifers: the influence of the unsaturated zone," Third annual and final report, Project No. A10-SWC-77, Hydraulic Eng. Lab., Technion, Haifa, Israel.

Kroszynski, U.I., 1975, "Flow in a vertical porous column drained at its bottom at constant flux," J. Hydrol., v.24, pp. 135-153.

Lamb, H., 1945, "Hydrodynamics," Sixth ed., Dover Publications.

Luthin, J.N., and Worstell, R.V., 1957, "The falling water table in tile drainage--a laboratory study," Soil Sci. Soc. Am. Proc., v.21, pp. 580-584.

Maasland, M., 1959, "Water table fluctuations induced by intermittent recharge," J. Geophys. Res., v.74, pp. 549-559.

Mansur, C.I., and Dietrich, R.J., 1965, "Pumping test to determine permeability ratio," Amer. Soc. Civil Eng. Proc., v.91, n.SM4.

Marino, M.A., 1967, "Hele-Shaw model study of the growth and decay of groundwater ridges," J. Geophys. Res., v.72, n.4, pp. 1195-1205.

Miller, E.E. and Miller, R.D., 1956, "Physical theory for capillary flow phenomena," J. Appl. Physics, v.27, n.4, pp. 324-332.

Murray, A.W., 1970, "Seepage face effect in unsteady groundwater flow," Ph.D. Dissertation, Dept. of Civil Eng., Univ. of Wisconsin, Madison.

Muskat, M., 1946, "The flow of homogeneous fluids through porous media," J.W. Edwards, Inc., 763 p.

Myers, L.E., and Van Bavel, C.H.M., 1962, "Measurement of water table elevations," Congr. Intern. Comm. Irrigation Drainage, 5th, 17.109-17.119.

Neuman, S.P., 1972, "Finite element computer programs for flow in saturated-unsaturated porous media," Second annual report, part 3, Project no. A10-SWC-77, Hydraulic Eng. Lab., Technion, Haifa, Israel.

_____, 1972, "Theory of flow in unconfined aquifers considering delayed response of the water table," Water Resour. Res., v.8, n.4.

_____, 1974, "Effect of partial penetration on flow in unconfined aquifers considering delayed gravity response," Water Resour. Res., v.10, n.2, pp. 303-312.

_____, 1975, "Analysis of pumping test data from anisotropic unconfined aquifers considering delayed gravity response," Water Resour. Res., v.11, n.2, pp. 329-342.

Nielsen, D.R., and Biggar, J. W., 1961, "Measuring capillary conductivity," Soc. Soil Sci., v.92, pp. 192-193.

Nielsen, D.R., Kirkham, D., and Perrier, E.R., 1960, "Soil capillary conductivity: comparison of measured and calculated values," Soil Sci. Soc. Amer. Proc., v.24, pp. 157-160.

Pinder, G.F., and Bredehoeft, J.D., 1968, "Application of the digital computer for aquifer evaluation," Water Resour. Res., v.4, n.5.

Polubarinova-Kochina, P.Y., 1962, "Theory of groundwater movement," (translated from Russian by J.M.R. DeWiest), Princeton Univ. Press, 613 p.

Prickett, T.A., 1965, "Type-curve solution to aquifer tests under water table conditions," J. Groundwater, v.3, n.3, p.5.

Prickett, T.A., and Lonnquist, C.G., 1971, "Selected digital computer techniques for groundwater resource evaluation," Ill. State Water Survey, Bull. 55, 62 p.

Prill, R.C., 1961, "Comparison of drainage data obtained by the centrifuge and column drainage methods, U.S. Geol. Surv. Prof. Pap. 424-D, Art. 434, pp. 399-401.

Richards, L.A., 1931, "Capillary conduction of liquids through porous mediums," Physics, v.1, pp. 318-333.

Rubin, J., 1968, "Theoretical analysis of two-dimensional transient flow of water in unsaturated and partly saturated soils," Soil Sci. Soc. Amer. Proc., v.32, n.5, pp. 607-615.

Shaw, F.S., and Southwell, R.V., 1941, "Relaxation methods applied to engineering problems, VII: Problems relating to the percolation of fluids through porous media," Proc. Royal Soc., A178, 1941.

Singh, R., 1972, "Mound geometry under recharge basins," Dept. of Civil Eng., Calif. State Univ., San Jose, Calif. (NSF research grant no. GK-18526).

Smith, W.O., 1967, "Infiltration in sands and its relation to ground-water recharge," Water Resour. Res., v.3, n.2, pp. 539-555.

Stallman, R.W., 1961, "Boulton's integral for pumping test analysis," U.S. Geol. Surv. Prof. Pap. 424-C.

Streltsova, T.D., 1972, "Unsteady radial flow in an unconfined aquifer," Water Resour. Res., v.8, n.4, p. 1059.

_____, 1973, "Flow near a pumped well in an unconfined aquifer under nonsteady conditions," Water Resour. Res., v.9, n.1,pp.227-235.

_____, and Rushton, K.R., 1973, "Water table drawdown due to a pumped well in an unconfined aquifer," Water Resour. Res., v.9, n.1, pp. 236-242.

Swartzendruber, D., 1966, "Soil water behavior as described by transport coefficients and function," from Advances in Agronomy, v.18, Academic Press, Inc., New York.

Taylor, G.S., and Luthin, J.N., 1969, "Computer methods for transient analysis of water-table aquifers," Water Resour. Res., v.5, n.1, pp. 144-152.

Terzidis, G., 1968, "Computational schemes for the Boussinesq equation," J. Irrig. and Drainage Div., Amer. Soc. Civil Eng. Proc., v.94, n.IR4, pp. 381-389.

Theis, C.V., 1935, "The relation between the lowering of the piezometric surface and the rate and duration of discharge of a well using ground-water storage," Trans. American Geophysical Union, 16th Annual meeting, pt. 2.

Thiem, G., 1906, "Hydrologische Methoden," Gebhardt, Leipzig, 56p.

Todsen, M., 1971, "On the solution of transient free-surface flow problems in porous media by finite-difference methods," J. Hydrol., v.12, pp. 177-210.

VanSchilfgaarde, J., 1963, "Transient design of drainage systems," Proc. Amer. Soc. Civil Eng., v.91, n.IR3, pp. 9-22.

VanSchilfgaarde, J., 1965, "Limitations of Dupuit-Forchheimer theory in drainage," Trans. Amer. Soc. Agric. Eng., v.8, n.4, pp. 515-519.

Verma, R.D., 1969, "Physical analysis of the outflow from an unconfined aquifer," Ph.D. Dissertation, Dept. of Civil Eng., Cornell Univ.

Verma, R.D., and Brutsaert, W., 1971, "Unsteady free surface groundwater seepage," J. Hydraulic Div., Proc. Amer. Soc. Civil Eng., v.97, n.HY8, pp. 1213-1228.

Wenzel, L.K., 1942, "Methods for determining permeability of water bearing materials, with special reference to discharging-well methods, with a section on direct laboratory methods and a bibliography on permeability and laminar flow by V.C. Fishel," U.S. Geol. Surv. Water Supply Pap. 887, 192 p.

Werner, P.W., 1957, "Some problems in nonartesian groundwater flow," Trans. AGU., V.38, n.4, pp. 511-518.

White, W.N., 1932, "A method of estimating ground-water supplies based on discharge by plants and evaporation of soil," U.S. Geol. Surv. Water Supply Pap. 659-A, 106 p.

Yeh, W.G., 1970, "Nonsteady flow to a surface reservoir," Proc. Amer. Soc. Civil Eng., v.96, n.HY3, pp. 609-618.

APPENDIX A

Input Data for the Computer Program of the Variably Saturated Flow Model by Kroszynski and Dagan, 1974

The flow domain is divided into rectangles in the r,z plane, and these in turn are divided into triangels; the total number of nodal points used is 550 (25 nodes in the z-direction and 22 in the r-direction, the radial and the vertical coordinates are shown below). The initial saturated thickness D is 10 meters; the horizontal and vertical conductivities are 40 m/day and 10 m/day respectively; the specific yield S_y is 0.2 and the discharge Q is 800 m^3/day. The well radius r_w is 0.1 meters.

Radial coordinates (meters): 0.1, 0.2, 0.3, 0.4, 0.5, 0.6, 0.7, 0.8, 1.0, 1.5, 2.0, 2.5, 3.0, 4.0, 5.0, 7.0, 10.0, 20.0, 50.0, 100.0, 500.0, 1000.0

Vertical coordinates (meters): 0.0, 1.0, 2.0, 3.0, 4.0, 5.0, 6.0, 7.0, 7.50, 8.0, 8.25, 8.5, 8.75, 9.0, 9.25, 9.5, 9.75, 10.0, 10.2, 10.4, 10.6, 10.8, 11.0, 11.5, 12.0

APPENDIX B

RESULTS OBTAINED FROM THE IMPROVED HORIZONTAL FLOW MODEL

DIMENSIONLESS AVERAGE DRAWDOWN ($4\pi TS/Q$)

C =0.005

τ_s =	0.1	0.2	0.4	0.6	0.8	1.0	2.0
.002	.535	.53	.53	.50	.466	.421	.194
.005	1.19	1.192	1.11	.996	.857	.715	.227
.01	1.8	1.75	1.564	1.311	1.05	.819	.228
.02	2.456	2.31	1.935	1.493	1.121	.841	0.229
.05	3.24	2.95	2.18	1.55	1.13	.843	0.239
.1	3.81	3.29	2.225	1.555	1.142	.845	.254
.3	4.52	3.41	2.241	1.565	1.159	.885	0.298
.6	4.8	3.51	2.242	1.6	1.22	.939	.390
1.	4.83	3.51	2.26	1.611	1.241	1.001	.496
10.	4.851	3.593	2.554	2.184	1.949	1.827	1.827
20.	4.858	3.695	2.823	2.508	2.475	2.475	2.475
40.	4.956	3.86	3.232	3.152	3.149	3.149	
100.			4.071	4.058	4.058	4.058	4.058
1000.	6.382	6.381	6.380	6.380	6.380	6.380	6.380
5000.	8.021	8.021	8.021	8.021	8.021	8.021	8.021
10000	8.730	8.730	8.730	8.730	8.730	8.730	8.730

C =0.01

τ_y \ ξ =	0.1	0.2	0.4	0.6	0.8	1.0	2.0
0.002	0.535	0.535	0.534	0.504	0.466	0.421	0.194
0.005	1.19	1.192	1.114	0.996	0.857	0.715	0.227
0.01	1.80	1.75	1.564	1.311	1.05	0.819	0.228
.02	2.456	2.31	1.935	1.493	1.121	.841	0.225
.05	3.24	2.95	2.18	1.55	1.13	.843	0.239
0.10	3.81	3.29	2.225	1.555	1.142	0.845	0.254
0.3	4.52	3.41	2.241	1.566	1.16	0.886	0.298
0.60	4.80	3.51	2.244	1.60	1.222	0.940	0.391
1.0	4.83	3.510	2.261	1.611	1.241	1.00	0.496
6.0	4.845	3.554	2.425	1.949	1.637	1.526	
10.0	4.853	3.596	2.558	2.188	1.954	1.831	1.831
20.0	4.861	3.701	2.335	2.16	2.483	2.483	2.48
40.0	4.961	3.869	3.244	3.165	3.161	3.161	3.161
1000.	6.483	6.435	6.435	6.435	6.435	6.435	6.435
5000.	8.104	8.104	8.104	8.104	8.104	8.104	8.104
10000	8.828	8.828	8.828	8.828	8.828	8.828	8.828

C = 0.03

τ_y \ ξ =	0.1	0.2	0.4	0.6	0.8	1.0	2.0
0.002	.535	.535	.534	.504	.466	.421	.194
0.005	1.19	1.192	1.114	0.996	0.857	0.715	0.227
0.01	1.80	1.75	1.564	1.311	1.05	0.819	0.228
.02	2.456	2.31	1.935	1.493	1.121	.841	0.225
.05	3.24	2.95	2.18	1.55	1.13	.843	0.239
0.10	3.81	3.29	2.225	1.555	1.142	0.845	0.254
0.3	4.52	3.41	2.241	1.566	1.16	0.886	0.30
0.60	4.80	3.51	2.244	1.60	1.222	0.940	0.391
6.0	4.848	3.561	2.436	1.961	1.648	1.537	
10.0	4.858	3.607	2.576	2.207	1.971	1.848	1.848
20.0	4.871	3.723	2.866	2.546	2.514	2.514	2.514
40.0	4.983	3.911	3.295	3.217	3.214	3.214	
100.0			4.179	4.168	4.168	4.168	4.168
1000.	6.711	6.664	6.664	6.664	6.664	6.664	6.664
50000	8.479	8.479	8.479	8.479	8.479	8.479	8.479
10000	9.273	9.273	9.278	9.278	9.278	9.278	9.278

C =0.05

ζ_g	ξ = 0.1	0.2	0.4	0.6	0.8	1.0	2.0
0.002	0.535	0.535	0.534	0.504	0.466	0.421	0.194
0.005	1.19	1.192	1.114	0.996	0.857	0.715	0.227
0.01	1.80	1.75	1.564	1.311	1.05	0.819	0.228
.02	2.455	2.31	1.935	1.493	1.121	.841	0.225
.05	3.24	2.95	2.18	1.55	1.13	.843	0.239
0.05	3.24	2.95	2.181	1.553	1.131	0.843	
0.10	3.81	3.29	2.225	1.555	1.142	0.845	0.254
0.3	4.52	3.41	2.241	1.566	1.16	0.886	0.301
0.60	4.80	3.51	2.244	1.60	1.222	0.940	0.391
6.0	4.852	3.568	2.447	1.974	1.659	1.547	
10.0	4.864	3.619	2.594	2.226	1.989	1.865	1.865
20.0	4.883	3.746	2.898	2.579	2.547	2.549	2.549
40.0	5.006	3.953	3.349	3.272	3.269	3.269	3.269
100.0			4.276	4.265	4.265	4.265	4.265
1000.	6.974	6.932	6.932	6.932	6.932	6.932	6.932
5000.	8.939	8.939	8.939	8.939	8.939	8.939	8.939

C = 0.08

τ_y \ ξ =	0.1	0.2	0.4	0.6	0.8	1.0	2.0
10000	9.845	9.845	9.845	9.845	9.845	9.845	9.845
0.002	0.535	0.535	0.534	0.504	0.466	0.421	0.194
0.005	1.19	1.192	1.114	0.996	0.857	0.715	0.227
0.01	1.80	1.75	1.564	1.311	1.05	0.819	0.228
0.02	2.456	2.31	1.935	1.493	1.121	0.841	0.225
0.05	3.24	2.95	2.181	1.553	1.131	0.843	0.239
0.10	3.81	3.29	2.225	1.555	1.142	0.845	0.254
6.0	4.857	3.578	2.464	1.992	1.677	1.564	
10.0	4.873	3.637	2.622	2.257	2.018	1.892	1.89
20.0	4.90	3.781	2.949	2.631	2.600	2.60	.60
40.0	5.040	4.019	3.437	3.363	3.362	3.362	3.362
100.0			4.441	4.430	4.430	4.430	4.430
1000.	7.467	7.437	7.437	7.437	7.437	7.437	7.437
5000.	9.900	9.900	9.900	9.900	9.900	9.900	9.900
10000	11.09	11.09	11.09	11.09	11.09	11.09	11.09

DIMENSIONLESS FREE SURFACE DRAWDOWN ($4\pi Ts^{\circ}/Q$)

C =0.005

τ_y \ ξ =	0.1	0.2	0.4	0.6	0.8	1.0	2.0
.1						.021	.023
.3				.042	.054	.062	0.071
.6			.053	.083	.106	.123	.144
1.	.012	.035	.088	.137	.175	.201	.244
6.	.072	.206	.498	.739	.908	1.018	1.261
10.	.12	.338	.794	1.136	1.357	1.491	1.742
20.	.238	.654	1.423	1.892	2.136	2.257	2.429
40.	.466	1.221	2.338	2.802	2.971	3.035	3.125
100.	1.101	2.524	3.715	3.933	3.991	4.01	4.049
1000.	5.536	6.268	6.382	6.382	6.382	6.382	6.382
10000	8.678	8.720	8.720	8.720	8.720	8.720	8.720

C =0.01

τ_y \ ξ =	0.1	0.2	0.4	0.6	0.8	1.0	2.0
0.1						0.021	0.023
.3				.042	.054	.062	0.071
0.6			0.053	.083	0.106	0.123	0.144
1.0	0.012	0.035	0.088	.137	0.175	0.202	0.244
6.0	0.072	0.20	0.49	0.739	0.90	1.01	1.263
10.0	0.120	0.338	0.794	.138	1.359	1.494	1.746
20.0	0.238	0.654	1.426	.897	2.142	2.263	2.437
40.0	0.466	1.223	2.345	.812	2.982	3.047	3.138
1000.	5.576	6.319	6.408	.435	6.435	6.435	6.435
10000	8.780	8.781	8.785	8.820	8.828	8.828	8.828

C =0.03

ζ_y \ ξ =	0.1	0.2	0.4	0.6	0.8	1.0	2.0
0.1						0.021	0.023
.3				.042	.054	.062	0.071
0.6			0.053	0.083	0.106	0.123	0.144
1.0	0.012	0.035	0.088	0.137	0.175	0.202	0.244
6.0	0.072	0.206	0.500	0.742	0.913	1.025	1.271
10.0	0.120	0.339	0.798	1.144	1.368	1.505	1.761
20.0	0.238	0.656	1.436	1.915	2.165	2.290	2.467
40.0	0.467	1.230	2.374	2.853	3.029	3.095	3.189
100.0	1.108	2.565	3.806	4.036	4.097	4.117	4.159
1000.	5.746	6.540	6.636	6.665	6.665	6.665	6.665
10000	9.222	9.222	9.222	9.222	9.222	9.222	9.222

C =0.05

ζ_y \ ξ =	0.1	0.2	0.4	0.6	0.8	1.0	2.0
.1						.021	.023
.3				.042	.054	.062	0.071
.6			.053	.083	.106	.123	.144
1.	.012	.035	.088	.137	.176	.202	.244
6.	.072	.206	.501	.745	.917	1.03	1.279
10.	.120	.339	.801	1.151	1.378	1.517	1.777
20.	.238	.658	1.447	1.935	2.190	2.317	2.500
40.	.469	1.238	2.404	2.897	3.078	3.147	3.245
100.	1.115	2.601	3.886	4.126	4.191	4.211	4.255
1000.	5.939	6.797	6.901	6.932	6.932	6.932	6.932
10000	9.779	9.789	9.843	9.844	9.844	9.844	9.844

C =0.08

$\tilde{\zeta}$ =	0.1	0.2	0.4	0.6	0.8	1.0	2.0
$\tilde{\zeta}_y$							
.1						.021	.023
.3				.042	.054	.062	0.071
.6			.053	.083	.107	.123	.144
1.	.012	.035	.088	.137	.176	.202	.245
6.	.072	.207	.503	.749	.924	1.038	1.292
10.	.120	.341	.806	1.161	1.393	1.535	1.803
20.	.239	.662	1.463	1.965	2.229	2.362	2.552
40.	.470	1.250	2.452	2.968	3.159	3.233	3.336
100.	1.124	2.657	4.021	4.280	4.350	4.372	4.419
1000.	6.289	7.279	7.401	7.438	7.438	7.438	7.440
10000	11.01	11.04	11.08	11.09	11.09	11.09	11.09

APPENDIX C

Program listing of the linearized Potential flow model (Integral equation) for the artificial ground water recharge (Hunt, 1970)

```
C      ARTIFICIAL GROUNDWATER RECHARGE MOUND ---LINEARIZED POTENTIAL FLOW
C                                        MODEL BY HUNT(1970)
C      EVALUATION OF THE INTEGRAL EQ. BY SIMPSON RULE
C      SPRIME=(SR)KHD/(EL**2)
C      XPRIME=X/L
C      DPRIME=D/L
C      ETA=SQRT(KV/KH)*L/D
C      TPRIME=(T*KH*D)/(SY*L**2)
       COMMON DPRIME,TPRIME,X
       FUNC(Y)=(SIN(Y)-COS(Y*A)/Y**2)*(1.-EXP(-((Y*TPRIME)/DPRIME)*TANH(Y
      1*DPRIME)))/TANH(Y*DPRIME)
       REAL INT,NEWINT
       READ(5,100)DPRIME
  100  FORMAT(F4.3)
       ETA=L/DPRIME
       WRITE(6,60) ETA
   60  FORMAT(10X,'ETA =',F3.4)
       WRITE(6,30)
   30  FORMAT(1H1,    44H     M      TPRIME        XPRIME          SRPRIME   ///)
C      RUN THROUGH A SERIES OF XPRIME VALUES
       DO 43 KKK=1,2
       X=.10+1.0*FLOAT(KKK-1)
C      RUN THROUGH A SERIES OF TPRIME VALUES
       DO 40 K=1,20
       TPRIME=0.0+FLOAT(K-1)
C      RUN THROUGH A SERIES OF M VALUES
       DO 50 KK=10,40,10
       M=KK
       FM=M
       H=FM/2.
       N=1
       TWO=0.0
       FOUR=FUNC(FM/2.)
       INT=(H/3.)*(4.*FOUR+FUNC(FM))
    5  H=H/2.
       N=2*N
       TWO=TWO+FOUR
       FOUR=0.0
       T=H
       DO 6 J=1,N
       FOUR=FOUR+FUNC(T)
    6  T=T+H+H
       NEWINT=(H/3.)*(2.*TWO+4.*FOUR+FUNC(FM))
       IF(ABS(INT-NEWINT).LT.0.0001.OR.N.GT.5000) GO TO 3
       INT=NEWINT
       GO TO 5
    3  NEWINT=NEWINT*2*DPRIME/3.14159
   50  WRITE(6,27) M,TPRIME,X,NEWINT
   27  FORMAT(2X,I7,F10.3,F10.4,F14.7)
   40  CONTINUE
   43  CONTINUE
       STOP
       END
```

This thesis is accepted on behalf of the faculty of the Institute by the following committee:

Ernst Wolfgang Groos.

Alan Shapley.

Lynn W. Gelhar

Date August 5, 1976.